

Morphological Crystallography



κρυσταλλος
krystallos “hard ice”
low quartz (α -SiO₂)

Crystals

- plane *faces*
- straight line *edges*
- point *vertices*

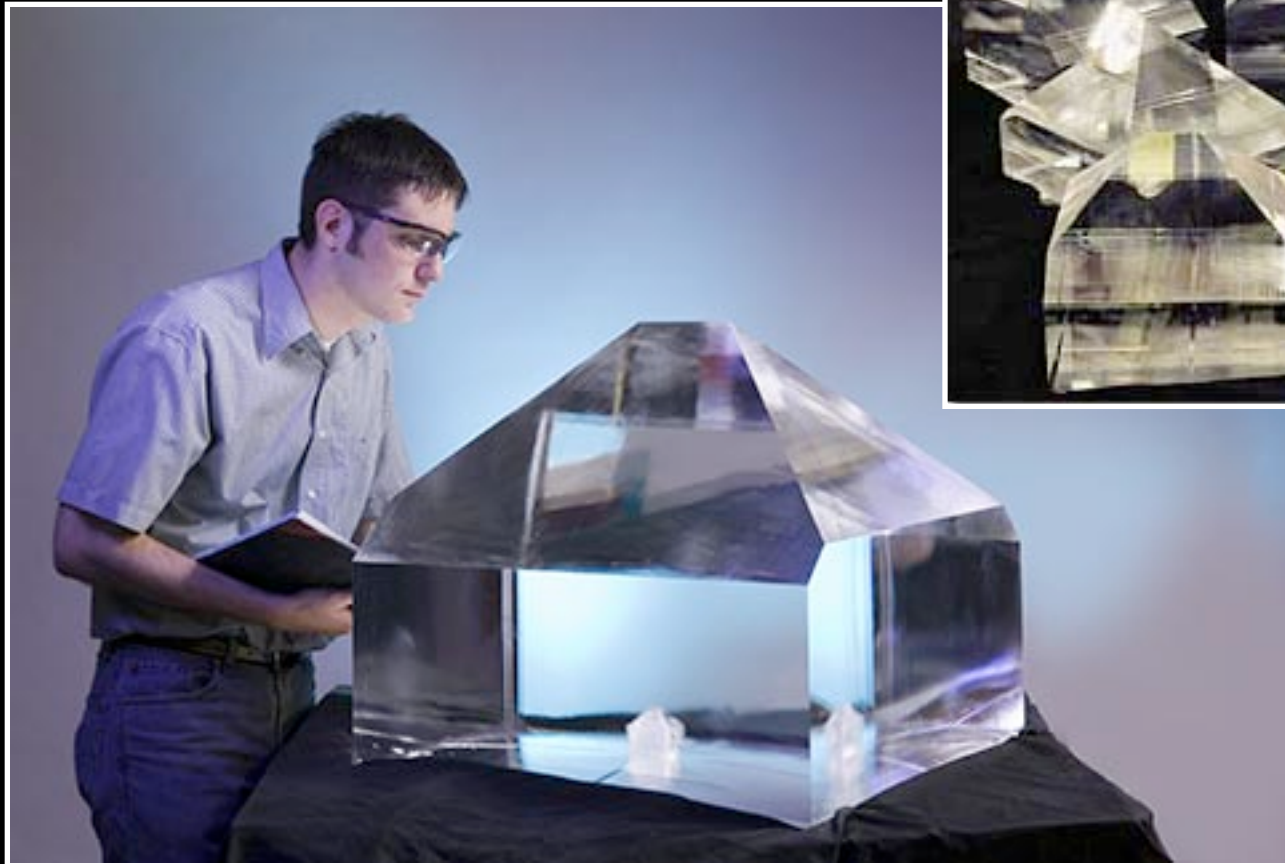
- constant interfacial angles
- rational intercepts

- 3-D periodic internal lattice



κρυσταλλος
krystallos “hard ice”
low quartz (α -SiO₂)

Large (~400 kg) KDP crystals
 KH_2PO_4 , sp. gp. *I* 4bar 2 d



Grown for fabricating frequency converters for high power laser systems for nuclear fusion experiments.

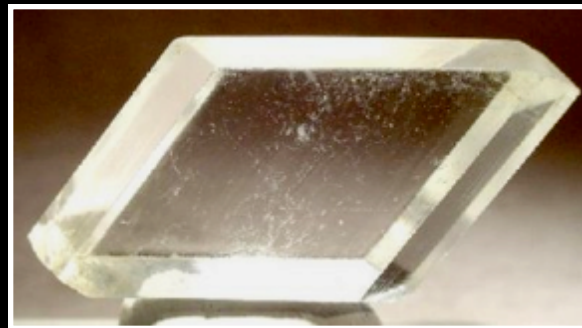
https://lasers.llnl.gov/programs/images/new_dkdp_crystal.jpg

<http://chemconnections.org/crystals/new/images/kdp.jpg>

Giant selenite gypsum crystals $\text{CaSO}_4 \cdot 2\text{H}_2\text{O}$ Cueva de los Cristales, Naica mine, Chihuahua, Mexico



Giant crystals grew over many millennia from satd. aq. soln. at const. 58°C temp. in flooded caverns, and were revealed when pumping for mining lowered the water table.

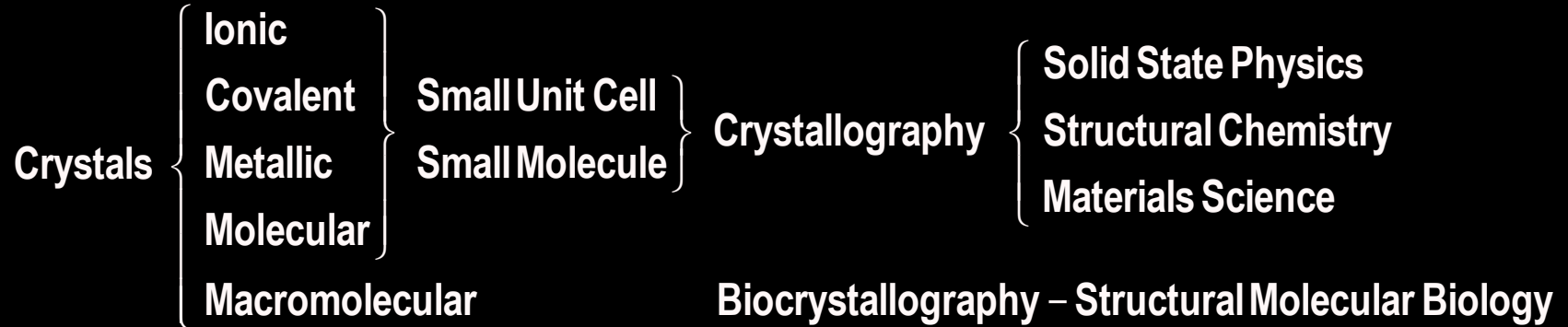


monoclinic point group $2/m$
space group $A2/a$





Crystals and Crystallographic Sciences



A Chronology of Crystallography

Classical antiquity

Greco-Roman thinkers – Nature of matter, polyhedral geometry, κρυσταλλος

1611 Johannes Kepler – Hexagonal snow crystals, hcp and ccp spheres

1600s René Descartes, Robert Hooke, Christiaan Huygens –
Speculations on periodic spheroid packing in crystals

1669 Nicolaus Steno (Niels Stensen),

1688 Domenico Gugliemini, and

1772 Jean-Baptiste Louis Romé de l'Isle – Law of Constant Interfacial Angles

1783 Abbé René-Just Haüy –

Law of Rational Indices, “*molécules intégrantes*,” unit cells

1839 William Hallowes Miller – stereographic projection, Miller indices

1849 Auguste Bravais – Lattice theory

1883 William J. Pope and William Barlow –

Speculations on atomic and ionic sphere-packing in crystals.

1890 Evgraf Stepanovich Federov,

1892 Arthur Moritz Schoenflies, and

1894 William Barlow (all three independently) – Space group theory






1883 Paul Heinrich Ritter von Groth – Chemical and optical crystallography

1895 Wilhelm Conrad Röntgen – X-rays

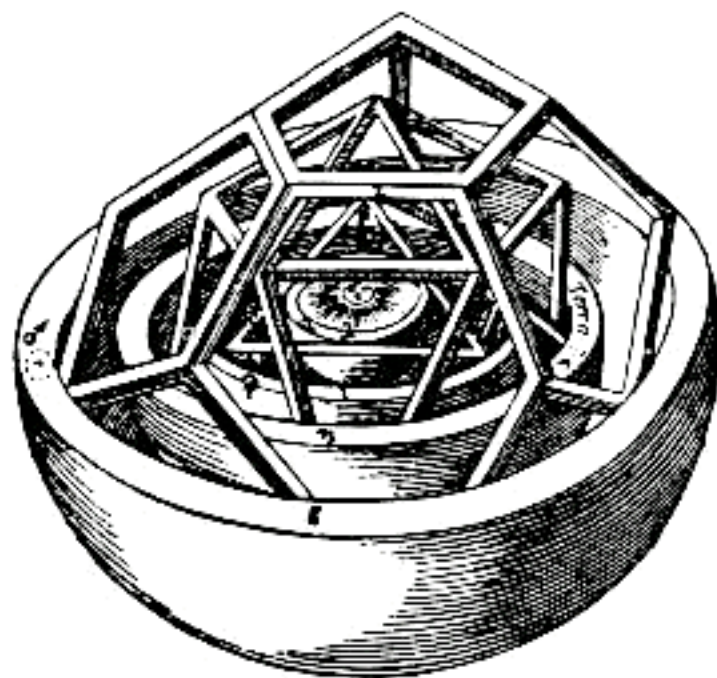
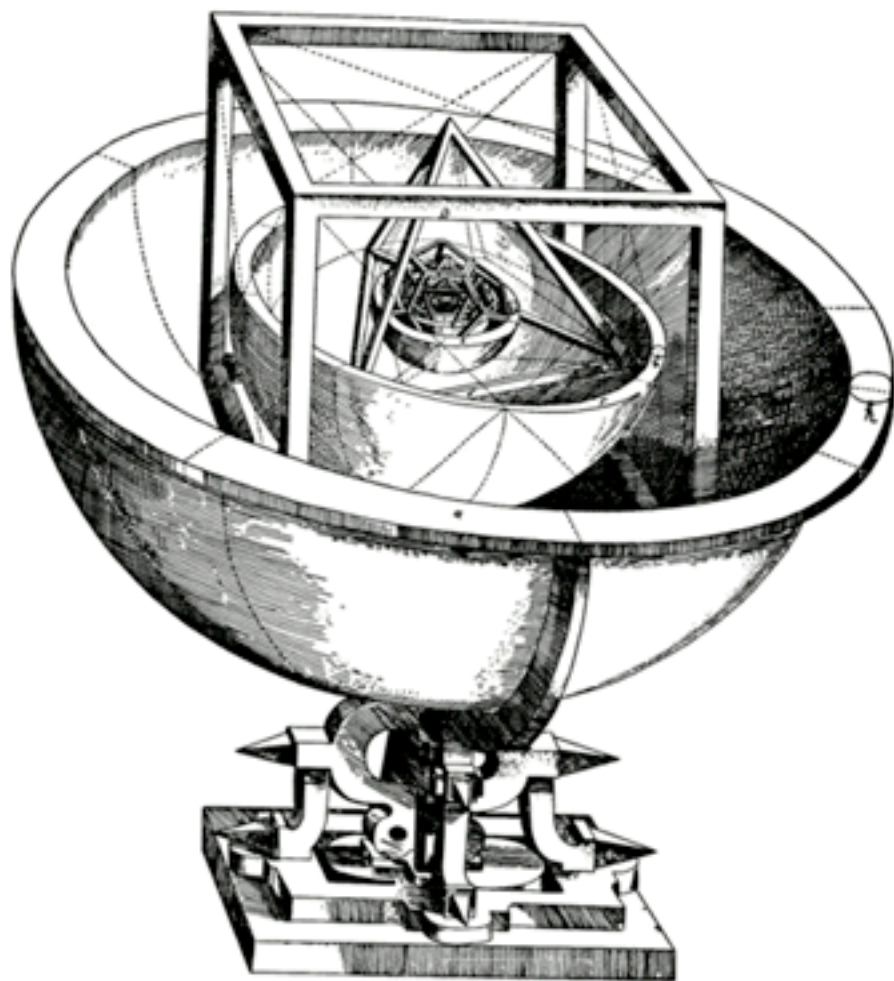
1912 Walther Friedrich, Paul Knipping, and Max von Laue – X-ray diffraction

1913 William Henry and William Lawrence Bragg – X-ray crystal structures

The Platonic Solids

Name	Image	Vertices V	Edges E	Faces F	Euler characteristic: $V - E + F$
Tetrahedron		4	6	4	2
Cube		8	12	6	2
Octahedron		6	12	8	2
Dodecahedron		20	30	12	2
Icosahedron		12	30	20	2

Kepler's Platonic solid model of the solar system from *Mysterium Cosmographicum* (1596)



Detailed view of the inner sphere

IOANNIS KEPLERIS C. MAIEST. MATHEMATICI STRENA

Seu
De Nive Sexangula.



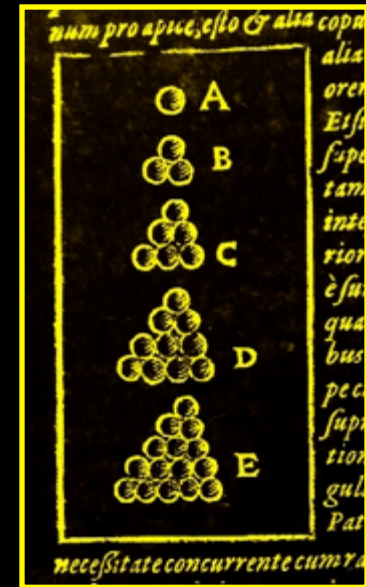
Cum Privilegio S. Cæs. Maiest. ad annos xv.
FRANCOFVRTI AD MOENVM,
apud Godofridum Tampach.
Anno M. DC. XI.

JOHANN KEPLER,
MATHEMATICIAN TO
HIS IMPERIAL MAJESTY

A NEW YEAR'S GIFT
OR
On the Six-Cornered Snowflake.

Copyright: Granted by His Imperial Majesty
for fifteen years.

Published by GODFREY TAMPACH at
FRANKFORT ON MAIN,
in the year 1611.



Johannes Kepler (1611)
On the Six-Cornered Snowflake



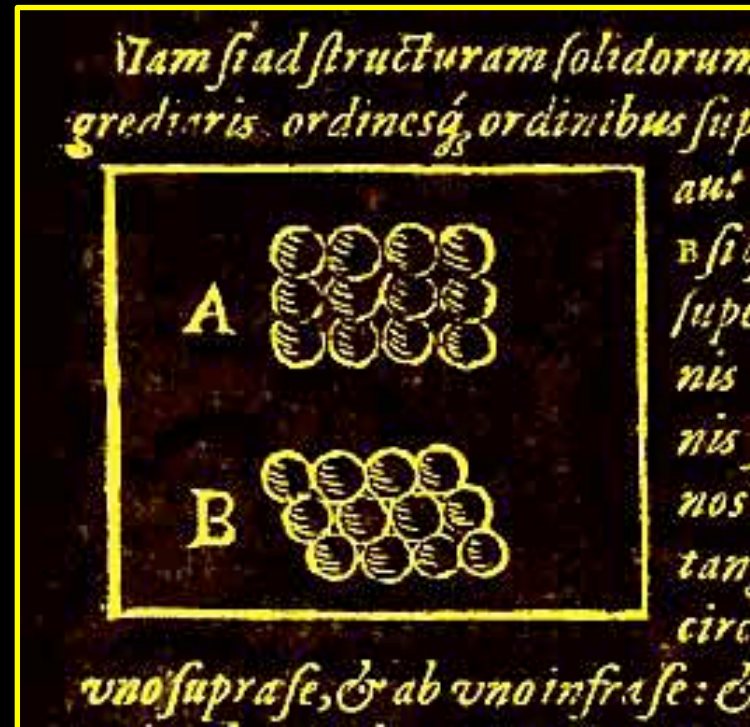
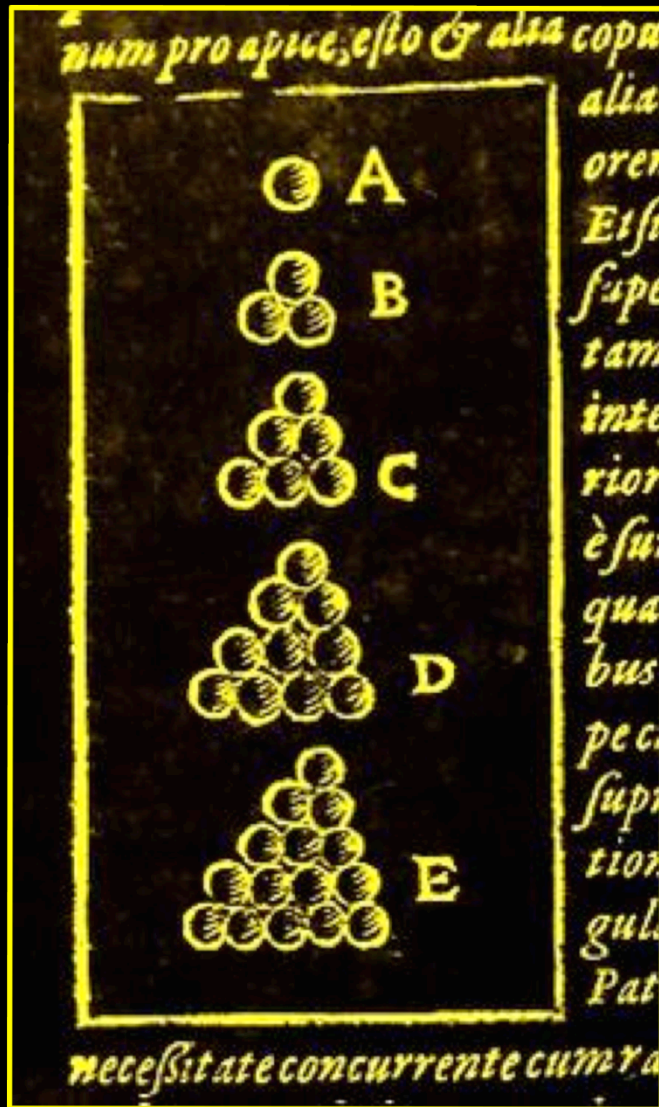
http://quinceandquire.typepad.com/quince_and_quire/2011/01/images-of-snow-crystals.html



*How full of the creative genius is the air in which these are generated!
I should hardly admire more if real stars fell and lodged on my coat.
Nature is full of genius, full of the divinity; so that not a snowflake
escapes its fashioning hand.*

—Henry David Thoreau (1817–1862)

Johannes Kepler (1611) On the Six-Cornered Snowflake



Kepler's conjecture (1611)

hcp and fcc-ccp densest packing of equal spheres

Computational proof by exhaustion (Thomas Hales, 1997)

<https://sites.google.com/site/thalespitt/>

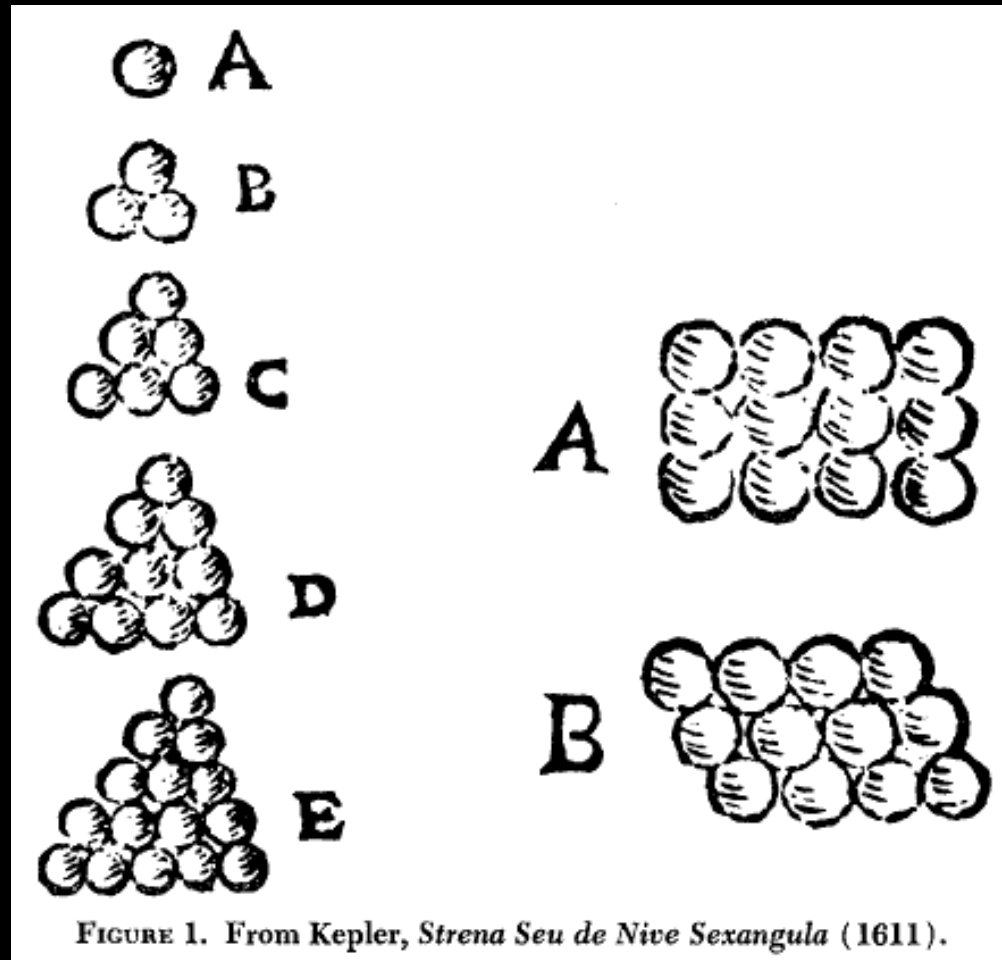


FIGURE 1. From Kepler, *Strena Seu de Nive Sexangula* (1611).

Cecil Schneer (1960). Kepler's New Year's Gift of a Snowflake. *Isis*, 51(4), 531-545.



"Each single plant has a single animating principle of its own, since each instance of a plant exists separately, and there is no cause to wonder that each should be equipped with its own peculiar shape. But to imagine an individual soul for each and any starlet of snow is utterly absurd, and therefore the shapes of snowflakes are by no means to be deduced from the operation of soul in the same way as with plants."

Johannes Kepler (1611). *De Nive Sexangula*
(*On the Six-Cornered Snowflake*).



"These were little plates of ice, very flat, very polished, very transparent, about the thickness of a sheet of rather thick paper...but so perfectly formed in hexagons, and of which the six sides were so straight, and the six angles so equal, that it is impossible for men to make anything so exact."

"I only had difficulty to imagine what could have formed and made so exactly symmetrical these six teeth around each grain in the midst of free air and during the agitation of a very strong wind, until I finally considered that this wind had easily been able to carry some of these grains to the bottom or to the top of some cloud, and hold them there, because they were rather small; and that there they were obliged to arrange themselves in such a way that each was surrounded by six others in the same plane, following the ordinary order of nature."

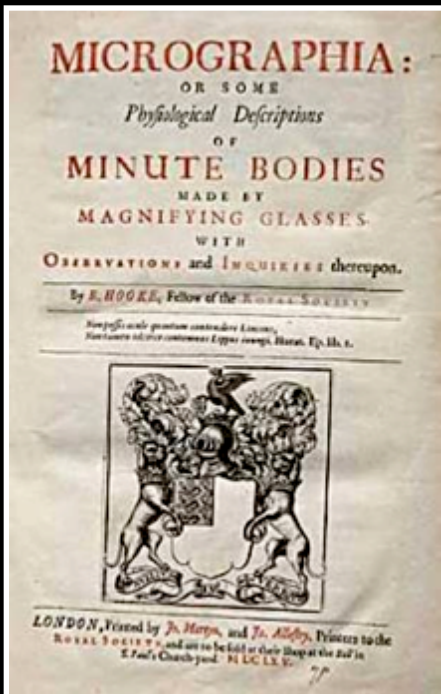
Rene Descartes (1635). Notes.

F.C. Frank (1974). Descartes' Observations on the Amsterdam Snowfalls of 4, 5, 6, and 9 February 1634. *J. Glaciology* 13, 535.

Robert Hooke (1635-1703)

In 1665 Robert Hooke published a large volume entitled *Micrographia*, containing sketches of practically everything Hooke could view with the latest invention of the day, the microscope. Included in this volume are many snow crystal drawings, which for the first time revealed the complexity and intricate symmetry of snow crystal structure.

Hexagonal Snow Crystals

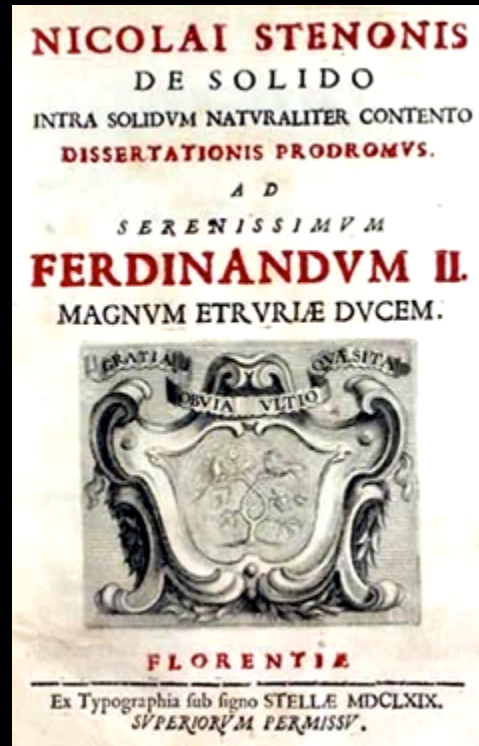


“The First Law of Crystallography” Steno’s Law of Constant Interfacial Angles (1669)

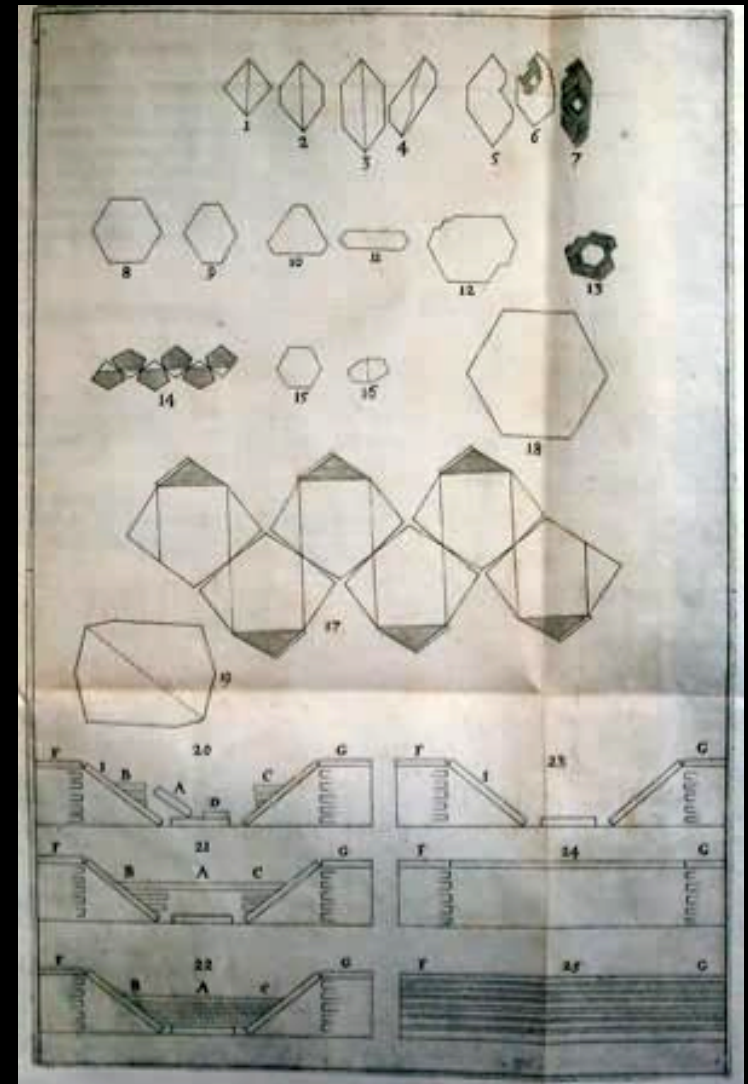
Niels Stensen
Nicolaus Steno



1638-1686



M.DC.LX.IX
1669



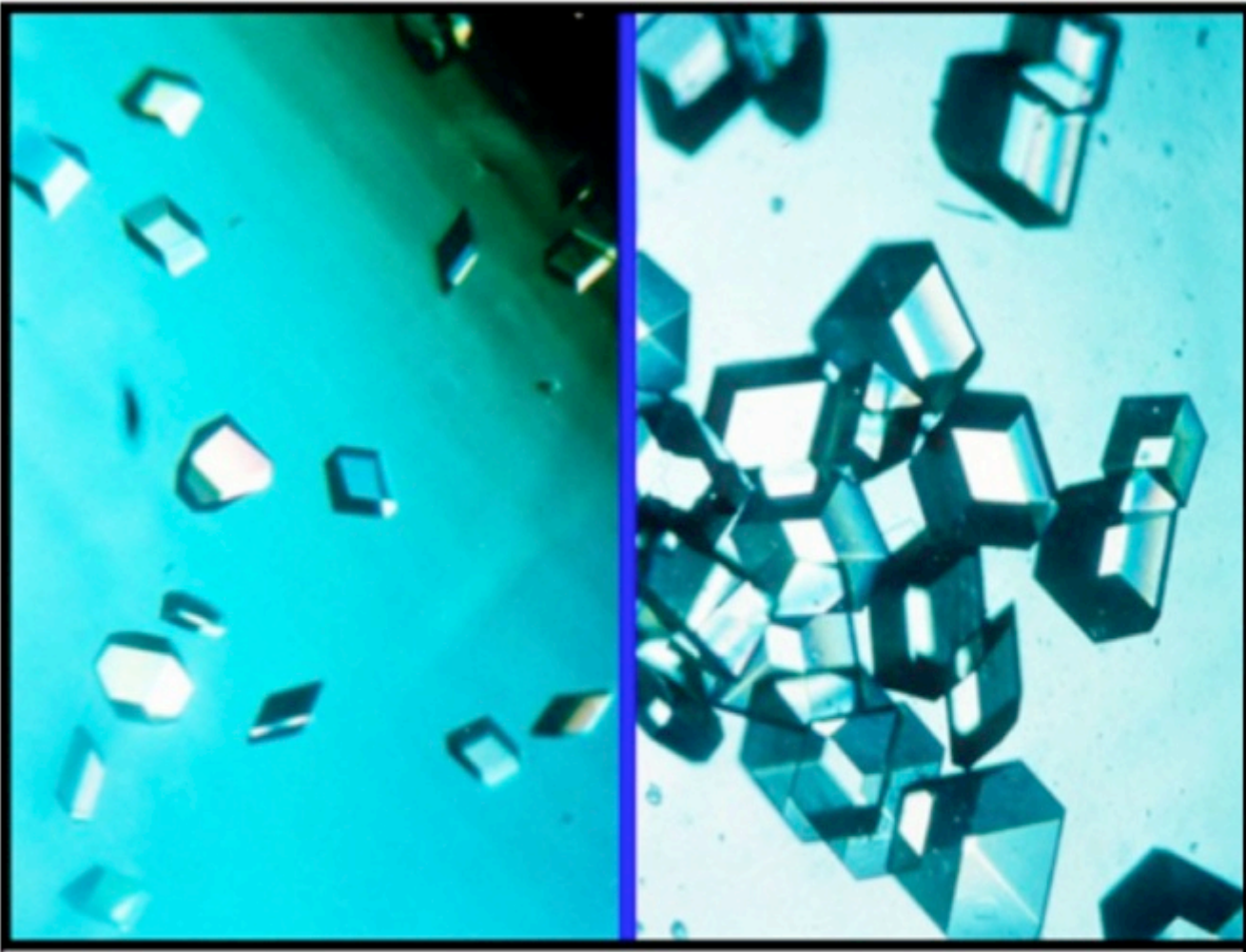
from Steno’s notebook

The First Law of Crystallography”
Steno’s Law of Constant Interfacial Angles (1669)

The angles between corresponding faces on crystals of any solid chemical or mineral species are constant and are characteristic of the species.

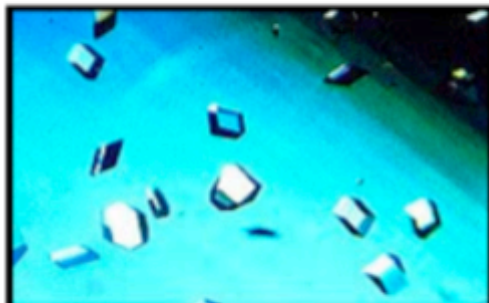
The interfacial angle is measured between face normals.

The law constant of interfacial angles holds for any two crystals a given species, whether they are natural or man-made, regardless of size or provenance.

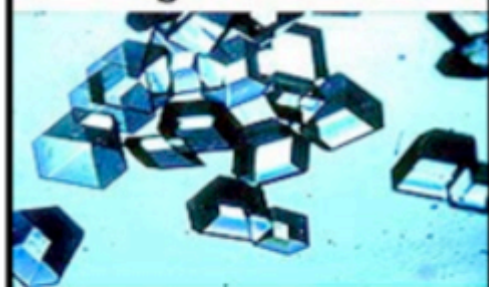


**Crystals of T_3R_3 human insulin
complexed with *p*-hydroxybenzamide**

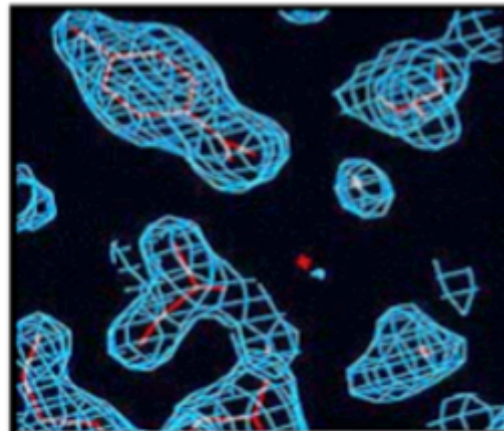
**NASA STS60 (Discovery, 1994): left, 1 G; right, μ G.
Both photomicrographs at the same magnification.**



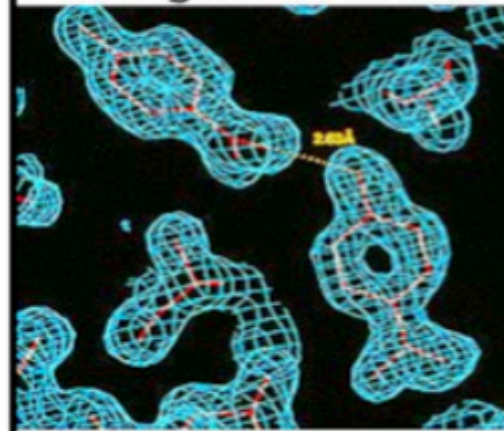
Earth-grown insulin



Space-grown insulin



Earth-grown insulin



Space-grown insulin

**Crystals of T_3R_3 human insulin
complexed with *p*-hydroxybenzamide**

NASA STS60 (Discovery, 1994): left, 1 G; right, μ G.

Earth grown (1 G) 1.9 Å resolution;

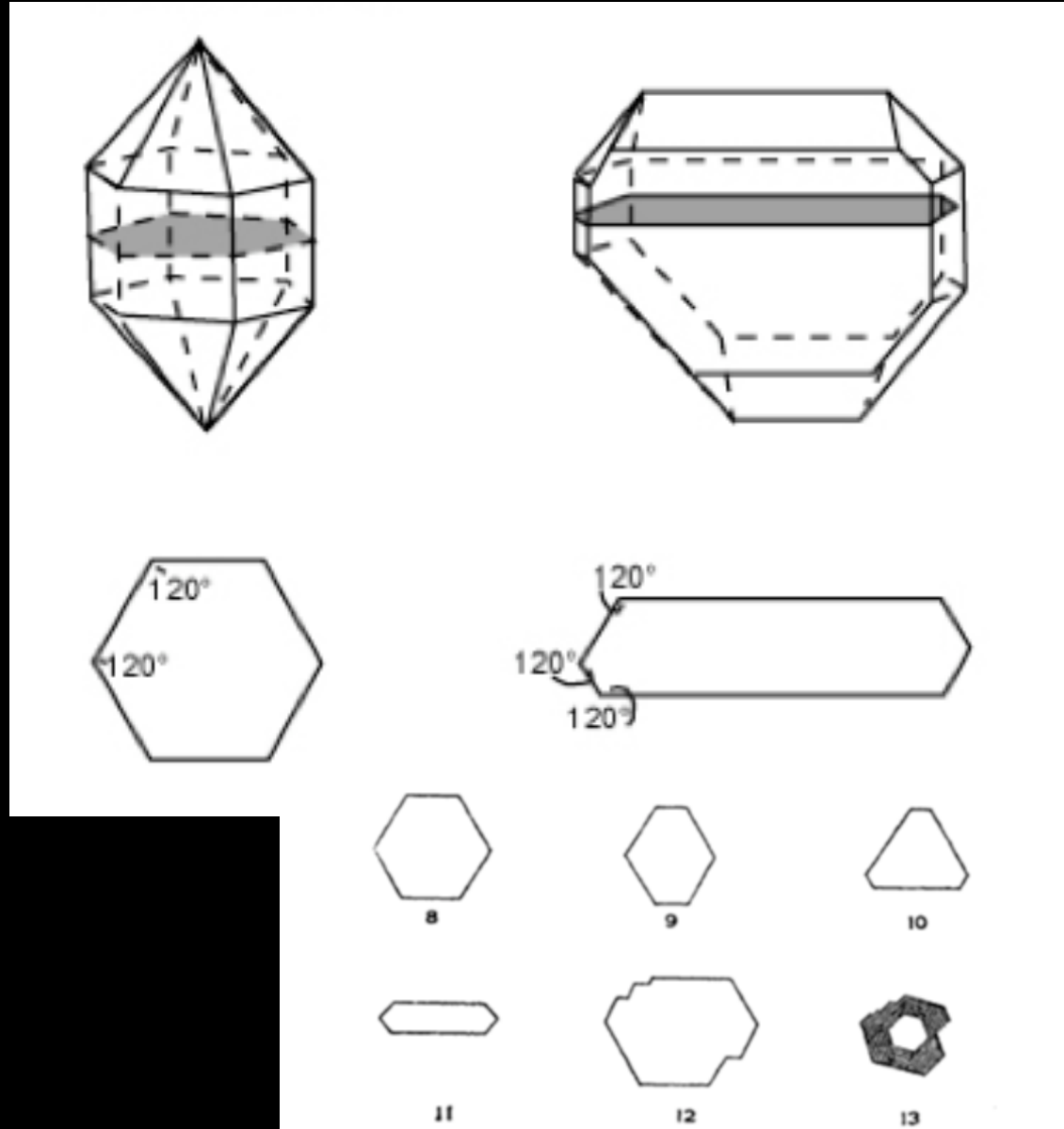
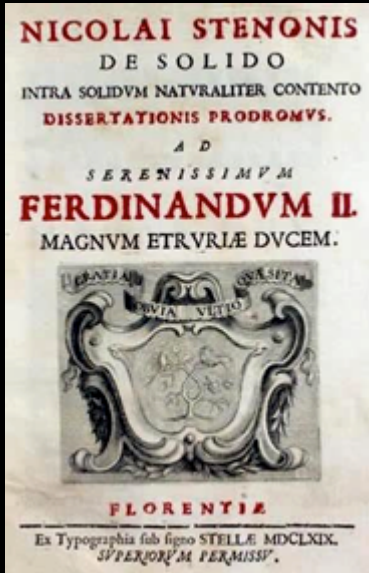
Space grown (μ G STS60) 1.4 Å resolution.

Photomicrographs at the same magnification.

Steno's Law of Constant Interfacial Angles



Niels Stensen
Nicolai Stenonis
Nicholas Steno
1628-1686



“The first law of crystallography”

The law of constant interfacial angles

[Nicolas Steno (Niels Stensen), 1669; Jean-Baptiste Romé de l'Isle, 1793]

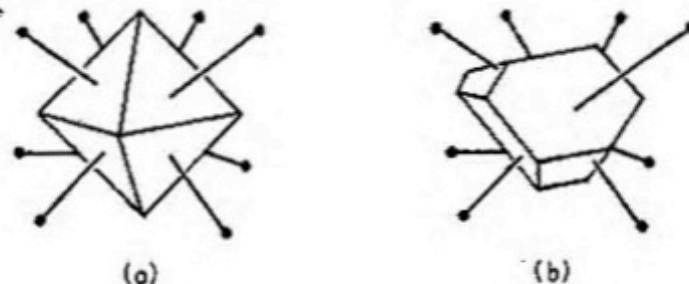


Fig. 2.5(a). Face normals of a regular octahedron.

Fig. 2.5(b). Same face normals as in Fig. 2.5(a) from octahedron of irregular growth.

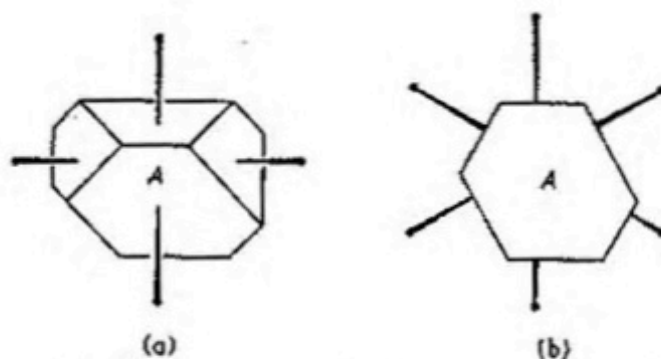
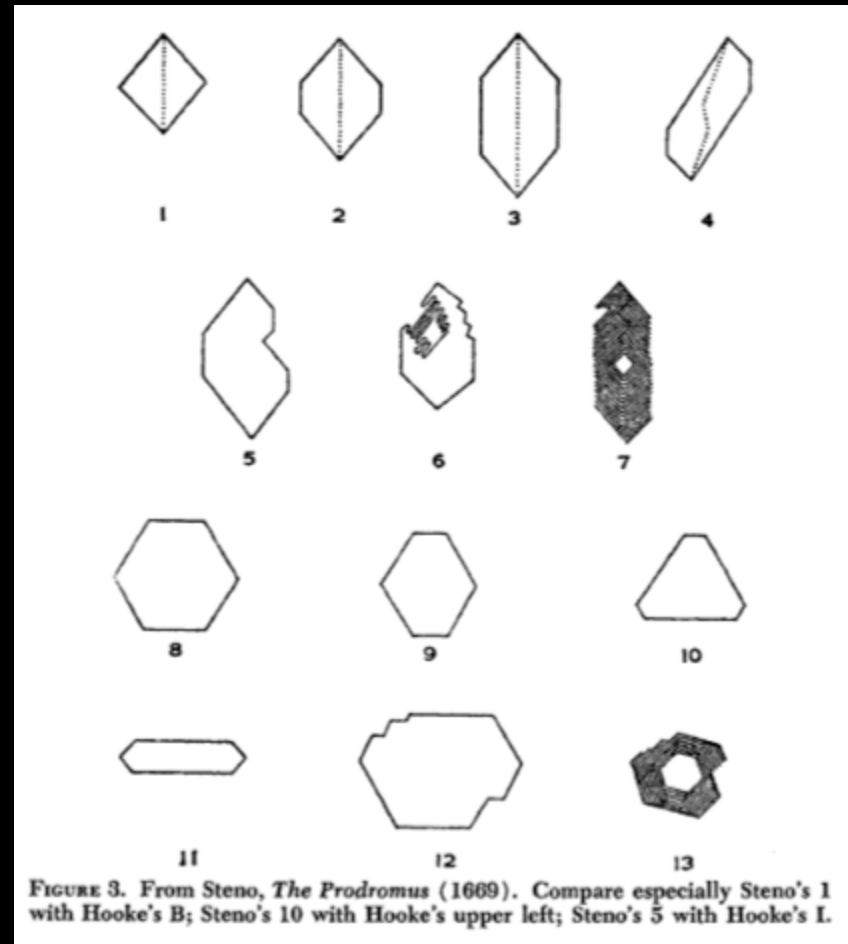
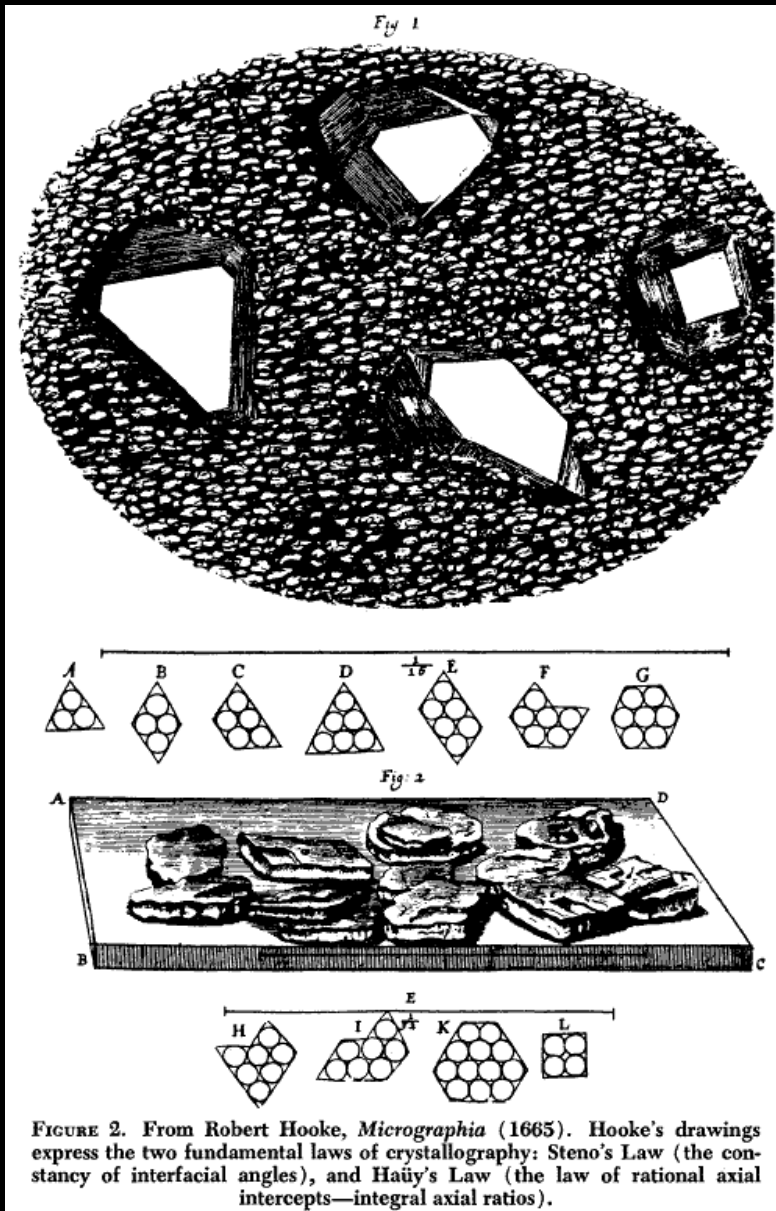


Fig. 2.6. Crystal of Fig. 2.5(b) showing (a) fourfold axis and (b) threefold axis.

Hooke (1665)

Steno (1669)



Quartz crystals
(1-7) elevations
(8-13) cross-sections

Confirmation of Steno's Law of Constant Interfacial Angles

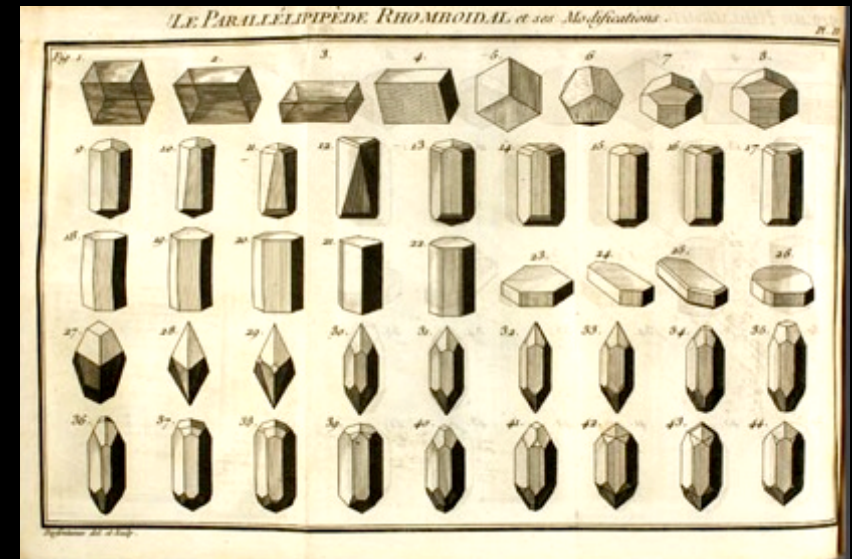
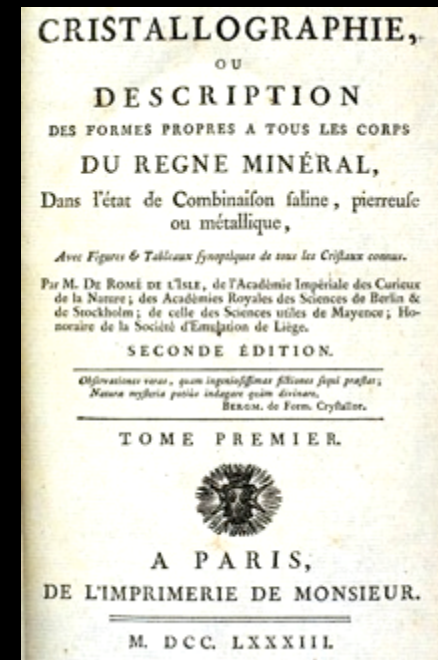


**Jean-Baptiste Louis Romé de l'Isle
(1736-1790)**

**Pre-Revolutionary French artillery officer
and by avocation a mineralogist**

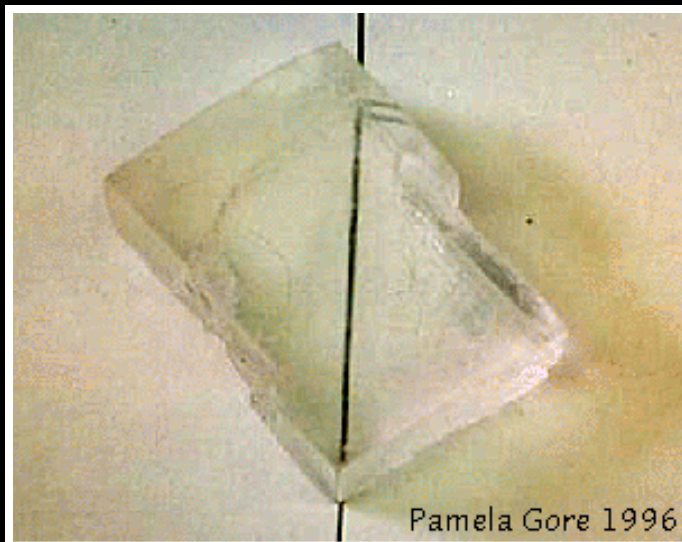
**Confirmed Steno's *Law of
Constant Interfacial Angles*
with hundreds of mineral crystals.**

***Essai de Cristallographie* (1772)
and
Cristallographie (1783).**



<http://www.ville-gray.fr/en/tourism-patrimony/culture-celebrities.php>
http://www.mineralogy.eu/bookarchive/r/RomeDeLisle_1783.html

Birefringent Iceland spar (calcite, CaCO_3)



120°
↻
→



http://www.museum.vic.gov.au/scidiscovery/images/mn006328_w150.jpg

<http://gpc.edu/~pgore/myphotos/calcdbl.gif>

Huygens' principle and birefringent Iceland spar

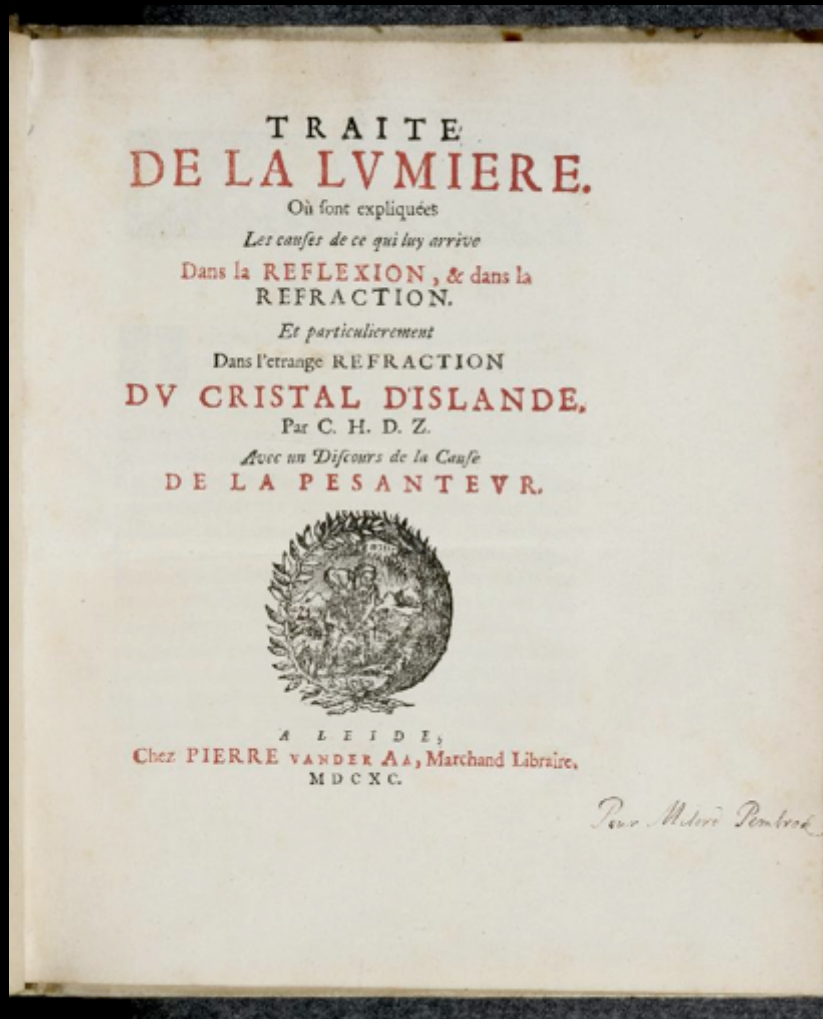


Christiaan Huygens (1629-1695)

"Huygens Principle" considers all points on a wavefront to be sources of spherical wavefronts that add up to build the propagating wavefront. Huygens realized that if the velocity of light varied with the direction the spheres would deform to ellipsoids and thus was able to explain the refraction law for crystals such as Iceland Spar.

Huygens (1678). *Traité de la Lumière.*

Christiaan Huygens (1629-1695)



Christiaan HUYGENS. *Traité de la Lumière.*

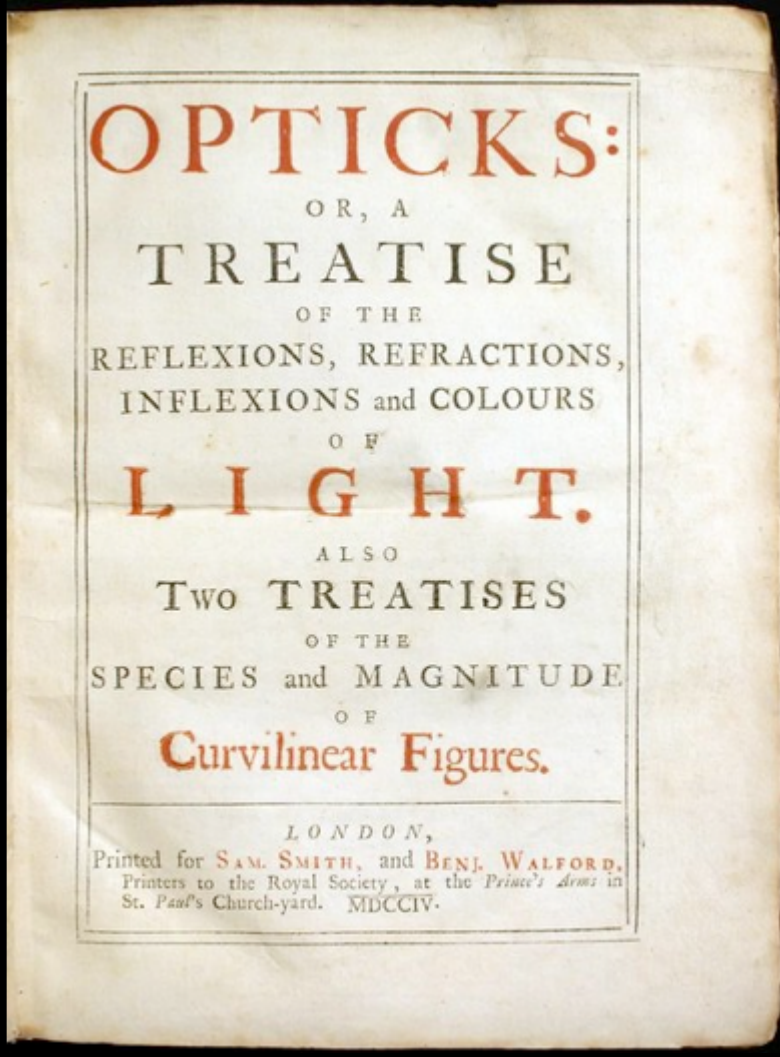
Où sont expliquées les causes de ce qui luy arrive dans la reflexion, & dans la refraction.

Et particulièrement dans l'etrange refraction du Cristal d'Islande....

Avec un discours de la cause de la pesanteur. MDCXC (1690).

http://www.jonathanahill.com/book.php?book_id=1242

Isaac Newton (1643-1727)



MDCCIV (1704)

<http://en.wikipedia.org/wiki/Opticks>

Birefringent Iceland spar (calcite, CaCO_3)



Huygens (1690)

Calcite (CaCO_3) cleavage rhombohedron

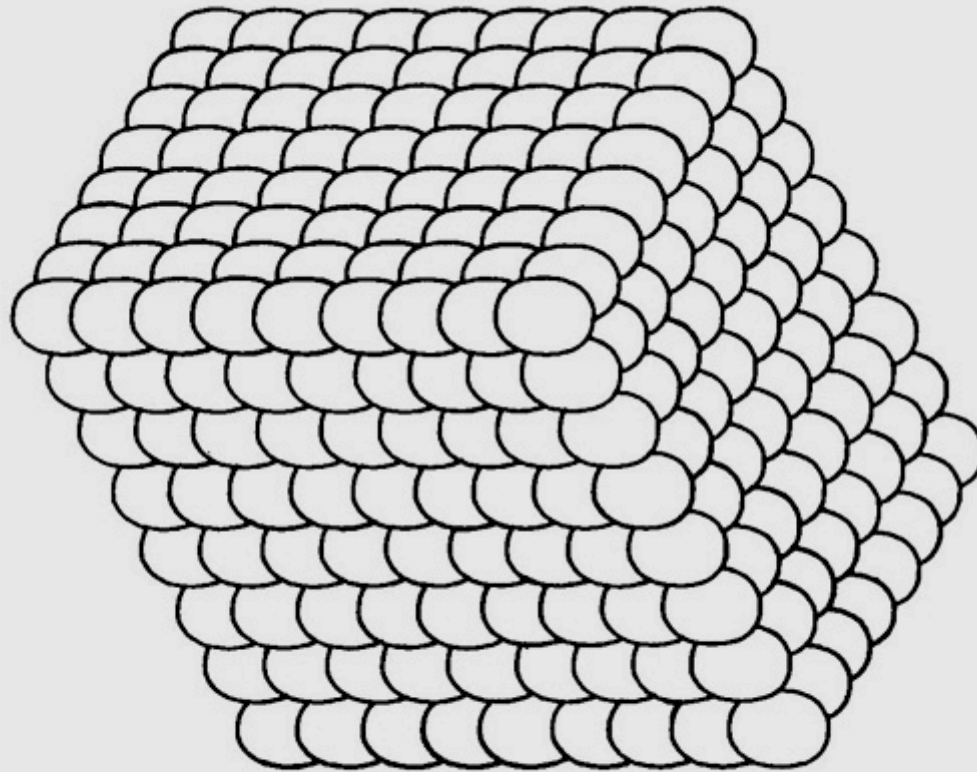


Fig. 1-24. Fine structure of the calcite cleavage rhombohedron according to Huygens. (Klug, *Am. Scientist*, 36, 377.)

Hypothetical ellipsoids rather than spheres in order to produce the rhomboid shape.

Huygens' (1690) calcite cleavage hypothesis

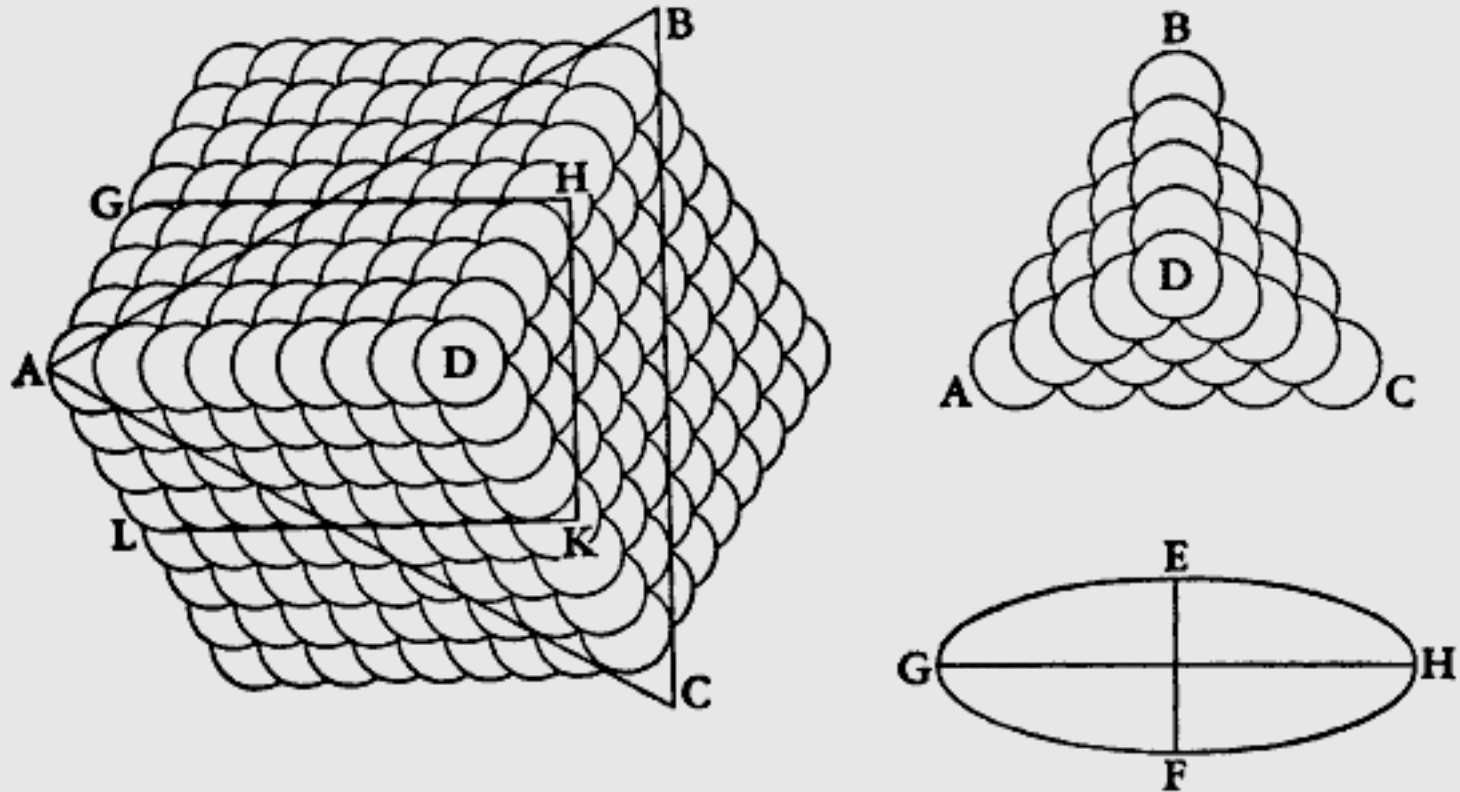
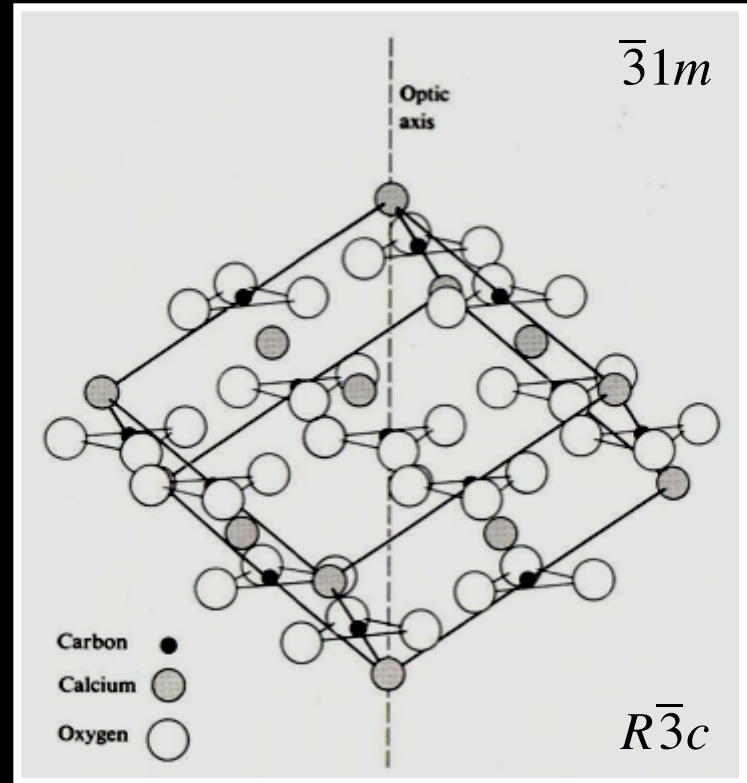
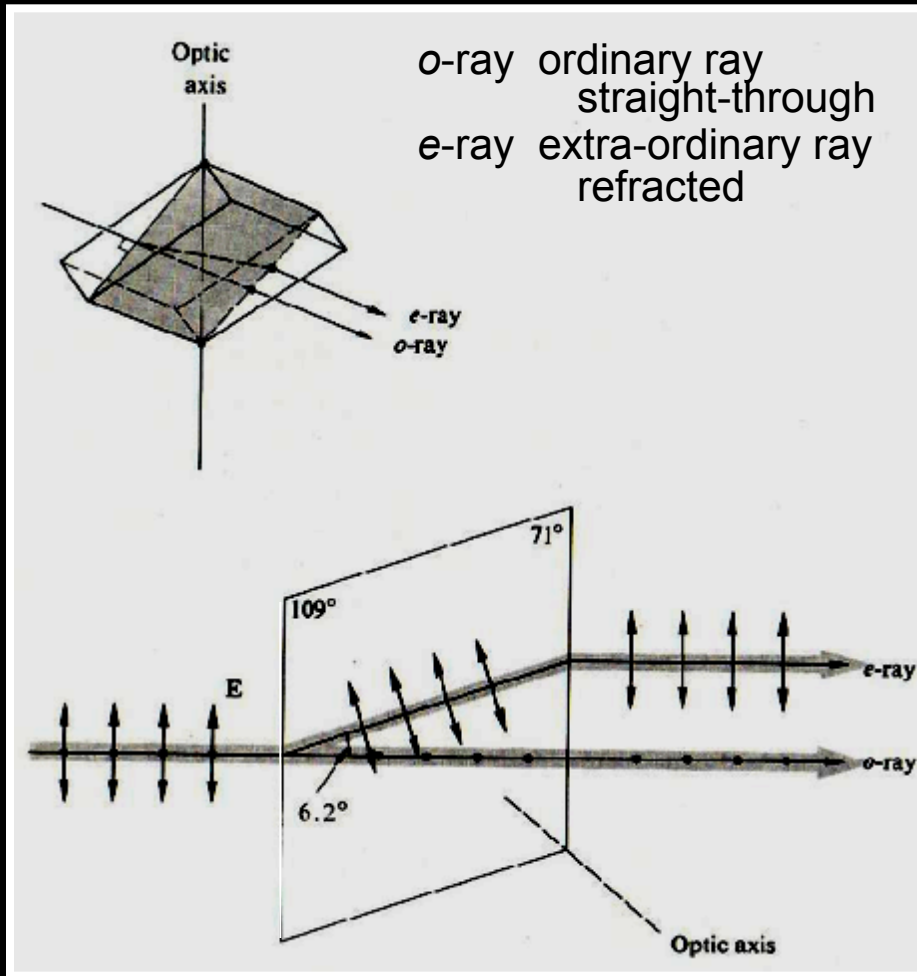


FIGURE 4. From Huygens, *Treatise on Light* (1690). Huygens' corpuscular model for Iceland spar (calcite) is the prototype for Haüy's Law of rational intercepts (integral axial ratios).

Calcite (CaCO_3) birefringence



$\{10\bar{1}4\}$ faces

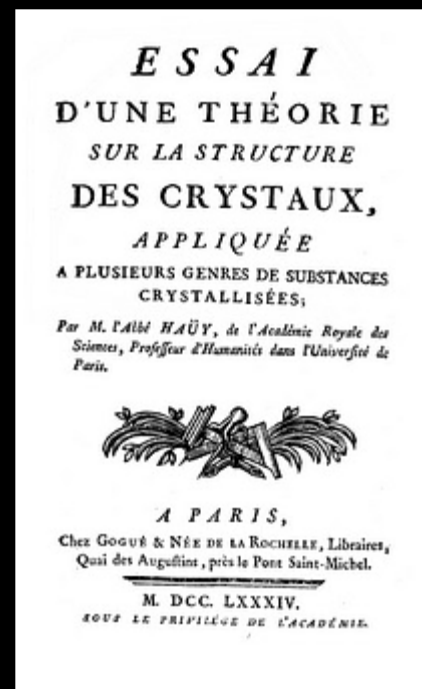
“The Second Law of Crystallography”

Haüy’s Law of Rational Intercepts (1784)

According to Haüy, if three non-coplanar edges of a crystal are taken to define the directions of three axes of a coordinate system, then the ratios of the axial intercepts of two crystal faces are always found to be rational fractions. That is, the lengths of the axial intercepts can be expressed as integer multiples of some elementary axial lengths.



**Abbé René-Just Haüy
(1743-1822)
making goniometric
measurements on a
calcite (CaCO₃) crystal**



**Monsieur l'Abbé HAÜY
M.DCC.LXXX.IV
1784**



**Abbé René-Just Haüy
(1743-1822)
making goniometric
measurements on a
calcite (CaCO_3) crystal**

ESSAI
D'UNE THÉORIE
SUR LA STRUCTURE
DES CRYSTAUX,
APPLIQUÉE
A PLUSIEURS GENRES DE SUBSTANCES
CRYSTALLISÉES;

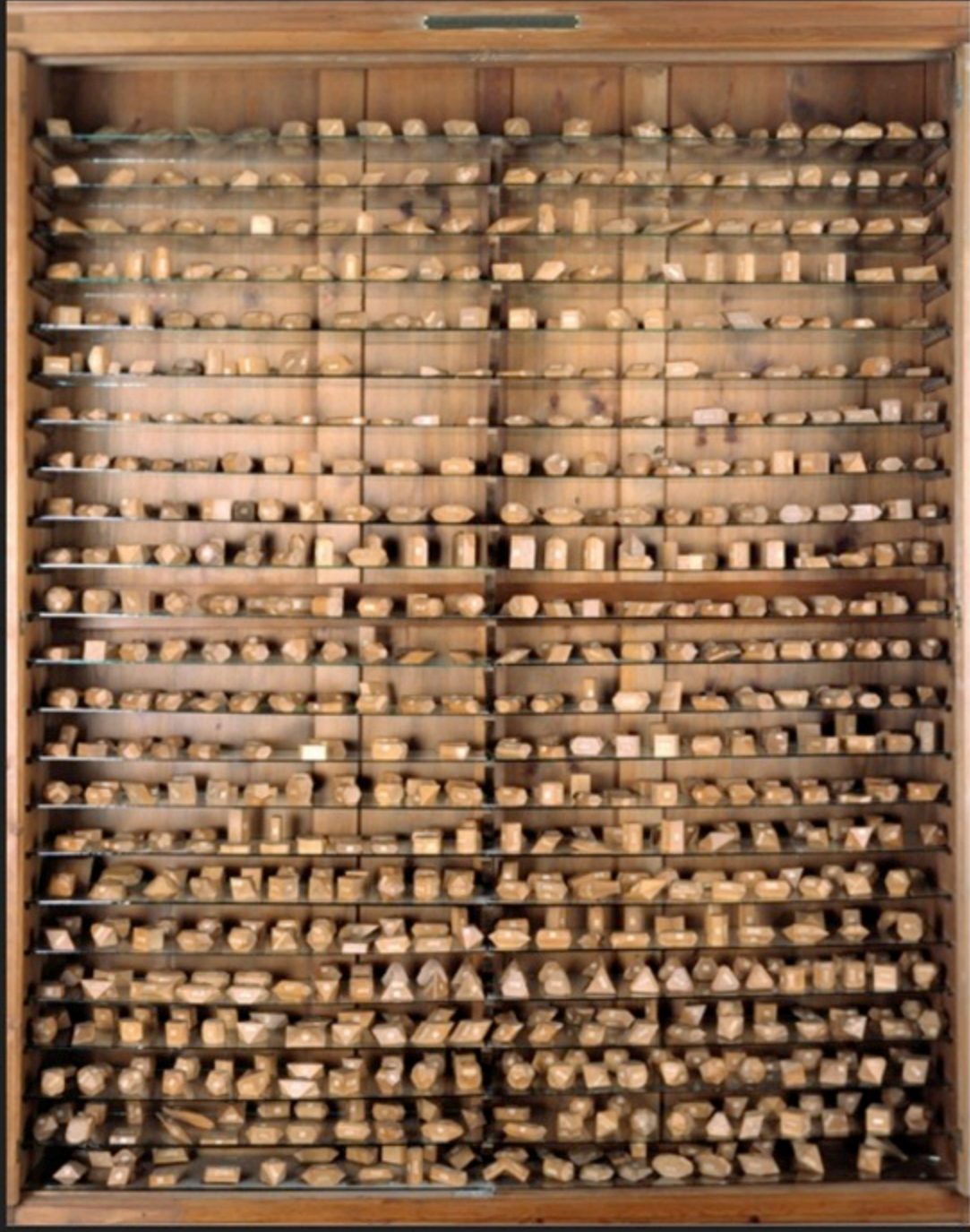
*Par M. l'Abbé HAÜY, de l'Académie Royale des
Sciences, Professeur d'Humanités dans l'Université de
Paris.*



A PARIS,
Chez GOGUÉ & NÉE DE LA ROCHELLE, Libraires,
Quai des Augustins, près le Pont Saint-Michel.

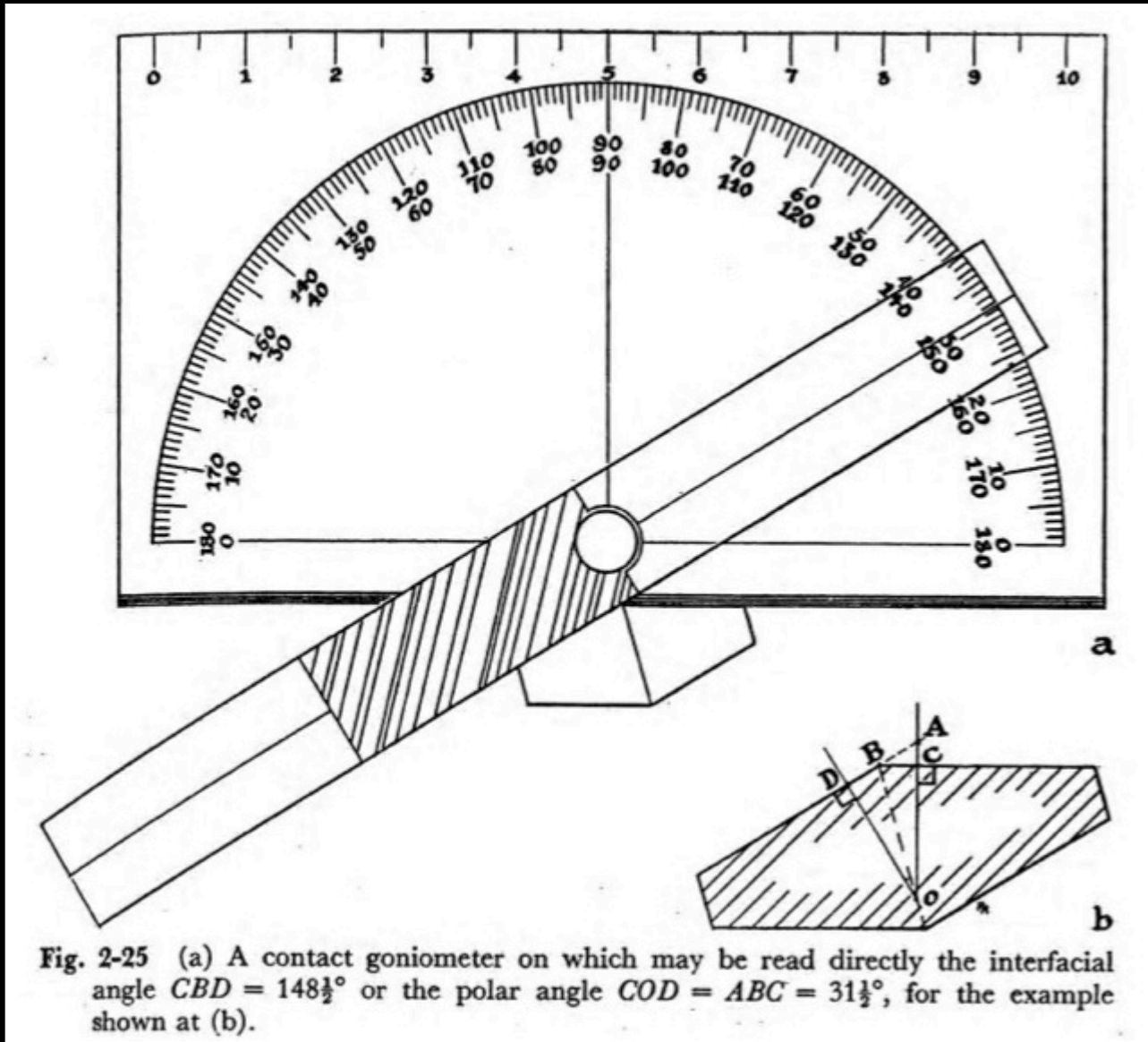
M. DCC. LXXXIV.
SOUS LE PRIVILÈGE DE L'ACADÉMIE.

**Monsieur l'Abbé HAÜY
M.DCC.LXXX.IV
1784**



**A collection of crystallographic solids
gifted by l'Abbe René Just Haüy (1743-1822)
to the Galician mathematician José Rodríguez González (1770-1824)**
http://www.xtal.iqfr.csic.es/Cristalografia/parte_12_1-en.html

Contact goniometer

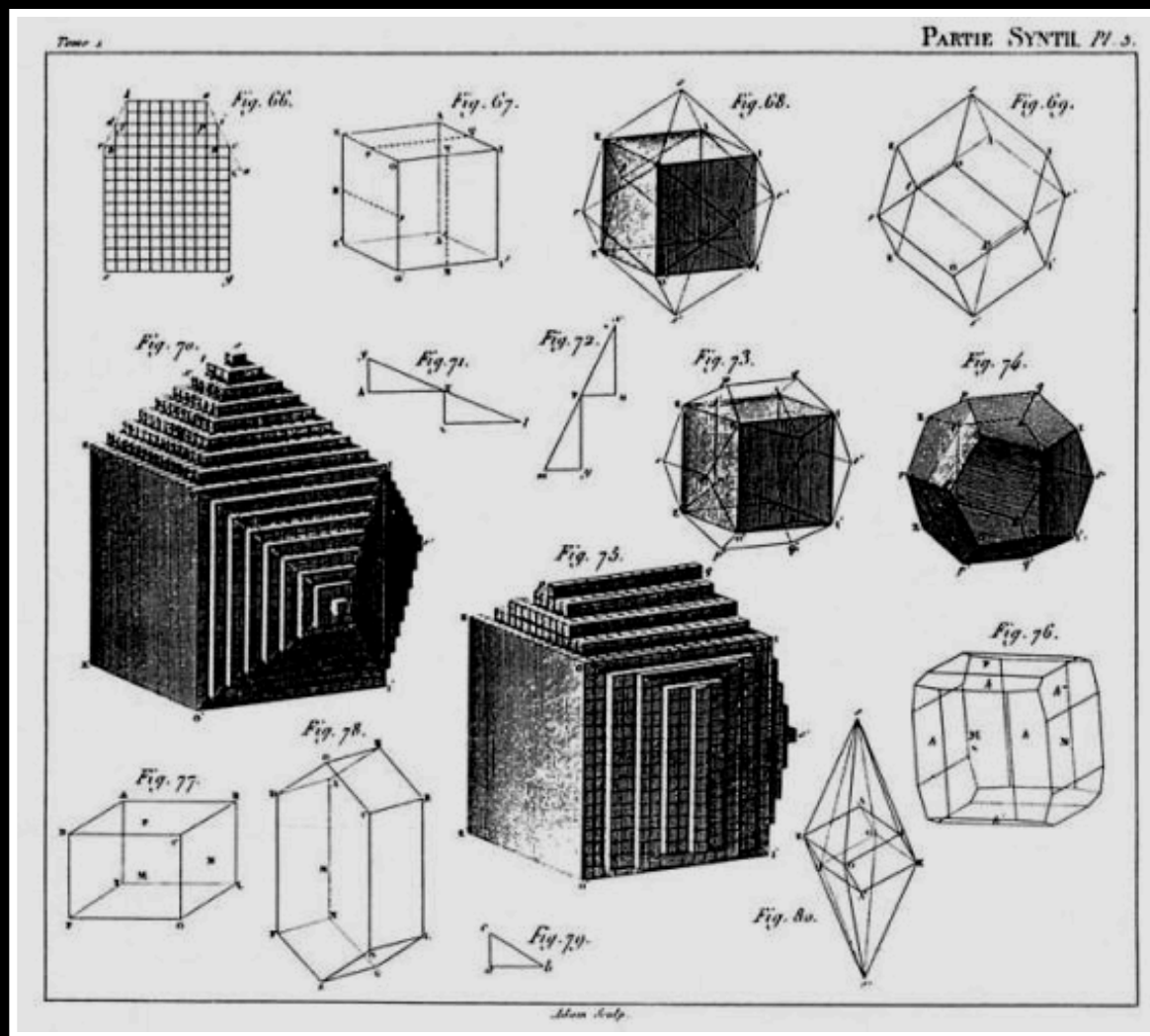




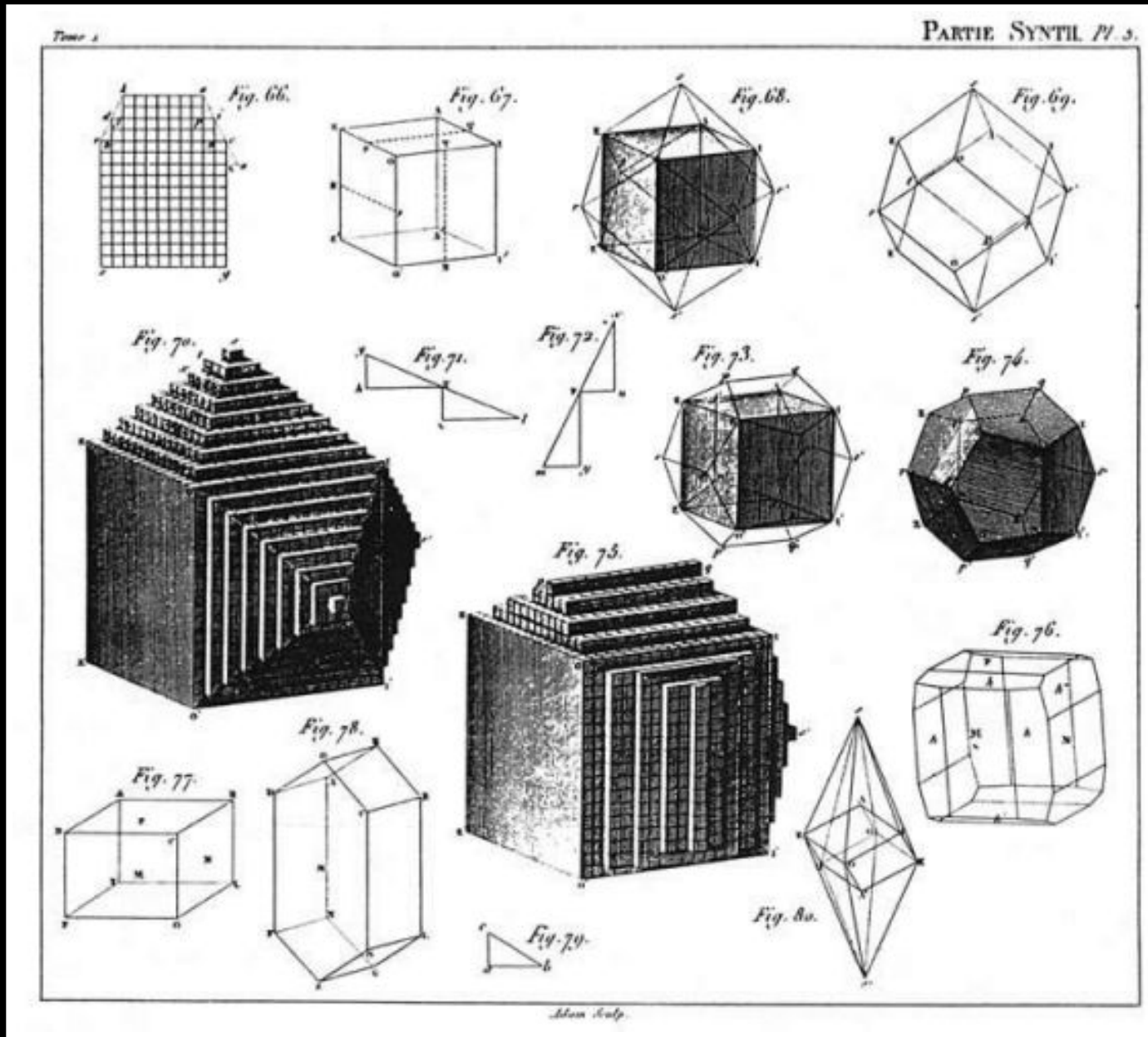
**Abbé René-Just Haüy
(1743-1822)
making goniometric
measurements on a
calcite (CaCO_3) crystal**

Haüy (1784)

The law of rational intercepts implies
“*molécules intégrantes*” or unit cells.



Haüy (1784). "molécules intégrantes" or unit cells



Two of Häüy's 1784 drawings of crystal structure models

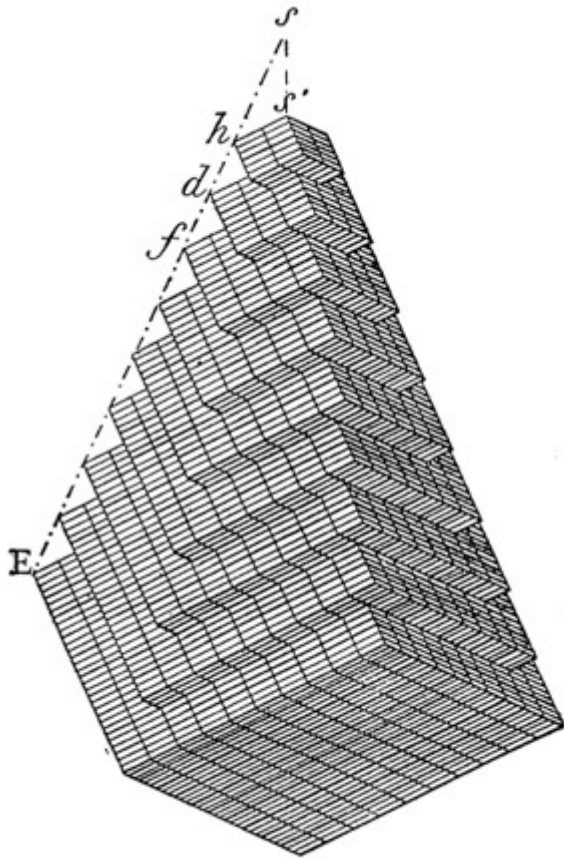


FIG. 49. A reproduction of one of Häüy's figures, showing how a crystal of dogtooth spar may be considered to be built up from rhombohedral units.

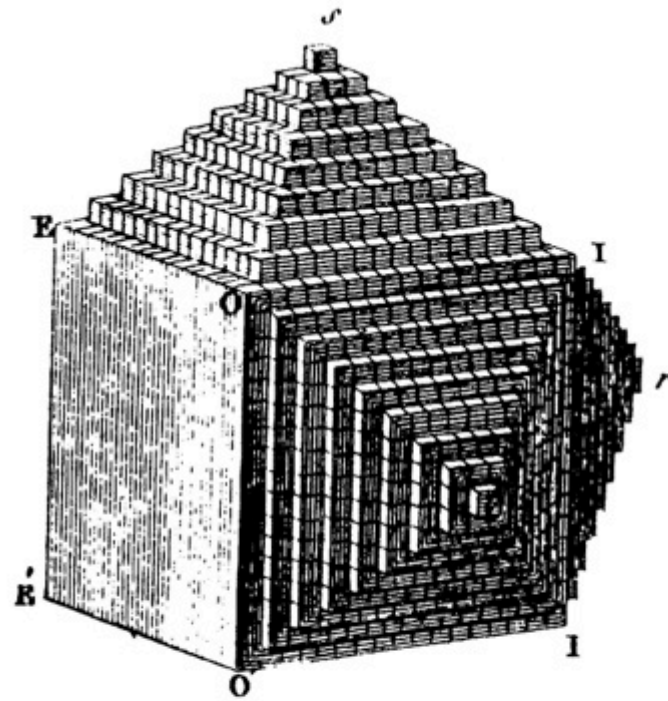


Fig. 17.2.1.1. Model of a crystal structure proposed by René Häüy in *Traite elementaire de Physique*, Vol. 1 [Paris: De L'Imprimerie de Delance et Lesueur, 1803]. This model, proposed in 1784, was the first to connect the external facets of a crystal with an underlying regular arrangement of building blocks.

**Development of a trigonal
scalenohedron
dogtooth spar crystal**

**Development of a cubic
rhombic dodecahedron**

Some Haüy constructions of crystal models (Abbé René-Just Haüy, 1784)

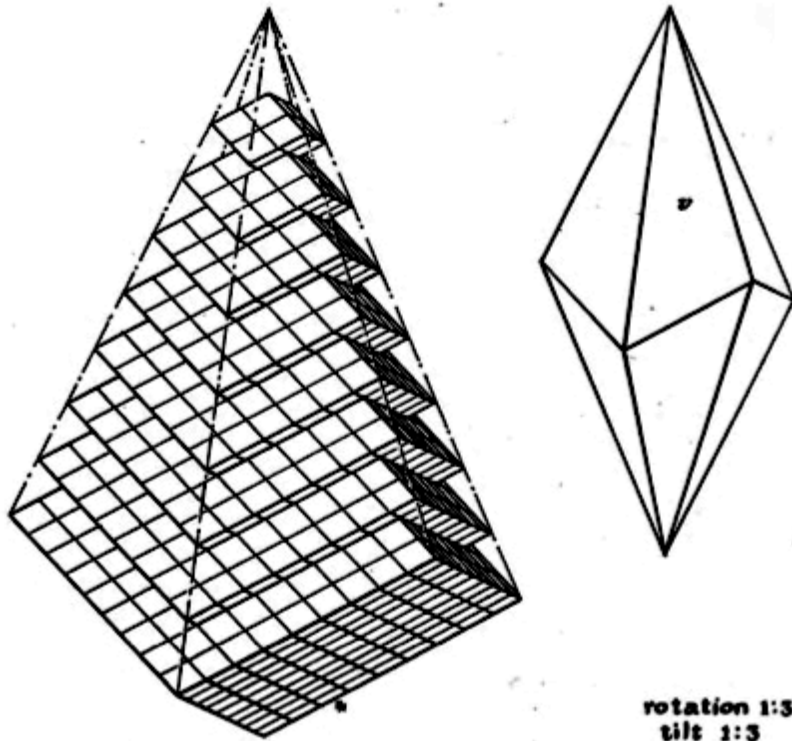


Fig. 2-1 Haüy's conception of structural units, with the shape of the cleavage rhombohedron, building up a crystal of calcite in the form of a scalenohedron $v(21\bar{3}1)$. [Left-hand drawing after Haüy.]

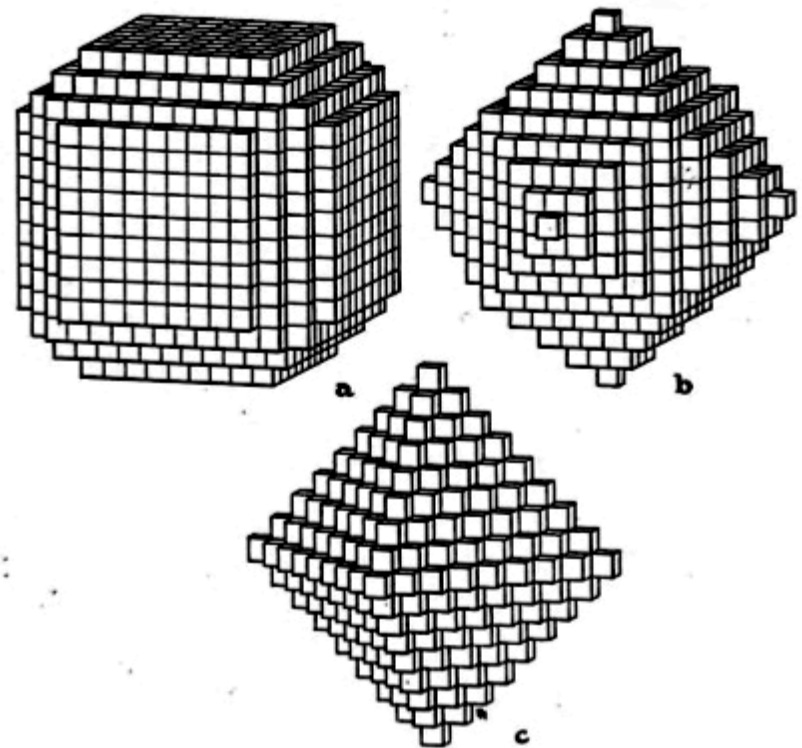


Fig 2-2 Haüy's conception of structural units, with the form of cleavage cubes of galena or halite, building up (a) a cube modified by dodecahedron faces, (b) a dodecahedron, (c) an octahedron.

trigonal calcite

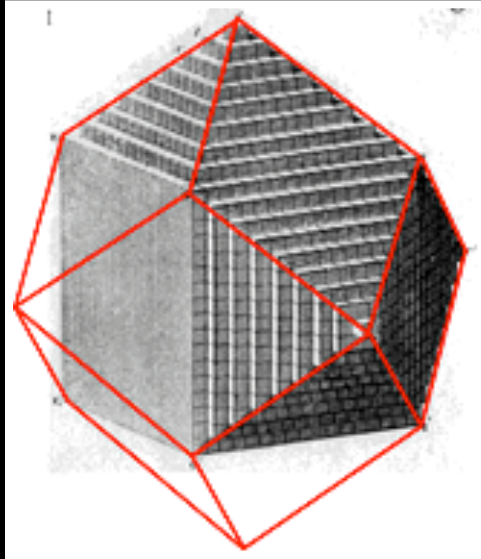
cleavage rhombohedron unit cell

cubic halite

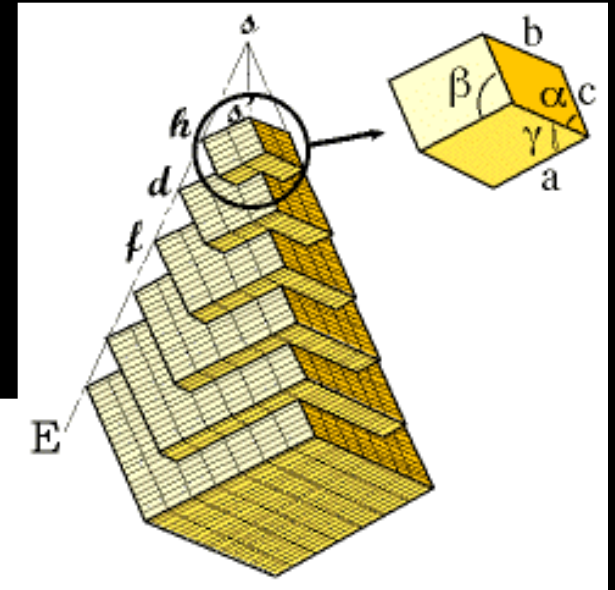
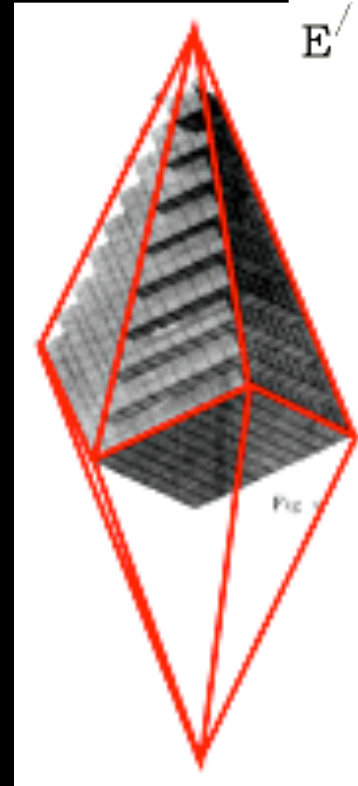
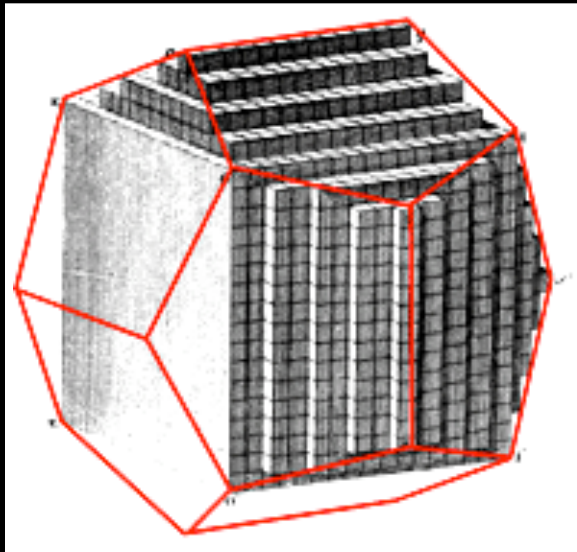
cleavage cube unit cell

Three of Haüy's 1784 crystal structure models

rhombic
dodecahedron

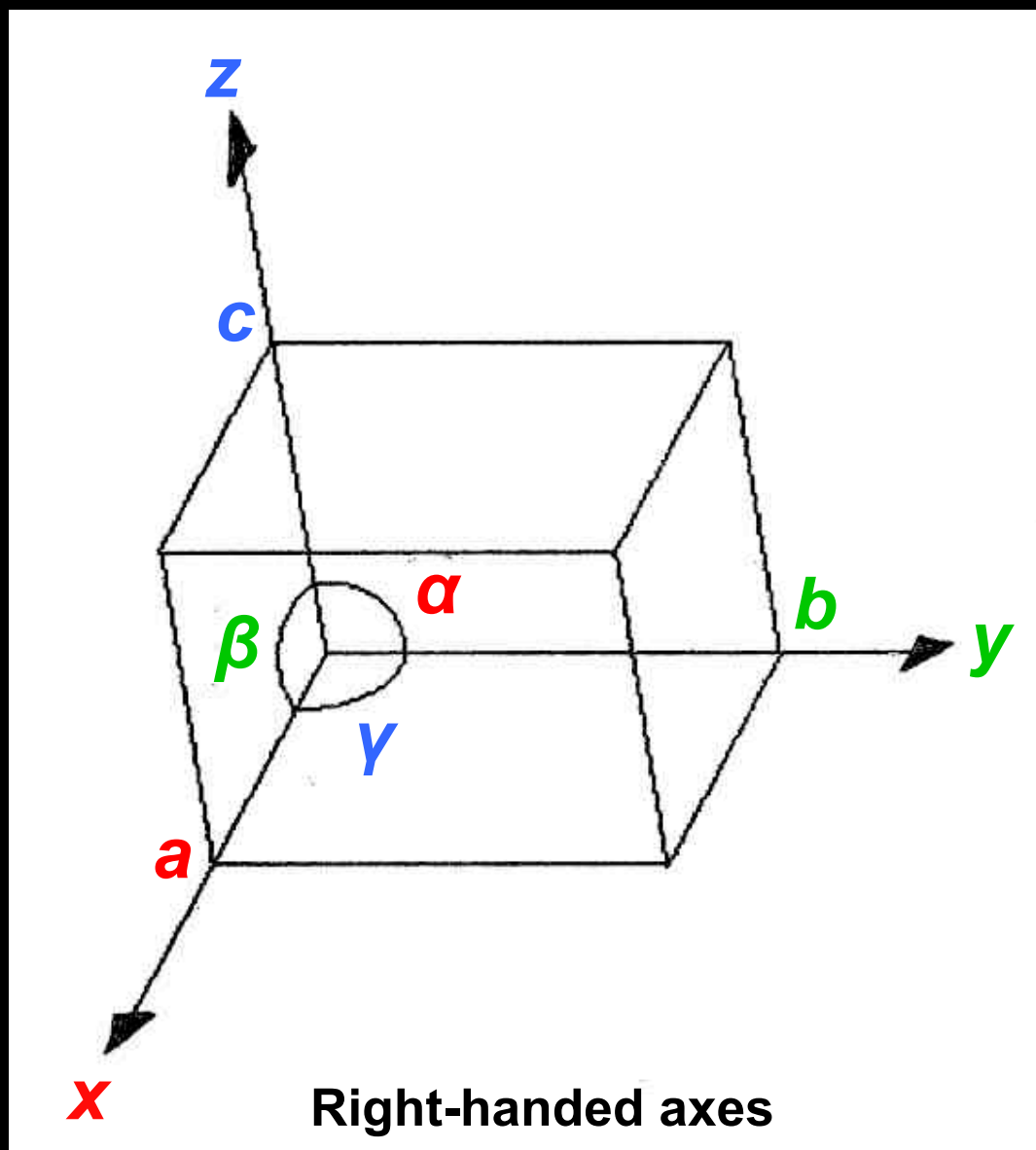


pentagonal
dodecahedron

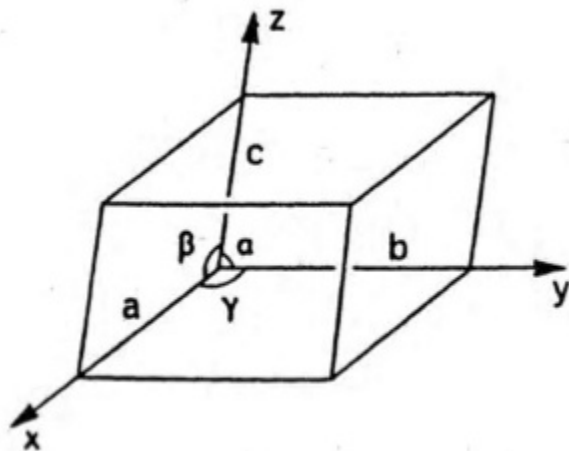


scalenohehedron

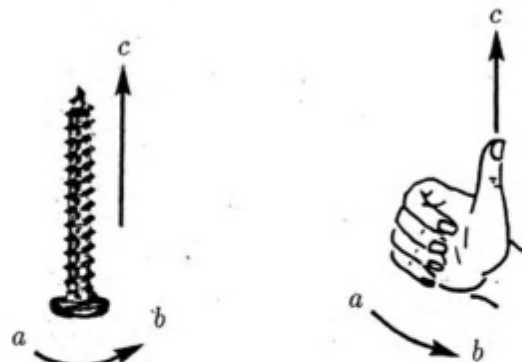
Crystallographic axes and unit cell dimensions



Crystallographic axes and lattice parameters



(a)



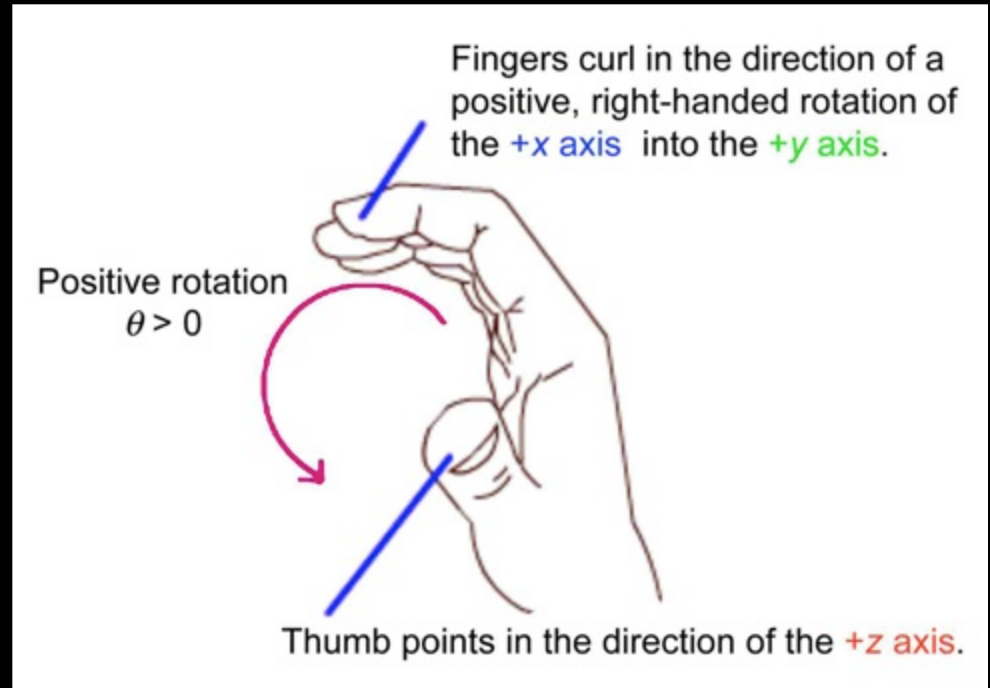
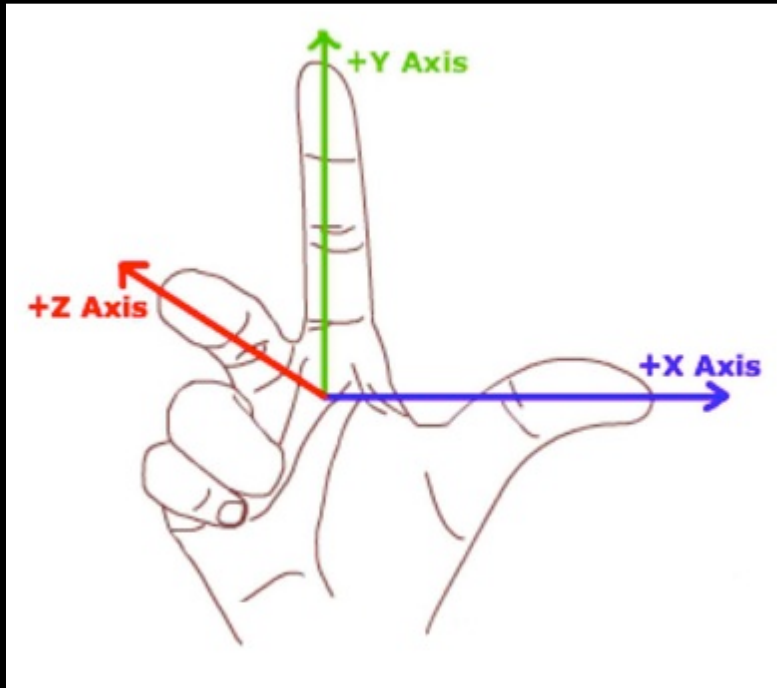
(b)

(c)

FIGURE 2.5. (a) A unit cell showing the axial lengths and interaxial angles. The directions of the axes are given in a right-handed axial system with a along the x direction and the angle γ between a and b . As a is moved to b , the screw (b) or thumb (c) proceeds in the c -direction, in a right-handed manner.

Jenny P. Glusker, with Mitchell Lewis and Miriam Rossi (1994).
Crystal Structure Analysis for Chemists and Biologists. New York: Wiley-VCH, Inc.

The Right-Hand Rule



Unit cell and crystal sizes

For a relatively large unit cell with dimensions

$$a \approx b \approx c \approx 100 \text{ \AA} = 100 \times 10^{-10} \text{ m},$$

the unit cell volume is

$$V_{\text{cell}} \approx 10^6 \text{ \AA}^3 = 10^{-24} \text{ m}^3.$$

And for a relatively small crystal with dimensions

$$\sim 100 \times 100 \times 100 \text{ \mu m} = 0.1 \times 0.1 \times 0.1 \text{ mm},$$

the crystal volume is

$$v_{\text{xtal}} \approx 10^{-3} \text{ mm}^3 = 10^{-12} \text{ m}^3.$$

Thus,

$$\frac{v_{\text{xtal}}}{V_{\text{cell}}} \approx 10^{12},$$

so that, even in a small crystal with a large unit cell, there are on the order of a *trillion*, i.e., a *million millions* of unit cells, and some $(10^{12})^{1/3} = 10^4$ or *ten thousand* unit cells along each crystal edge!

Solvent volume fraction and Matthews coefficient in protein crystals

$$f_{\text{solv}} = \frac{V_{\text{solv}}}{V_{\text{cell}}} = 1 - \frac{V_{\text{prot}}}{V_{\text{cell}}} = 1 - \frac{Z M_r m_u \bar{v}_{\text{prot}}}{10^{-24} V_{\text{cell}}} = 1 - 1.23 \frac{Z M_r}{V_{\text{cell}}}$$

V_{cell} unit cell volume (\AA^3),

M_r molar mass (Da) of protein in the asymmetric crystal chemical unit,

Z number of asymmetric crystal chemical units per unit cell,

m_u atomic mass constant, $m_u = m(^{12}\text{C})/12 = 1.66 \times 10^{-24} \text{ g Da}^{-1}$, and

\bar{v}_{prot} partial specific volume of the protein, which is assumed to be the same from one protein to the next, and the same in hydrated crystals as in aqueous solution.

$$\bar{v}_{\text{prot}} = \frac{1}{M_r} \left(\frac{\partial V}{\partial n_{\text{prot}}} \right)_{P, T, n_{\text{solv}}} \approx 0.74 \text{ mm}^3 \text{ mg}^{-1}, \quad \frac{1}{\bar{v}_{\text{prot}}} \approx 1.35 \text{ mg mm}^{-3}$$

The quantity $V_M = V_{\text{cell}} / (Z M_r)$ is called the Matthews coefficient.

$$1.6 \text{ \AA}^3 \text{ Da}^{-1} < V_M < 4.9 \text{ \AA}^3 \text{ Da}^{-1}, \quad \langle V_M \rangle \approx 2.2 \text{ \AA}^3 \text{ Da}^{-1}$$

$$25\% < f_{\text{solv}} < 75\%, \quad \langle f_{\text{solv}} \rangle \approx 45\%$$

Matthews, B.W. (1968). Solvent Content of Protein Crystals. *J. Mol. Biol.* **33**, 491-497.

Kantardjeff, K., & Rupp, B. (2003). Matthews coefficient probabilities: Improved estimates for unit cell contents of protein, DNA, and protein-nucleic acid crystals. *Protein Science*, **12**, 1865-1871.

Bulk Solvent Correction

Protein crystals average ~50% by volume bulk solvent, much of it liquid-like water.

The protein and bulk solvent regions have

$$\langle \rho_{\text{prot}} \rangle \approx 0.43 \text{ e \AA}^{-3} \quad \text{and} \quad 0.33 \text{ e \AA}^{-3} < \langle \rho_{\text{solv}} \rangle < 0.41 \text{ e \AA}^{-3}$$

pure H₂O 4-M (NH₄)₂SO₄
~ half sat'd

The protein and solvent regions are Babinet-complimentary, opposite-phase scattering masks. Thus,

$$F_{\text{total}} = F_{\text{prot}} + F_{\text{solv}},$$

$$F_{\text{solv}} \approx -F_{\text{prot}} k_{\text{solv}} \exp\left(-2\pi^2 \frac{\langle u_{\text{solv}}^2 \rangle}{d_{hkl}^2}\right),$$

$$F_{\text{total}} \approx F_{\text{prot}} \left[1 - k_{\text{solv}} \exp\left(-2\pi^2 \frac{\langle u_{\text{solv}}^2 \rangle}{d_{hkl}^2}\right) \right] = F_{\text{prot}} \left\{ 1 - k_{\text{solv}} \exp\left[-B_{\text{solv}} \left(\frac{\sin \theta_{hkl}}{\lambda}\right)^2\right] \right\},$$

where

$$B = 8\pi^2 \langle u^2 \rangle.$$

Typical values for the bulk solvent parameters are

$$k_{\text{solv}} \approx \frac{\langle \rho_{\text{solv}} \rangle}{\langle \rho_{\text{prot}} \rangle} \quad 2.5 < \langle u_{\text{solv}}^2 \rangle < 5 \text{ \AA}^2$$

$$0.75 < k_{\text{solv}} < 0.95 \quad 200 < B_{\text{solv}} < 400 \text{ \AA}^2$$

The seven crystal systems and fourteen Bravais lattices



Auguste Bravais
1811-1863

Nom du Système	simple	corps centré	2 faces centrées	faces centrées
triclinique $a \neq b \neq c$ $\alpha \neq \beta \neq \gamma \neq 90^\circ$				
monoclinique $a \neq b \neq c$ $\alpha = \gamma = 90^\circ \neq \beta$				
orthorhombique $a \neq b \neq c$ $\alpha = \beta = \gamma = 90^\circ$				
rhomboédrique $a = b = c$ $\alpha = \beta = \gamma \neq 90^\circ$				
quadratique $a = b \neq c$ $\alpha = \beta = \gamma = 90^\circ$				
hexagonal $a = b \neq c$ $\alpha = \beta = 120^\circ \neq \gamma = 90^\circ$				
cubique $a = b = c$ $\alpha = \beta = \gamma = 90^\circ$				

The Seven Crystal Systems

System	Defining Symmetry	Unit Cell Conditions
Triclinic	1-fold identity or inversion symmetry	none
Monoclinic	one 2-fold rotation or roto-inversion axis	$\alpha = \gamma = 90^\circ$
Orthorhombic	three perpendicular 2-fold rotation or roto-inversion axes	$\alpha = \beta = \gamma = 90^\circ$
Tetragonal	one 4-fold rotation or roto-inversion axis	$a = b$ $\alpha = \beta = \gamma = 90^\circ$
Trigonal	one 3-fold rotation or roto-inversion axis	<i>H</i> : $a = b$ $\alpha = \beta = 90^\circ, \gamma = 120^\circ$ <i>R</i> : $a = b = c$ $\alpha = \beta = \gamma < 90^\circ$
Hexagonal	one 6-fold rotation or roto-inversion axis	$a = b$ $\alpha = \beta = 90^\circ, \gamma = 120^\circ$
Cubic	four intersecting 3-fold axes	$a = b = c$ $\alpha = \beta = \gamma = 90^\circ$

Roto - inversion axes

$$\bar{1} \equiv i$$

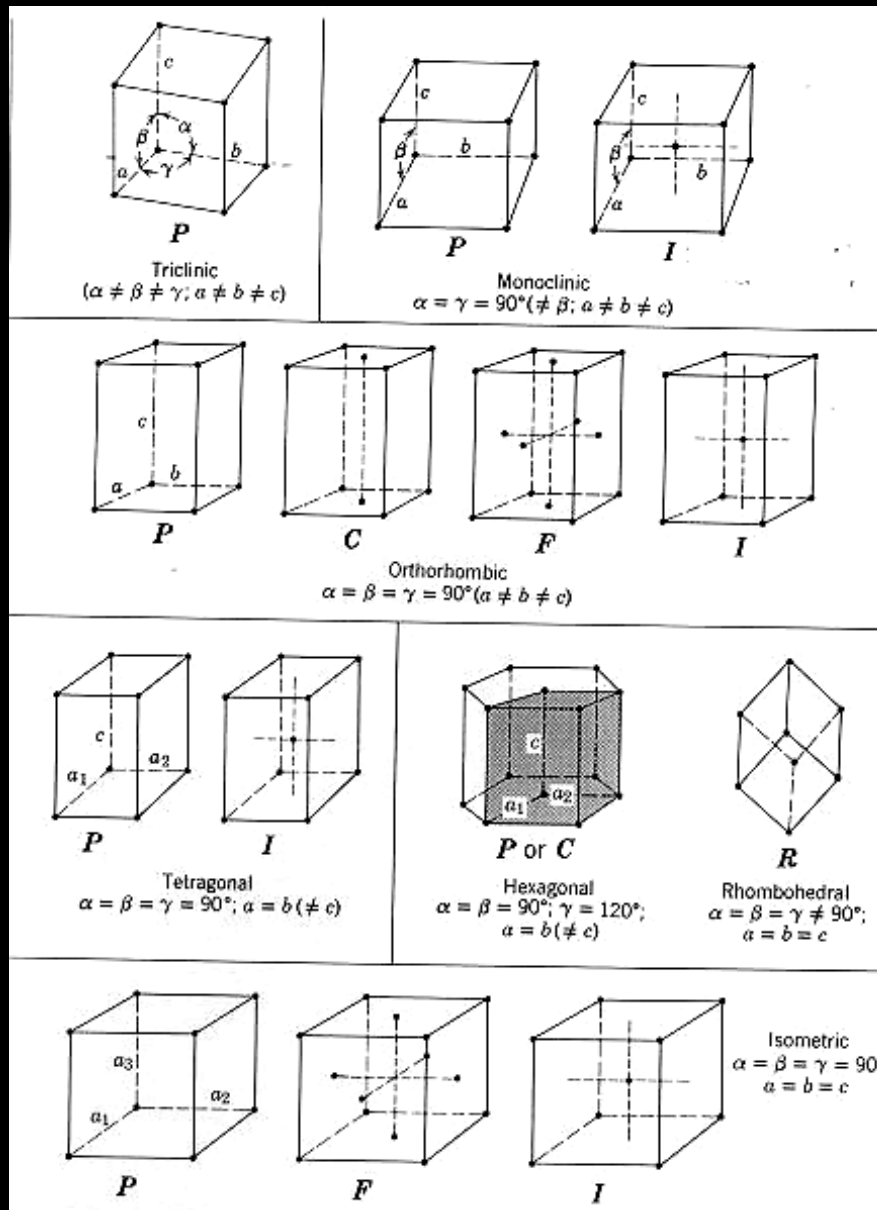
$$\bar{2} \equiv m$$

$$\bar{3} \equiv 3 + i$$

$$\bar{4}$$

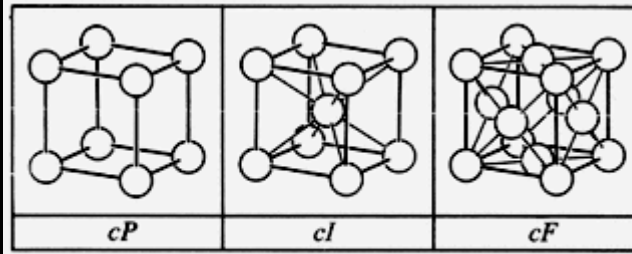
$$\bar{6} \equiv 3 / m$$

The 14 Bravais lattices

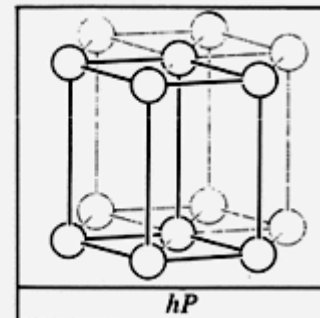


The 14 Bravais lattices

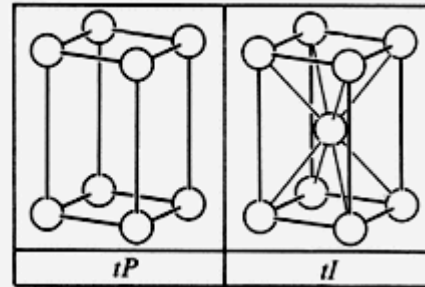
cubic



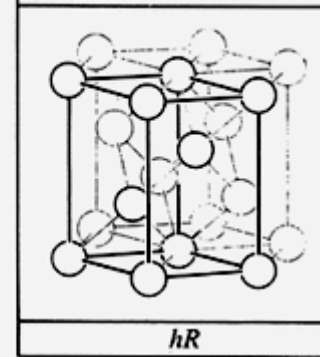
trigonal



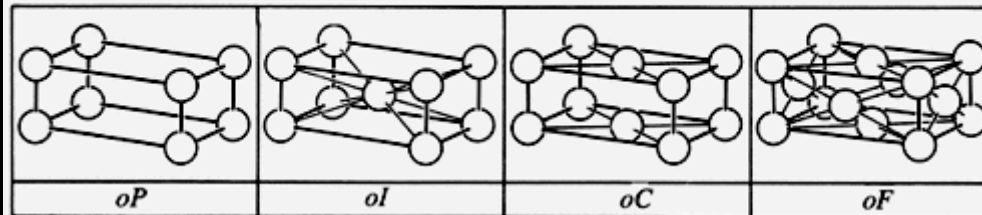
tetragonal



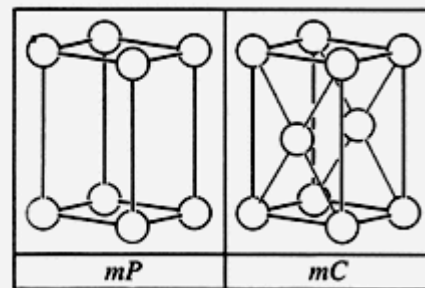
rhombohedral



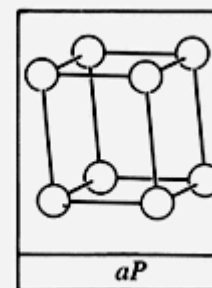
orthorhombic



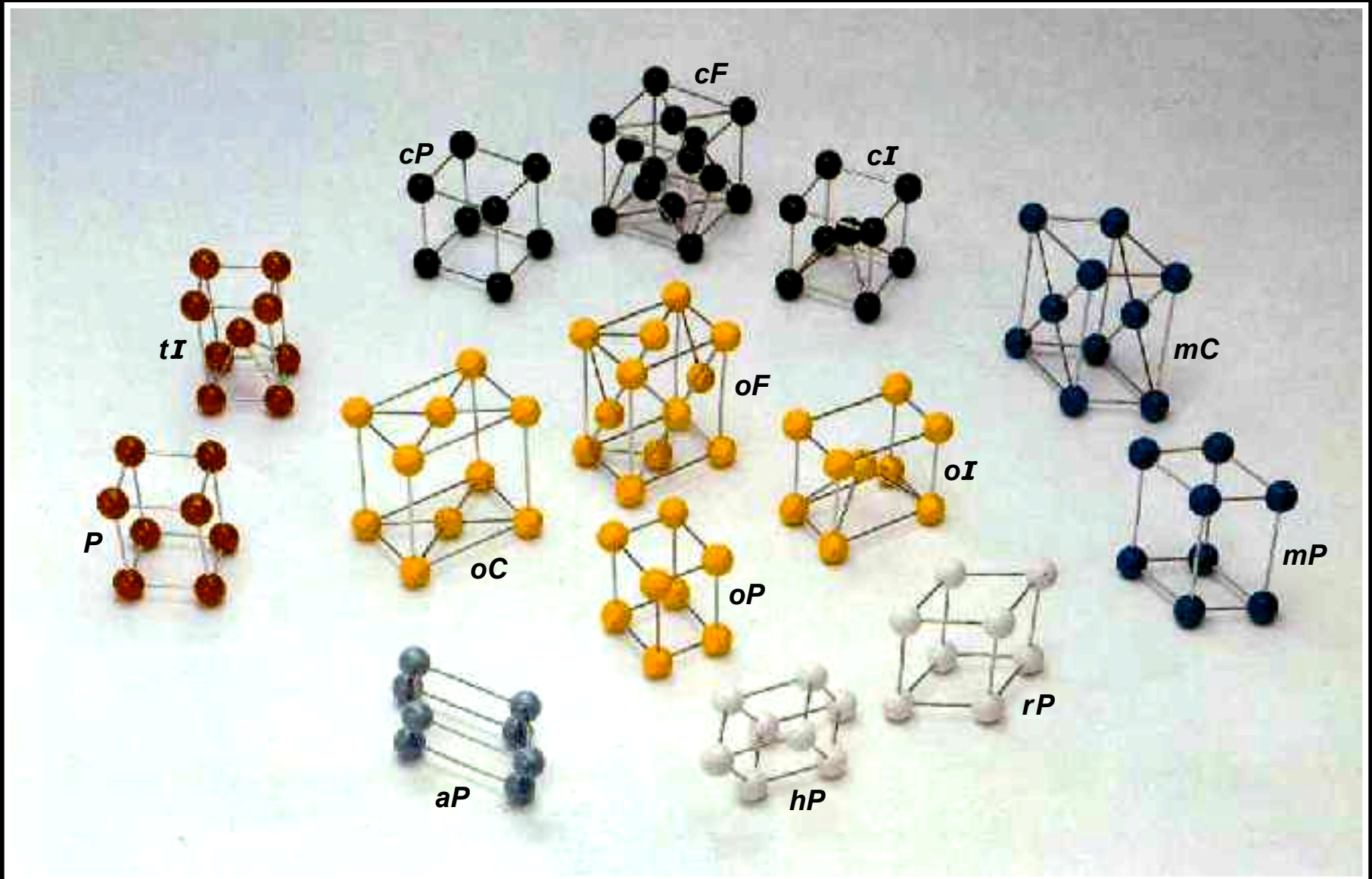
monoclinic



(anorthic)
triclinic



Models of the 14 Bravais lattices



Crystallographic Symmetries Hierarchy

7 crystal systems

14 Bravais lattices

{ **6 primitive**
8 centered

32 crystallographic point groups

{ **11 centrosymmetric - Laue groups**
{ **11 noncentrosymmetric, chiral**
10 noncentrosymmetric, polar

230 space groups

{ **93 centrosymmetric**
24 Patterson space groups
137 noncentrosymmetric
{ **65 chiral (enantiomorphic) space groups**
72 polar space groups

1-, 2-, and 3-D lattices

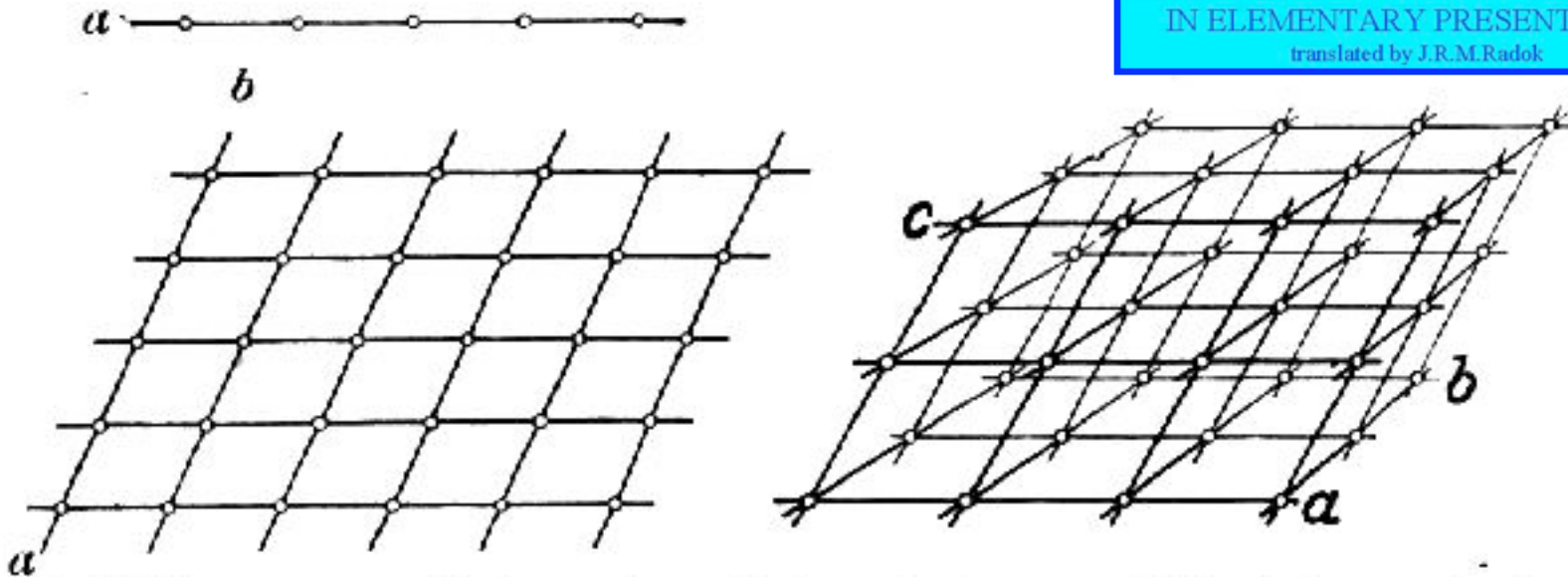


Fig. 154 Arrangement of points and translations a b c in a crystal; In a b the net-, in abc the lattice-arrangement. Points are indicated by circles, translations by lines.

Rainer Radok, 1.10.2001, radok81@bkk2.loxinfo.co.th
28/2 Mu 13 Nongnae 24120, Thailand
038-523492

http://en.wikipedia.org/wiki/Arnold_Berliner
www.austms.org.au/Gazette/2005/Mar05/radok.pdf

<http://kr.cs.ait.ac.th/~radok/physics/>
<http://kr.cs.ait.ac.th/~radok/physics/d2.htm#definite%20direction>

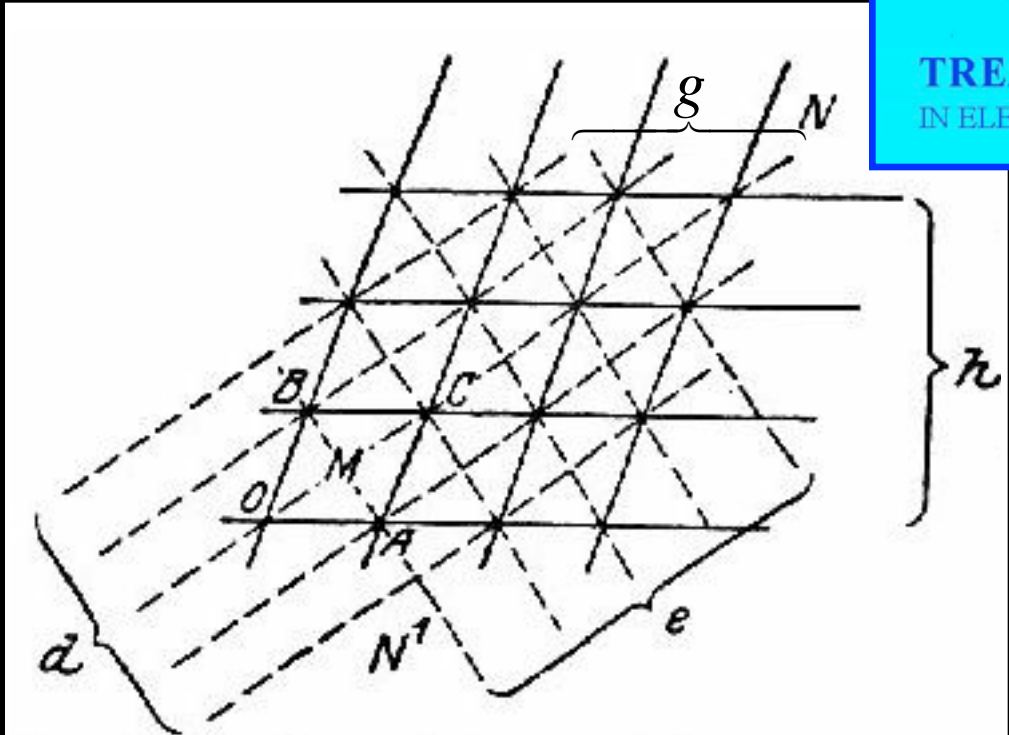
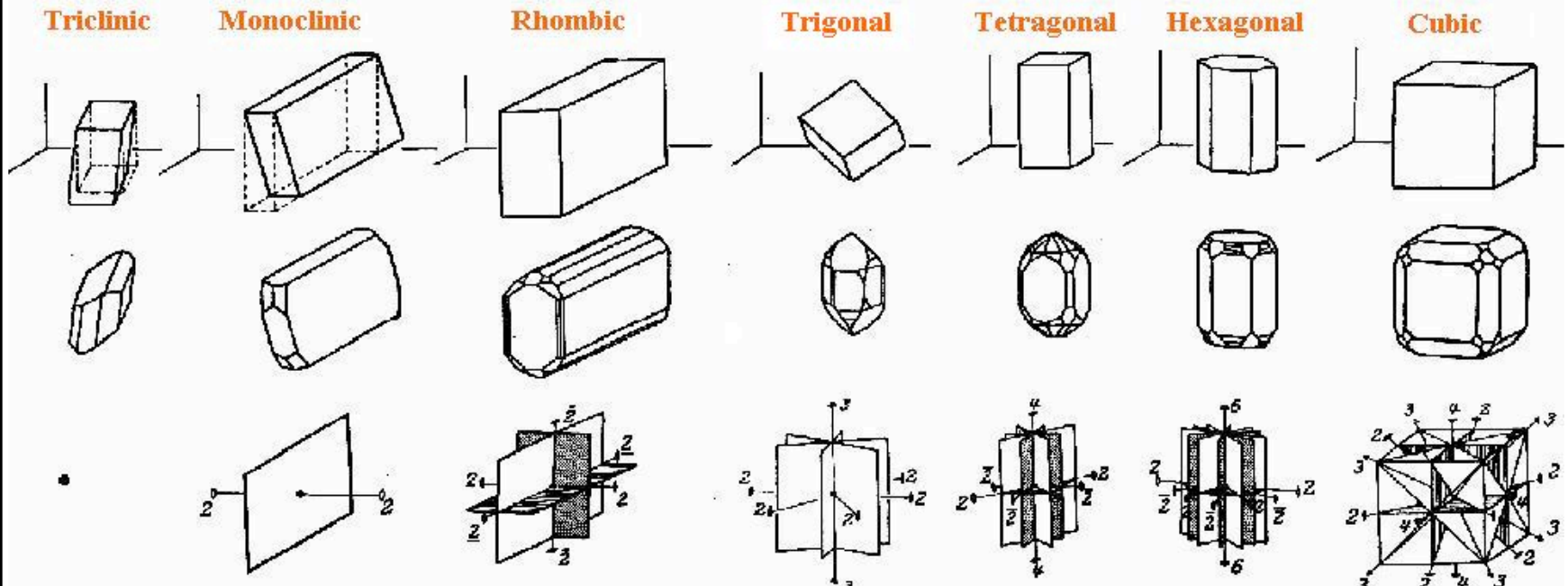


Fig. 155 Positions of the translation nets N and N' in the point net of a crystal

Fig. 156 Seven crystal systems and the elementary bodies of their translation lattices



The top row shows the simplest, crystal forms with the least faces which have the full symmetry of the respective crystal systems. The natural forms of the crystals derive from them by addition of other planes the positions of which arise in the simplest manner, for example, diagonal planes.

The second row shows corresponding forms of boundaries of natural crystals.

The third row shows the characteristic symmetry groups in symbolic representation:

the axes of rotation with the numbers 2, 3, 4 and 6 - those which are not equivalent and in pairs are distinguished by 2, 2 and 2;

the planes of reflection in the geometrically standard of a plane - different reflection planes are shaded for the sake of clearness;

the symmetry centre is indicated by a point •.

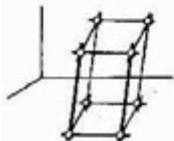
<http://kr.cs.ait.ac.th/~radok/physics/>



TREATISE OF PHYSICS
IN ELEMENTARY PRESENTATION
translated by J.R.M. Radok

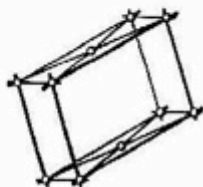
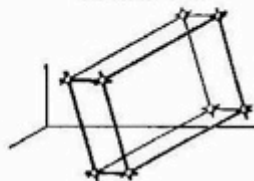
Fig. 156 continued: The elementary bodies of the point- and translation- lattice.

Triklin



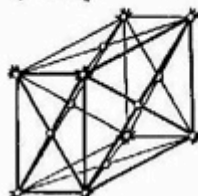
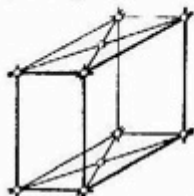
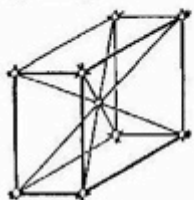
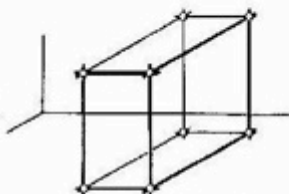
Three obliquely angled axes, One translation lattice, (Boric acid, copper sulfate)

Monoklin



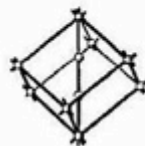
Two obliquely angled axes and one on the plane of which perpendicular all unequal, two translation lattices. (Iron sulfate, gypsum, mica, sugar of milk, sugar cane, sulphur, soda, acidity of wine.)

Rhombish



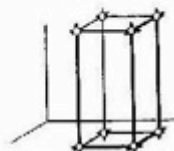
Three unequal, mutually perpendicular axes, 4 translation lattices. (Epsom salt, topaz, sulphur, iodine)

Trigonal



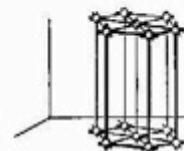
Three equal axes at equal angles, two translation lattices. The lattice derived from the second elementary body is identical to that derived from the hexagonal one. (Antimony, arsenic, ice, graphite, graphite, natron-saltpeter, quartz, bismuth, cinnabar)

Tetragonal



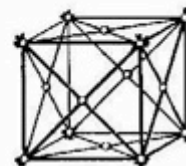
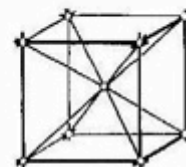
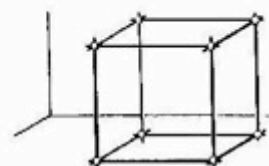
One principal axis and two secondary axes, perpendicular to it and to one another, two (Tin, zircon)

Hexagonal



One principal axis and three equal secondary axes, perpendicular to it angles of 60 degree to each other, one translation lattice (Beryl, zinc)

Cubic



Three mutually perpendicular equal axes, three translation lattices. (Alum, lead, diamond, iron, gold, copper, platinum, mercury, ammoniac, silver, rock-salt.)

The elementary bodies are the smallest and at the same time simplest (that is, have fewest faces) parallelepipeds of the point lattice, which have still the full symmetry of the crystal systems above. The directions of their edges are chosen as crystallographic axes. If repeated parallel in the three dimensions as in Fig. 154, every elementary body yields the corresponding translation lattice.

<http://kr.cs.ait.ac.th/~radok/physics/>

LEHRBUCH DER PHYSIK
 IN ELEMENTARER DARSTELLUNG
 VON
 ARNOLD BERLINER
 JULIUS SPRINGER  BERLIN 1935
TREATISE OF PHYSICS
 IN ELEMENTARY PRESENTATION
 translated by J.R.M. Radok

LEHRBUCH DER PHYSIK

IN ELEMENTARER DARSTELLUNG

VON

ARNOLD BERLINER

JULIUS SPRINGER



BERLIN 1935

TREATISE OF PHYSICS

IN ELEMENTARY PRESENTATION

translated by J.R.M.Radok

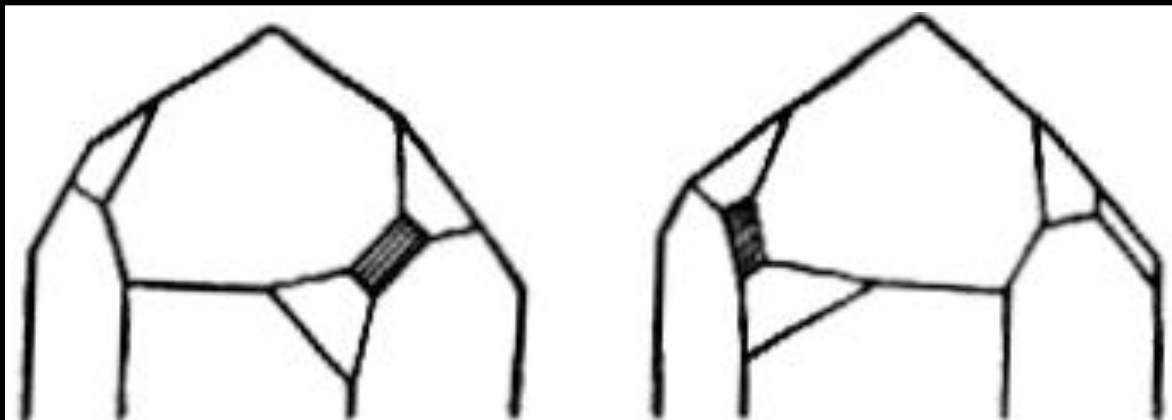
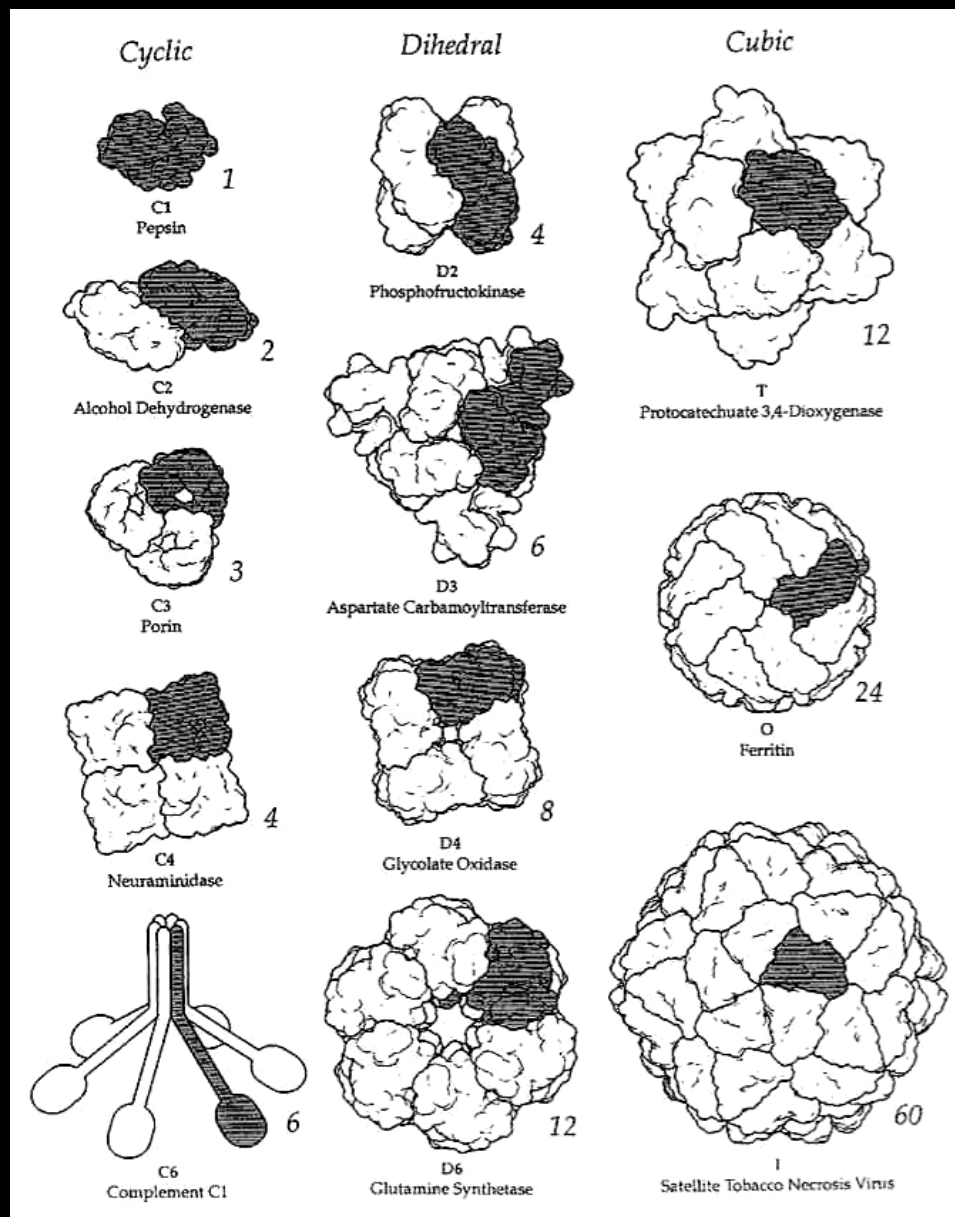


Fig. 152 Enantiomorphous crystals
(ἐν-αντιος = opposite)

Crystallographic point groups of protein homooligomers



Crystal habit is variable,
depending on crystal growth conditions,
but interfacial angles are constant.

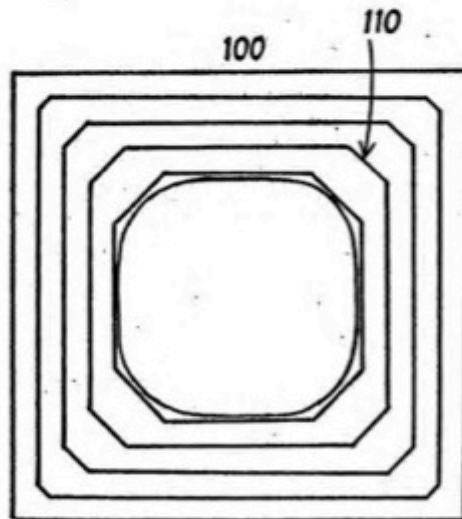


FIG. 8. A rounded crystal of sodium chlorate, on being put into super-saturated solution, develops 110 and 100 faces. The more rapidly growing 110 faces are subsequently eliminated.

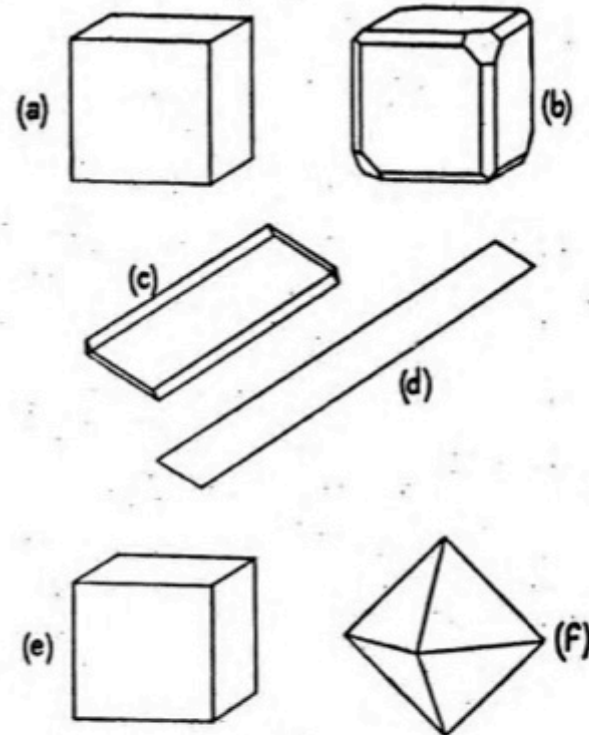


FIG. 3. Variation of crystal shape with conditions of growth. Sodium chlorate, NaClO_3 , grown (a) rapidly and (b) slowly; gypsum, $\text{CaSO}_4 \cdot 2\text{H}_2\text{O}$, grown (c) slowly and (d) rapidly; sodium chloride, NaCl , grown (e) from pure solution and (f) from solution containing 10 per cent. of urea.

Fast growing faces “grow out of the crystal.”

Some symmetric cubic crystal habits

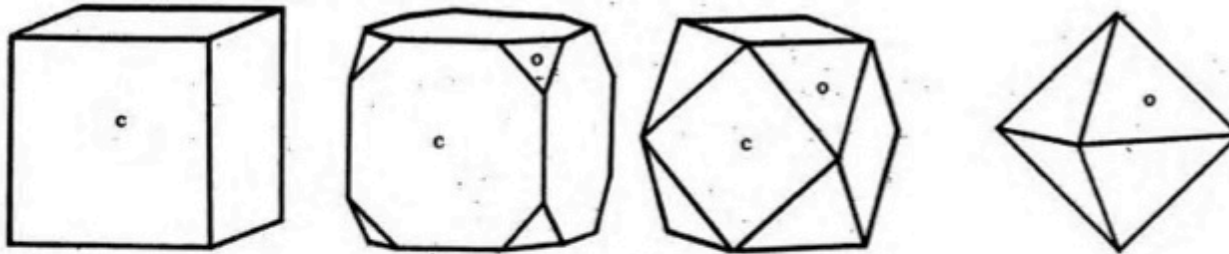


Figure 17: from cube to octahedron (cube face *c*, octahedron face *o*)

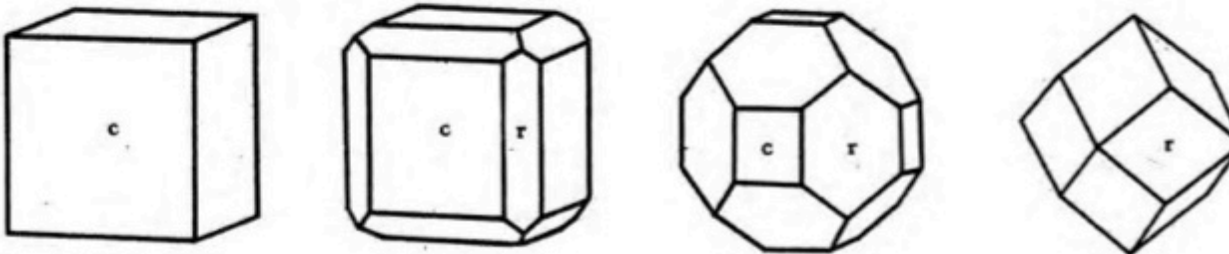


Figure 18: from cube to rhombic dodecahedron (faces *c* and *r* respectively)

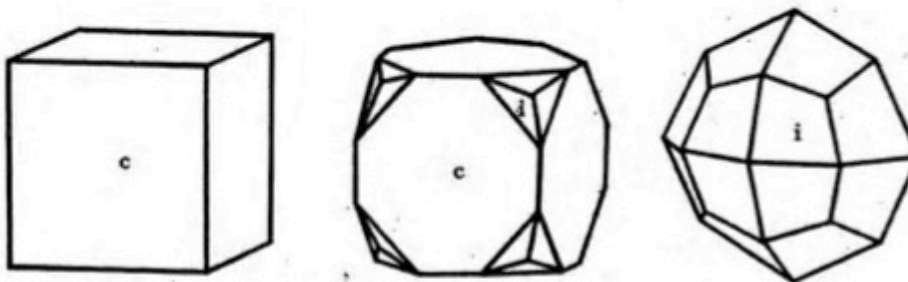


Figure 19: from cube to icositetrahedron (faces *c* and *i* respectively)

Some additional symmetric cubic crystal habits

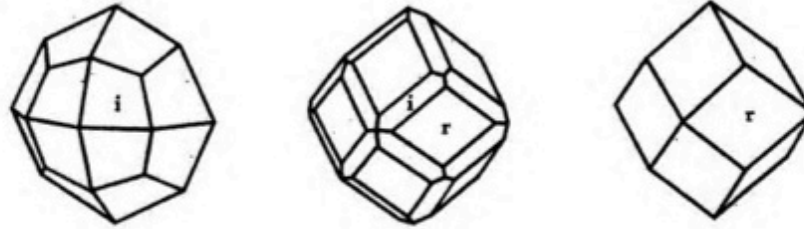


Figure 20: from icositetrahedron to rhombic dodecahedron (faces *i* and *r* respectively)

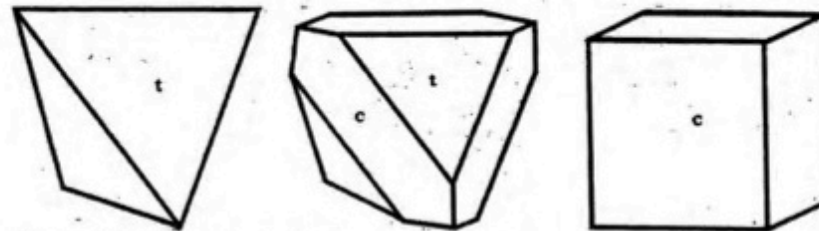


Figure 22: from tetrahedron to cube (faces *t* and *c* respectively)

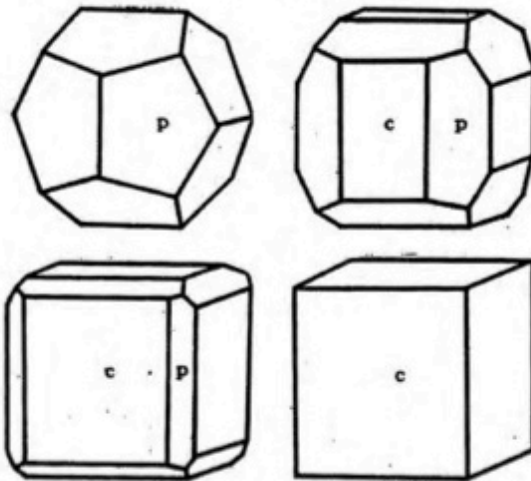


Figure 23: from pentagonal dodecahedron to cube (faces *p* and *c*)

Protein crystals are not perfect inside

Figure 3-11 Atomic force microscope images of crystal growth. (Panel A)

The atomic force microscope images of the 001 surface of glucose isomerase show the two most common growth patterns observed in crystal growth: step growth starting from 2-dimensional nucleation islands (A, left image) and a double-spiral growth pattern (A, right image). Panel B shows formation of supercritical 2-dimensional nuclei on the 001 surface of cytomegalovirus (CMV), a member of the herpes virus family. As indicated by the arrows, in this case only two virions (B, left image) suffice to generate a critical nucleus from which new step growth commences (B, right image). Images courtesy of Alexander McPherson and Aaron Greenwood, University of California, Irvine.

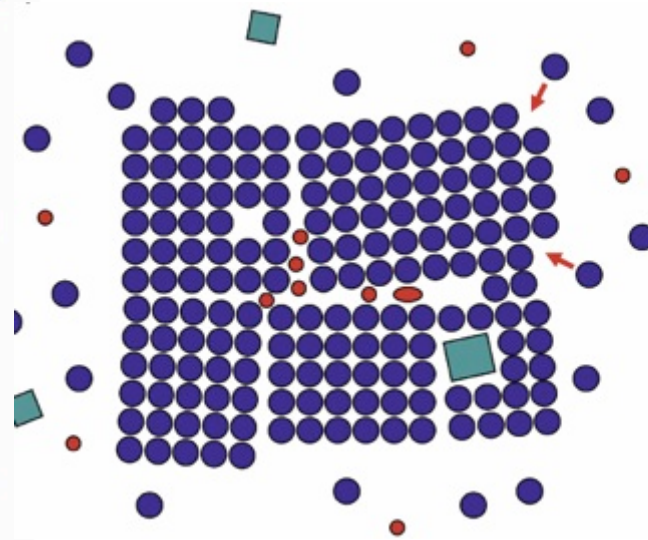
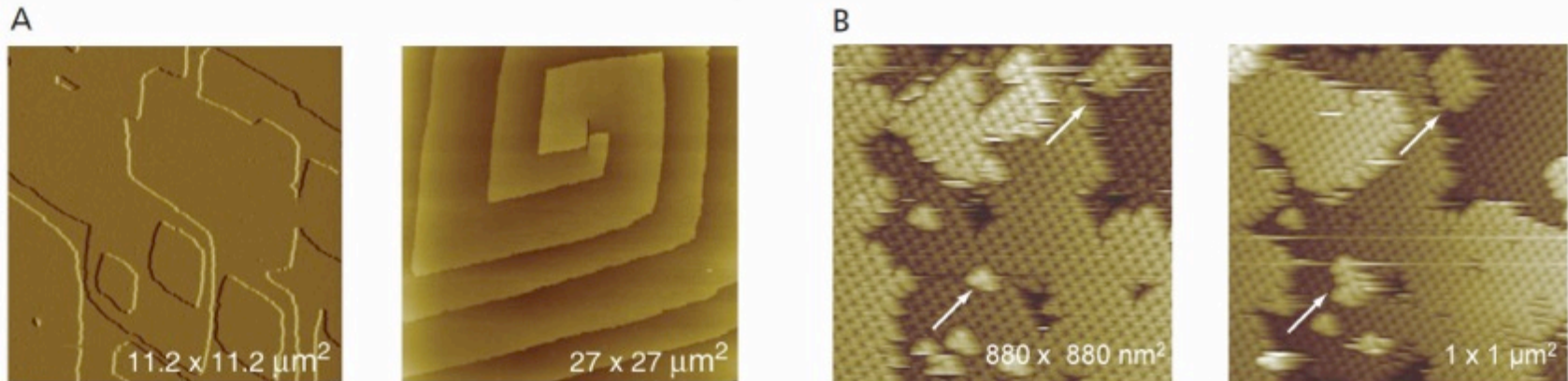


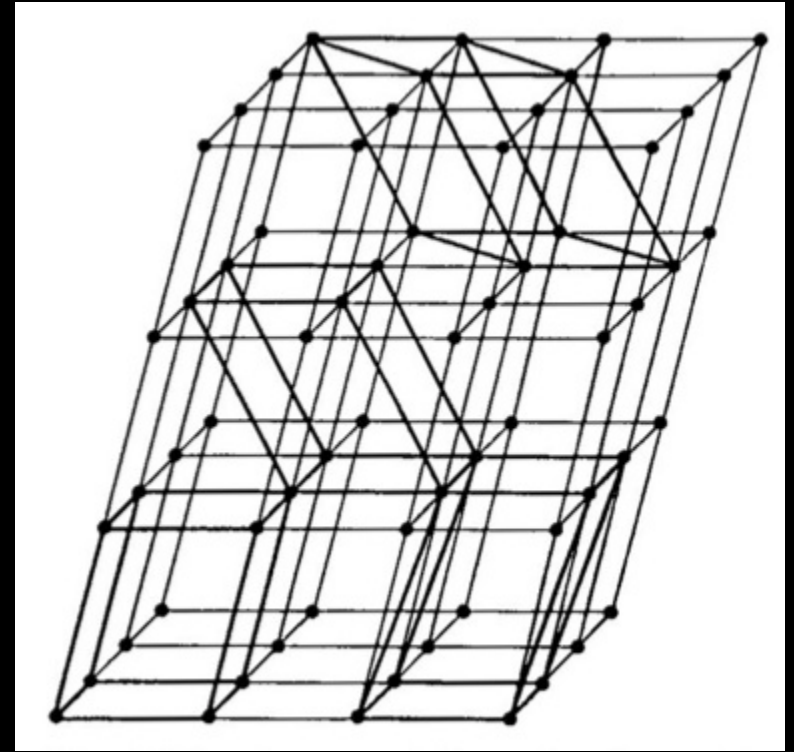
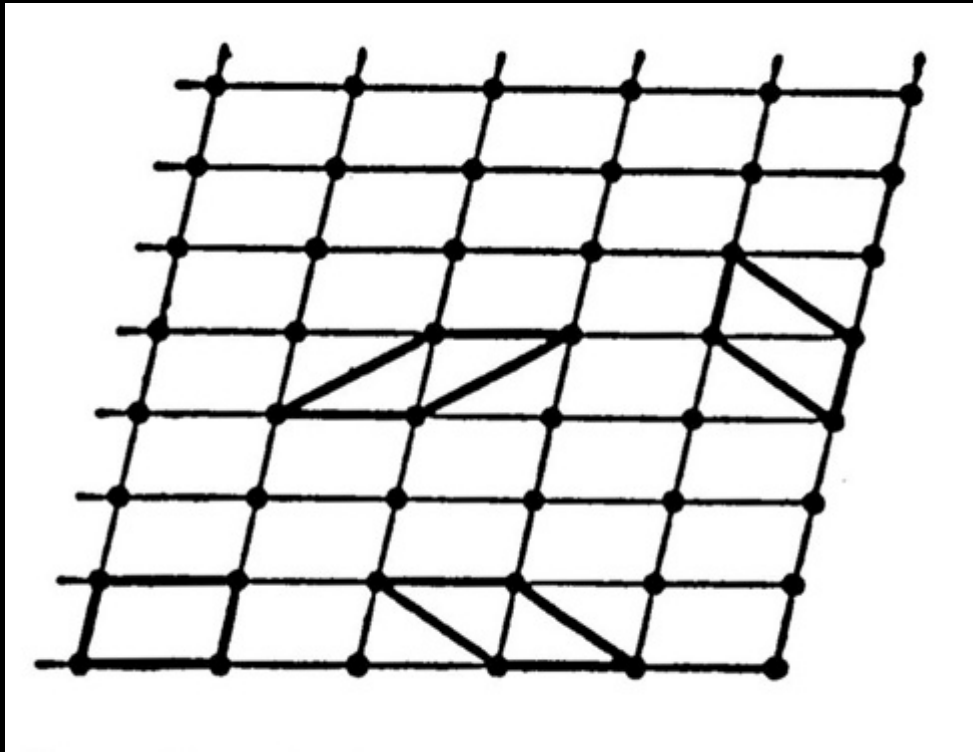
Figure 3-12 Growth of a real mosaic crystal. The schematic drawing shows a crystal growing in a solution of protein molecules (blue spheres). Small impurities (red) and some larger detritus (green squares) are also present in the solution. New molecules attach preferentially to steps and edges (red arrows) and we can recognize a growth defect in the form of a hole; impurities are enclosed at the domain boundaries; and a larger piece of detritus is incorporated at a domain boundary. Individual domains can be substantially misaligned, in this case about 6°; such a highly mosaic crystal would not be useful for diffraction experiments.

Phenomena of mosaicity and twinning complicate data collection

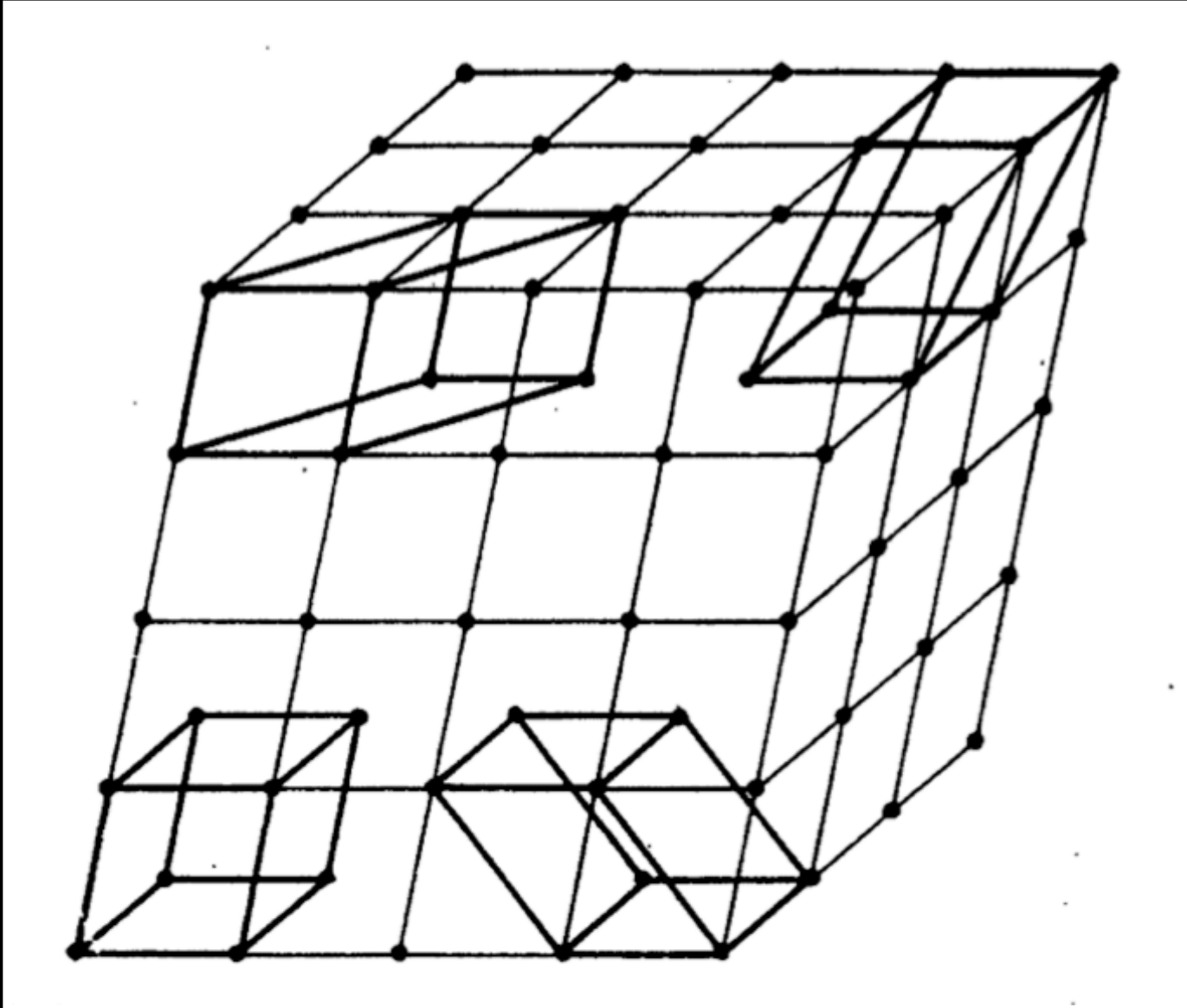


<http://escher.epfl.ch/eCrystallography/>

Alternative *primitive* unit cells for a given point lattice



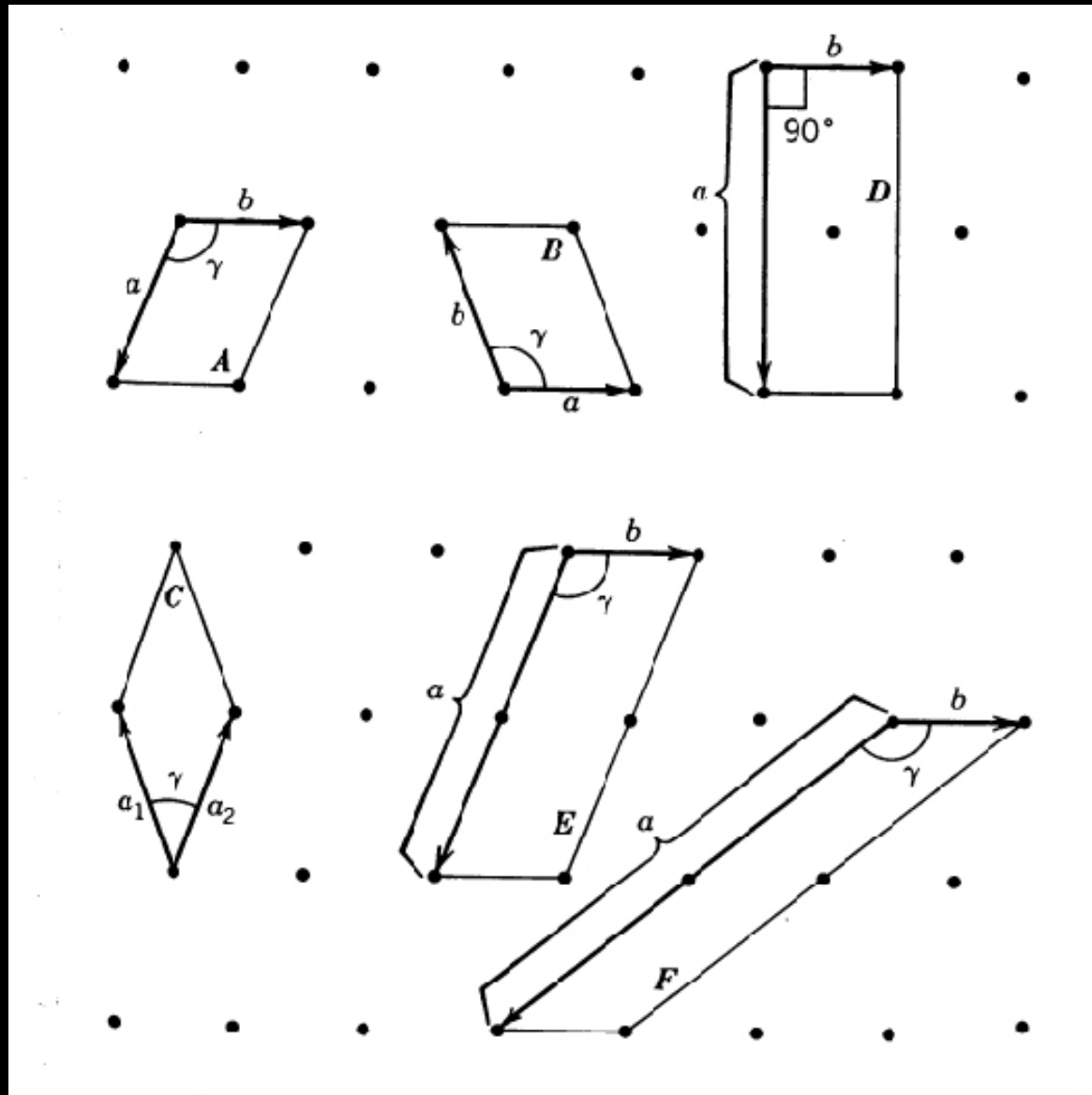
Alternative primitive unit cells in the same space lattice

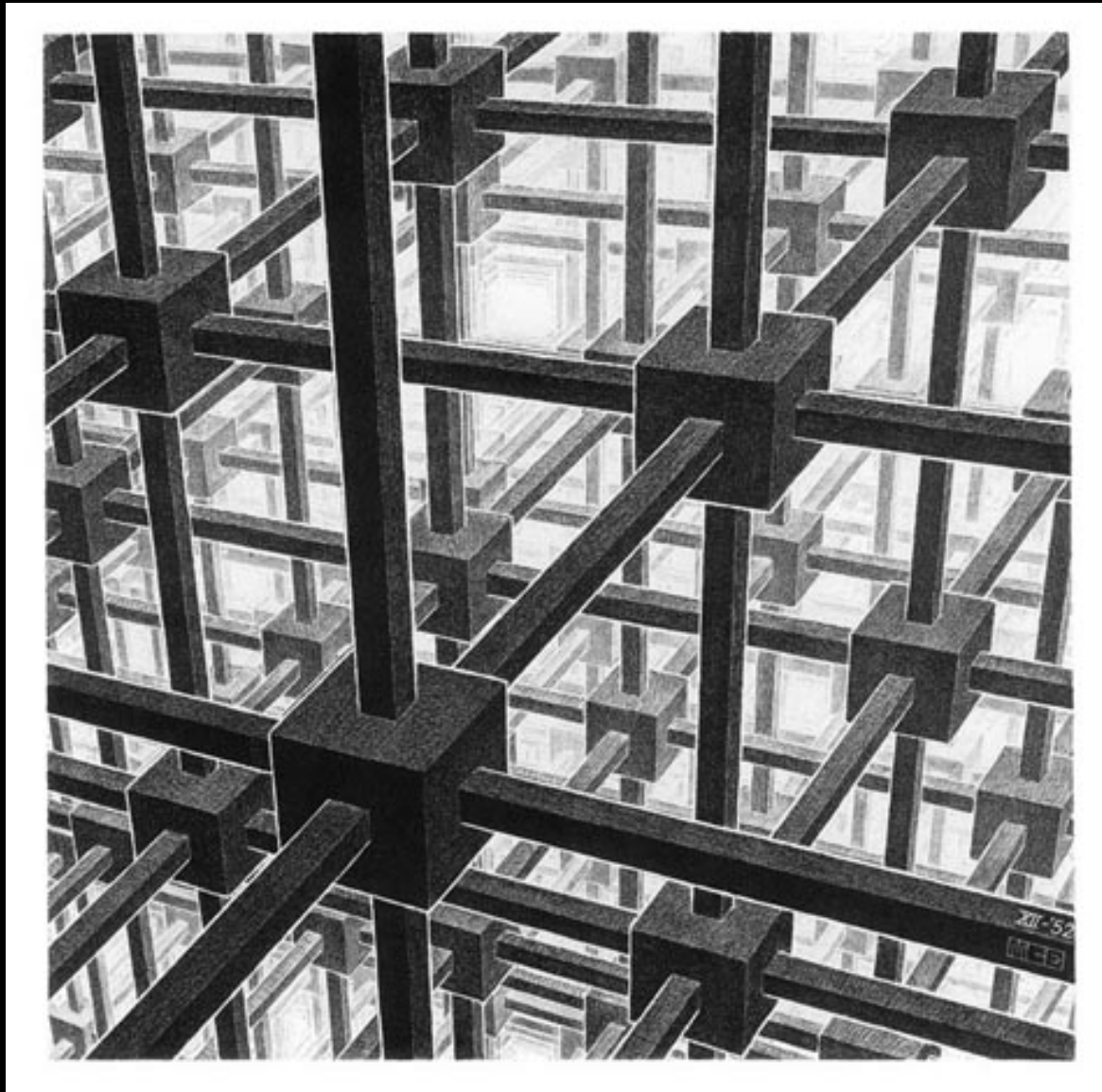


Henry S. Lipson (1970). *Crystals and X-Rays*. London: Wykeham Publications.

Alternative unit cells on a given plain lattice:

one face-centered (D), two side-centered (E,F), and three primitive cells (A,B,C)





<http://www.meta-library.net/cqmedia/esch-body.html>

Alternative primitive unit cells in the same space lattice

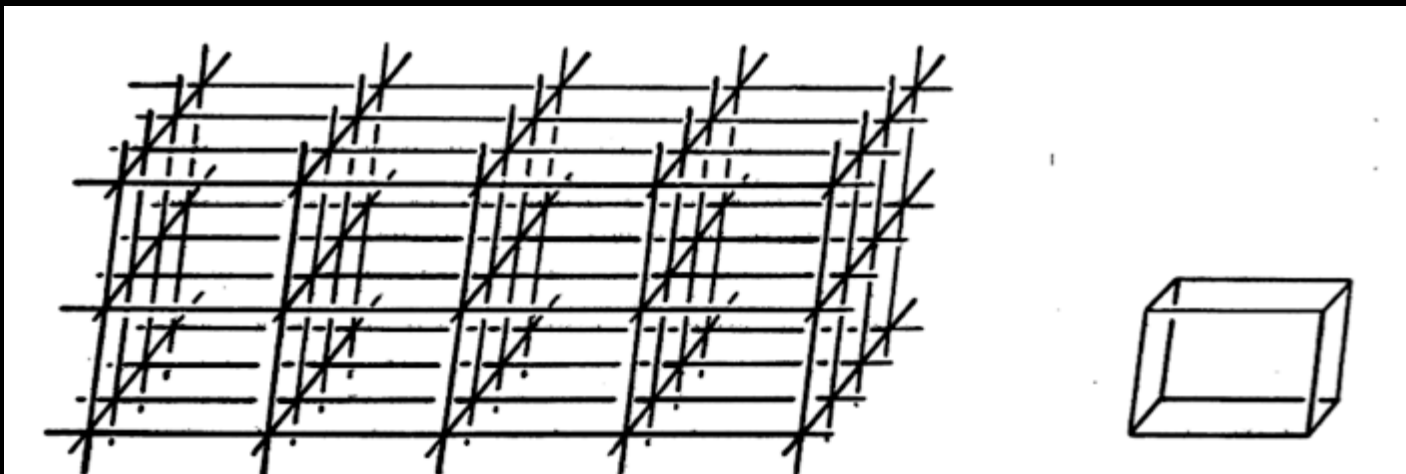


Fig. 2.8. Crystal lattice and one unit cell.

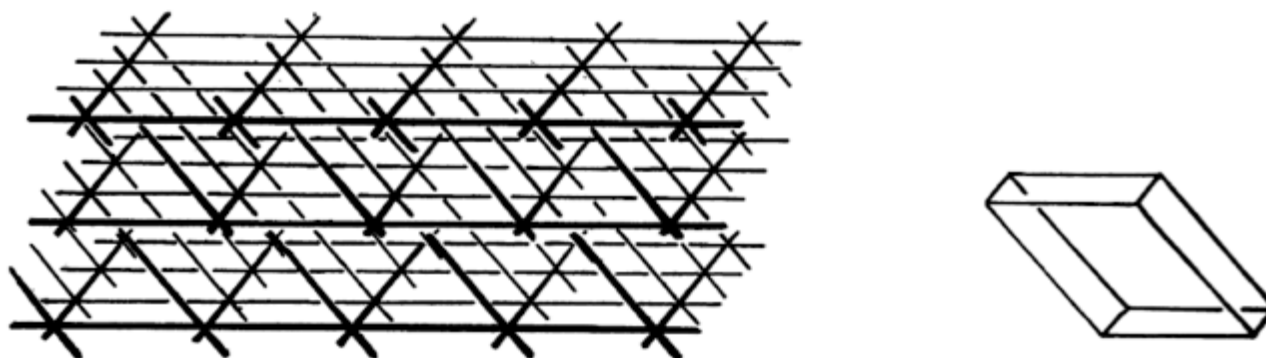
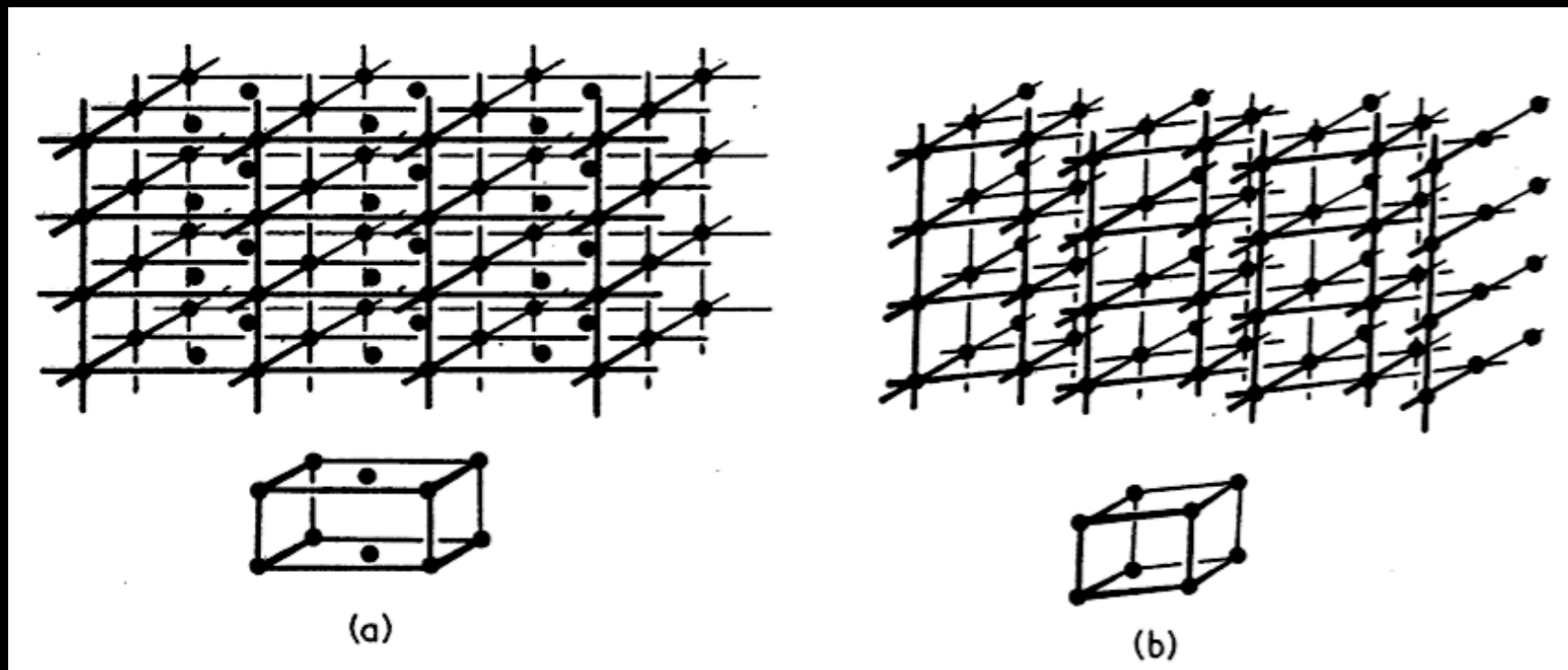


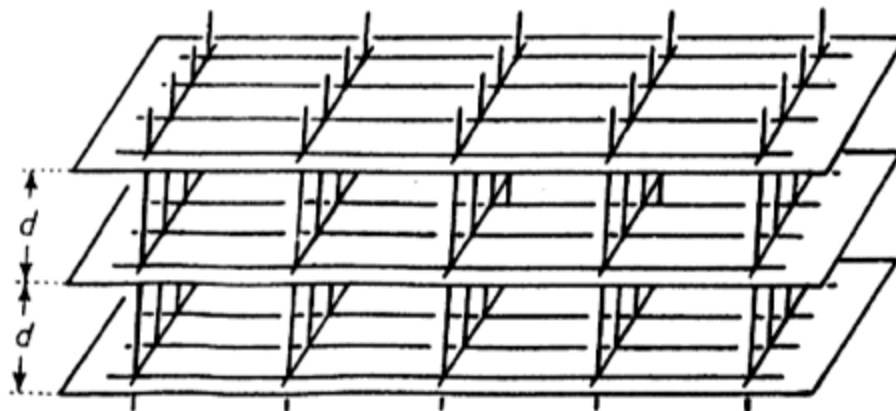
Fig. 2.9. Alternative lattice (and one unit cell) to that in Fig. 2.8.

Primitive and Centered Lattices and Unit Cells

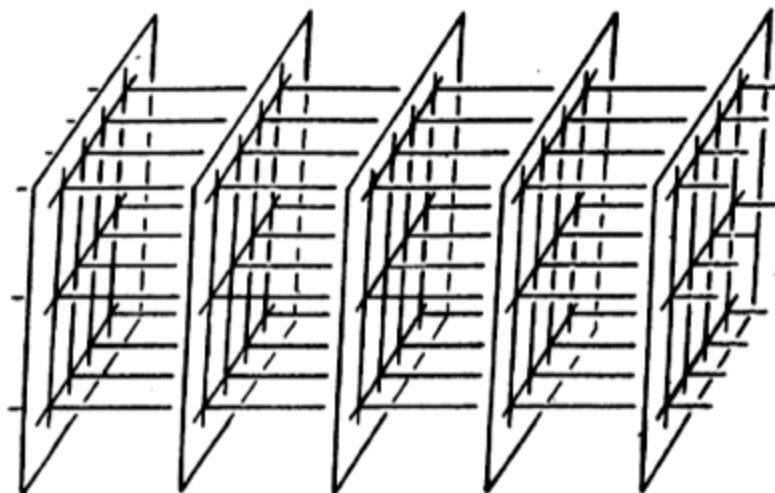
- (a) A centered lattice and unit cell have
- (b) an equivalent primitive lattice and unit cell



Two different families of lattice planes in the same lattice

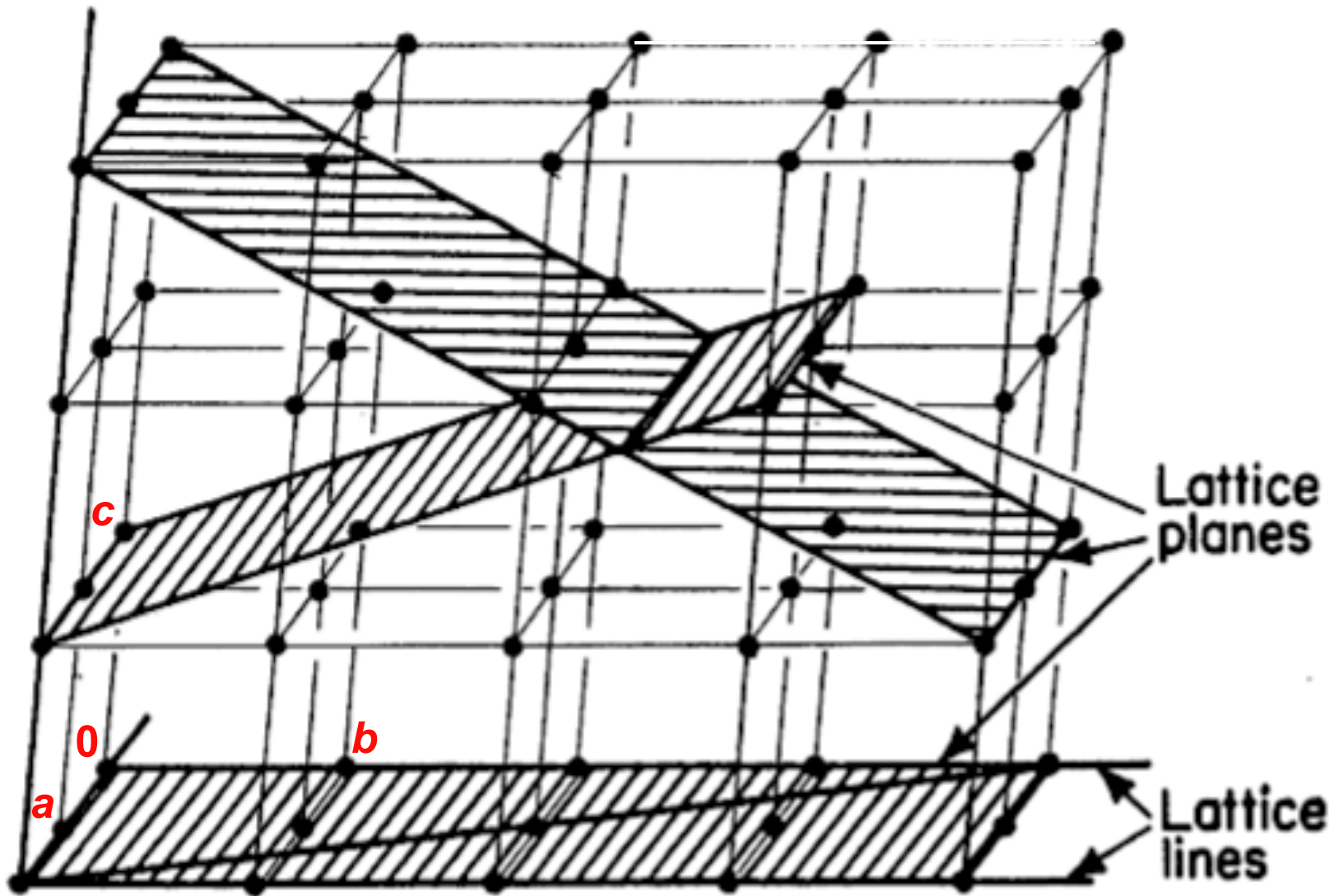


(a)



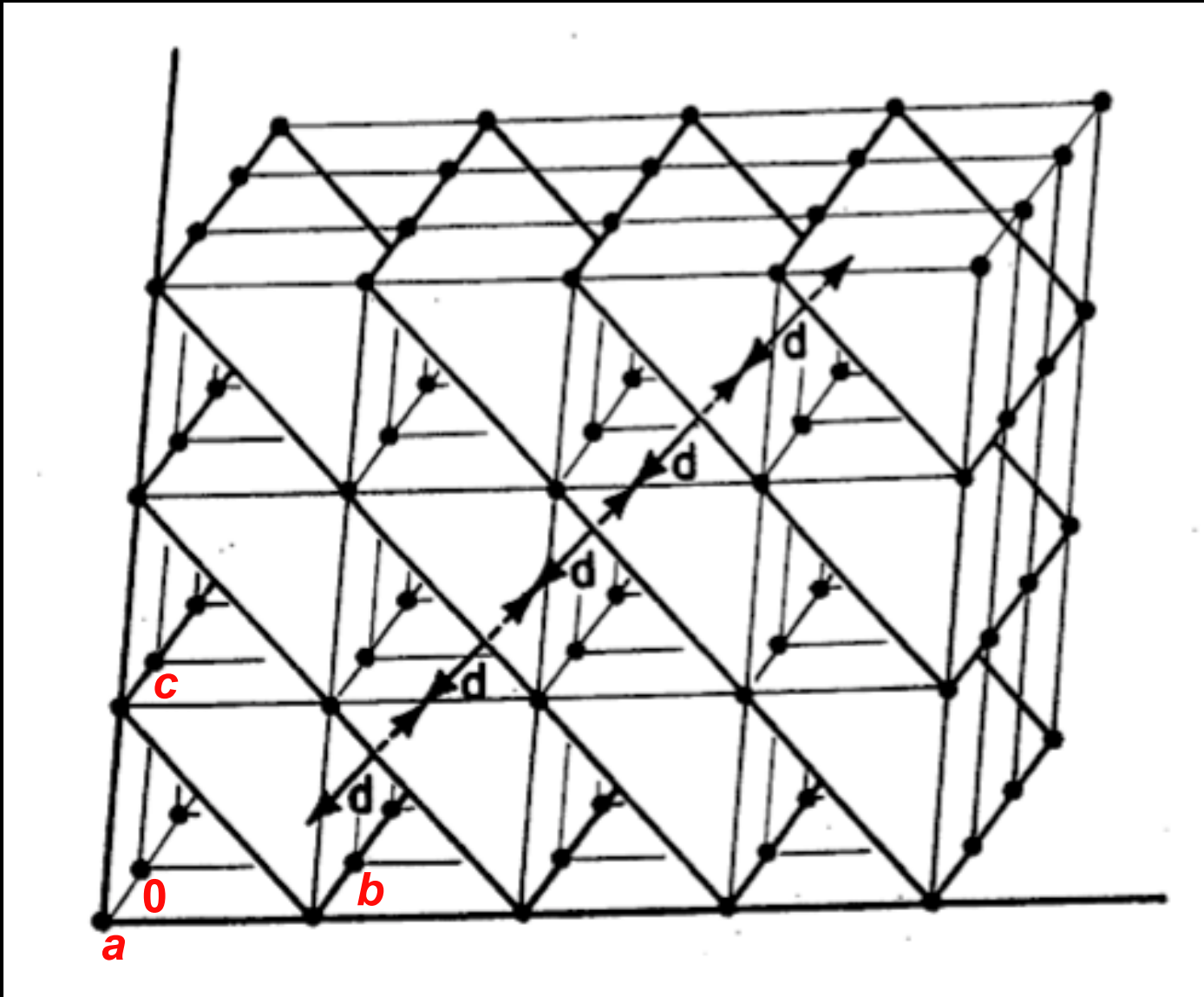
(b)

Lattice points, lattice rows, and lattice planes



Henry S. Lipson (1970). *Crystals and X-Rays*. London: Wykeham Publications.

Families of equidistant lattice planes pass through *all* the lattice points.



Every family of lattice planes passes through *all* the lattice points.

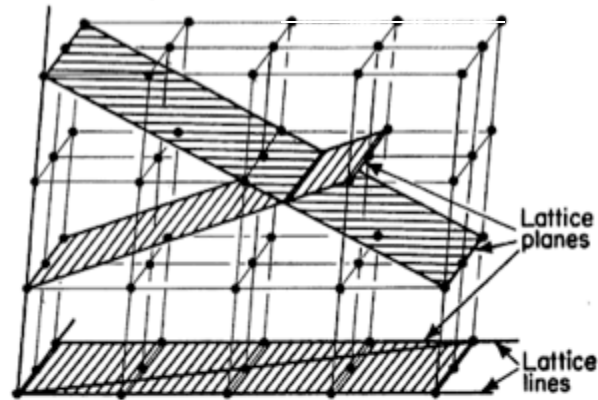
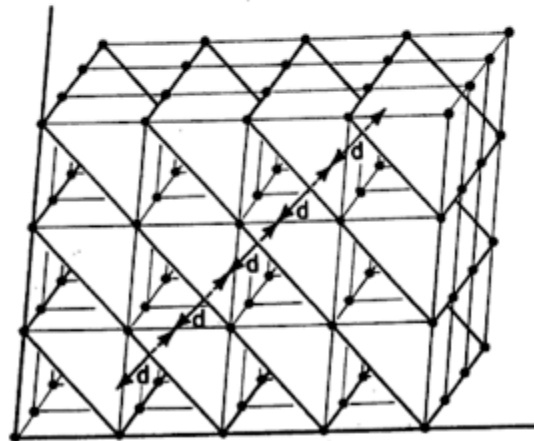
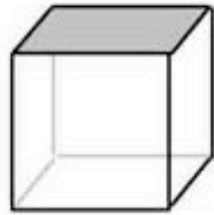


Fig. 3.7. Lattice lines or rows and lattice planes.

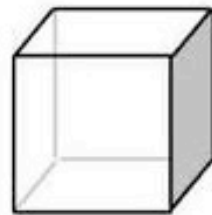


A set of equidistant planes passing through all the lattice points shown in fig. 3.7.

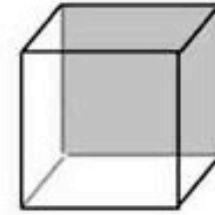
Some Cubic Lattice Planes



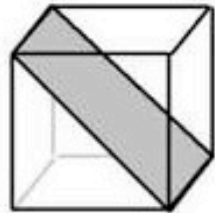
(001)



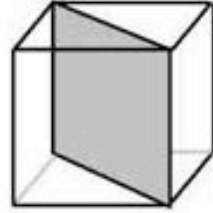
(100)



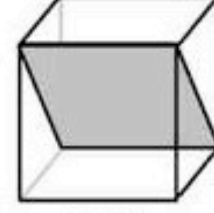
(010)



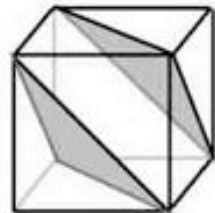
(101)



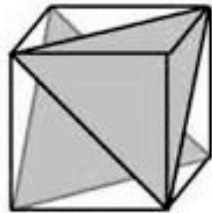
(110)



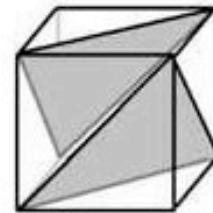
(011)



(111)



(1 $\bar{1}$ 1)



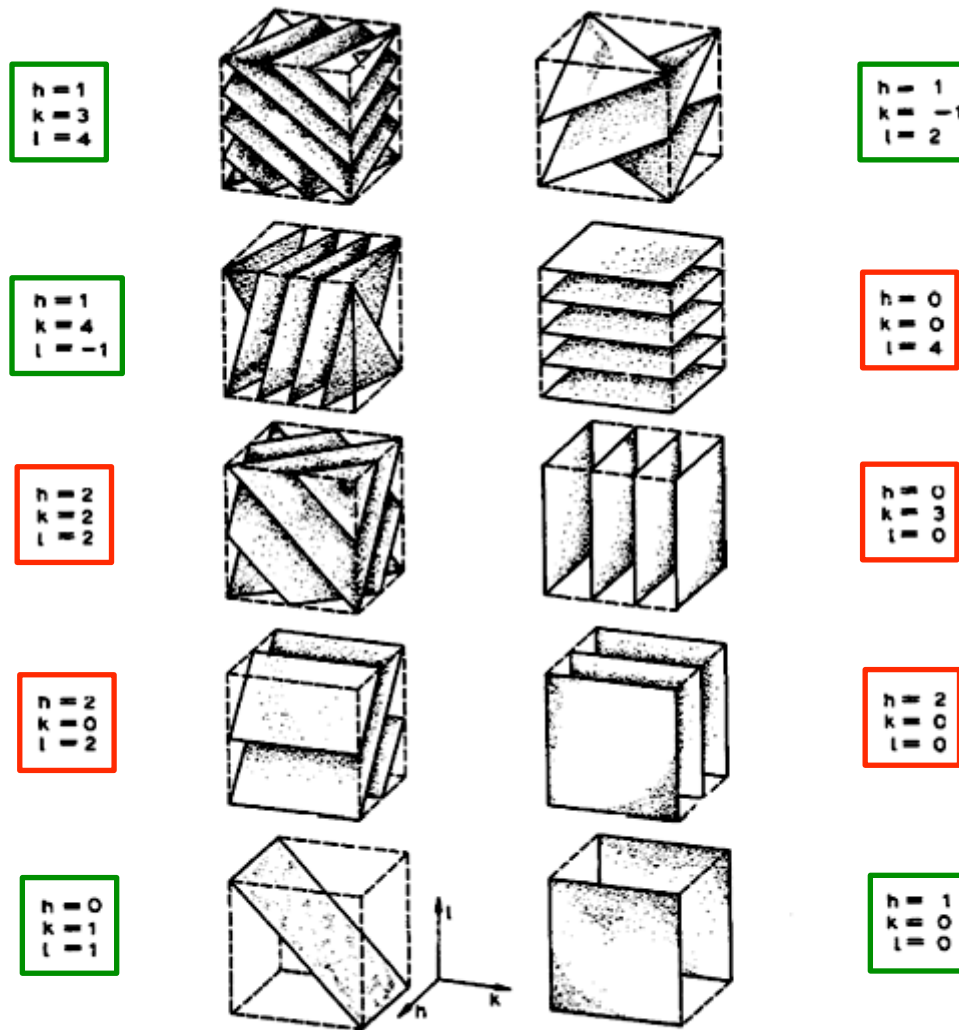
($\bar{1}$ 11)

Actual and Virtual Lattice Planes

660

1962 M.F.PERUTZ

co-prime indices have no common factor > 1



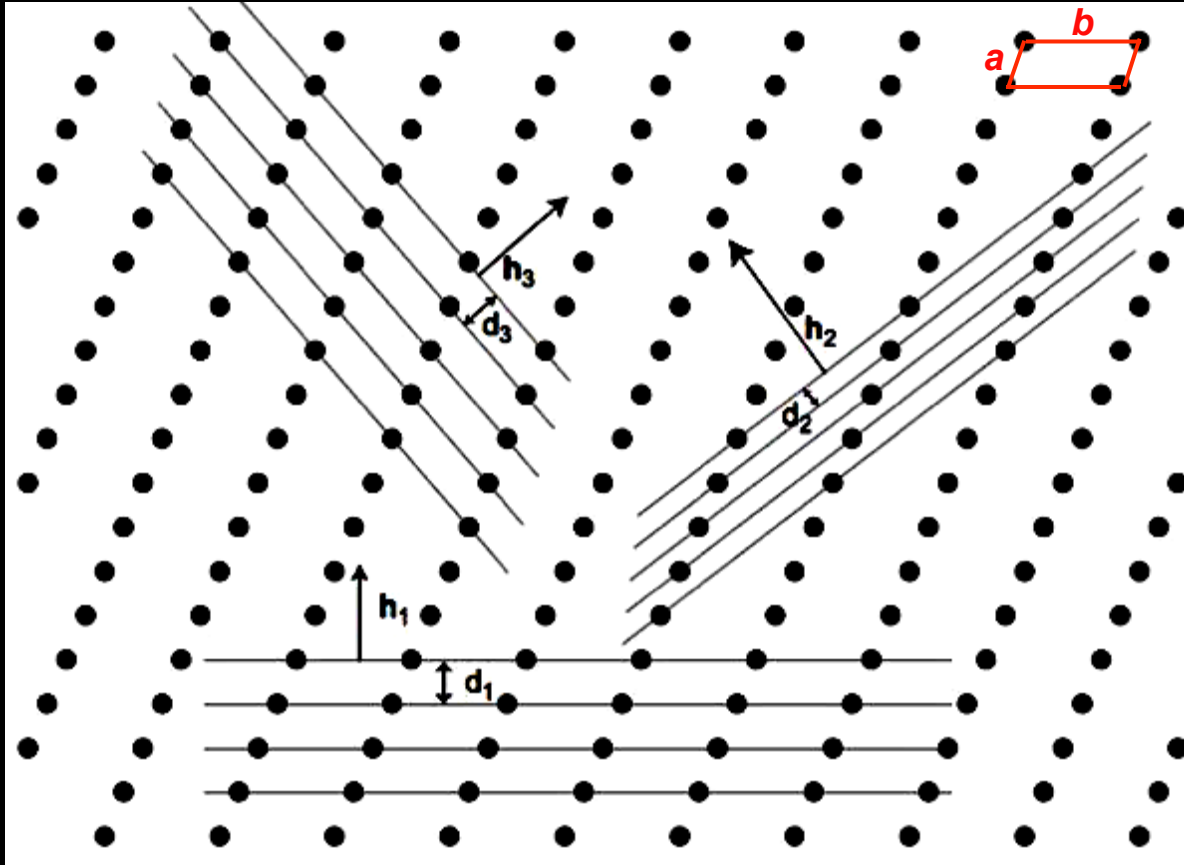
composite indices have a common factor > 1

Fig. 7. Set of three-dimensional fringes used to build up image of the electron density. (Reproduced, by permission, from W. de Beauclair, "Verfahren und Geräte zur mehrdimensionalen Fouriersynthese", Akademie-Verlag, Berlin, 1949.)

Max Perutz, Nobel Lecture (1962).

http://www.doitpoms.ac.uk/tlplib/miller_indices/lattice_index.php

Families of equally spaced lattice planes



$$h_1 \quad h_1 k_1 l_1 \quad 1 \ 0 \ 0$$

$$h_2 \quad h_2 k_2 l_2 \quad 1 \ 3 \ 0$$

$$h_3 \quad h_3 k_3 l_3 \quad -1 \ 2 \ 0$$

$$d_1 > d_3 > d_2$$

$$d_{100} > d_{-120} > d_{130}$$

The higher the indices, the smaller the interplanar spacing,
and the lower the reticular density.

Lattice Points, Lattice Lines, Lattice Planes, and Rational Indices

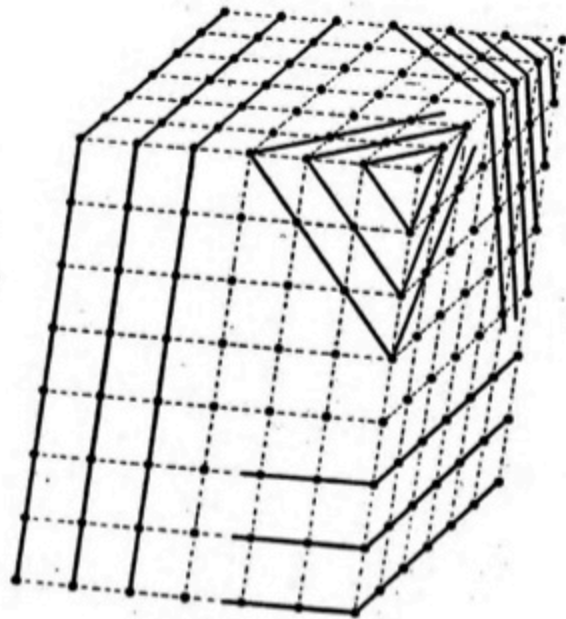


FIG. 7. Dividing a crystal into layers. A few of the simpler ways. (Each dot is a lattice point.)

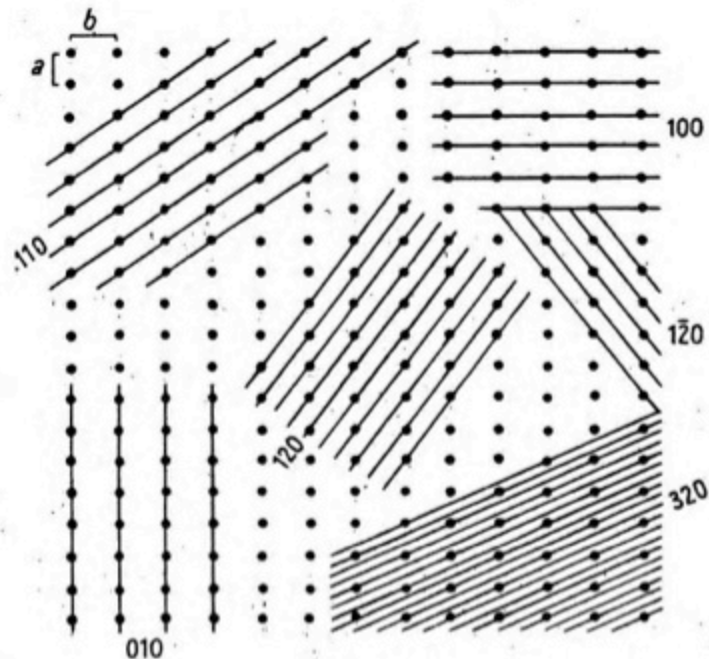


FIG. 9.

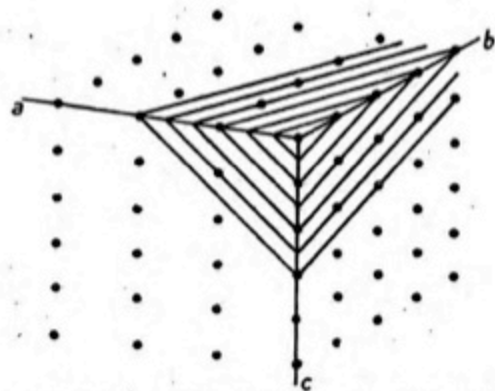


FIG. 10. This set of parallel planes has indices 312.

lattice points

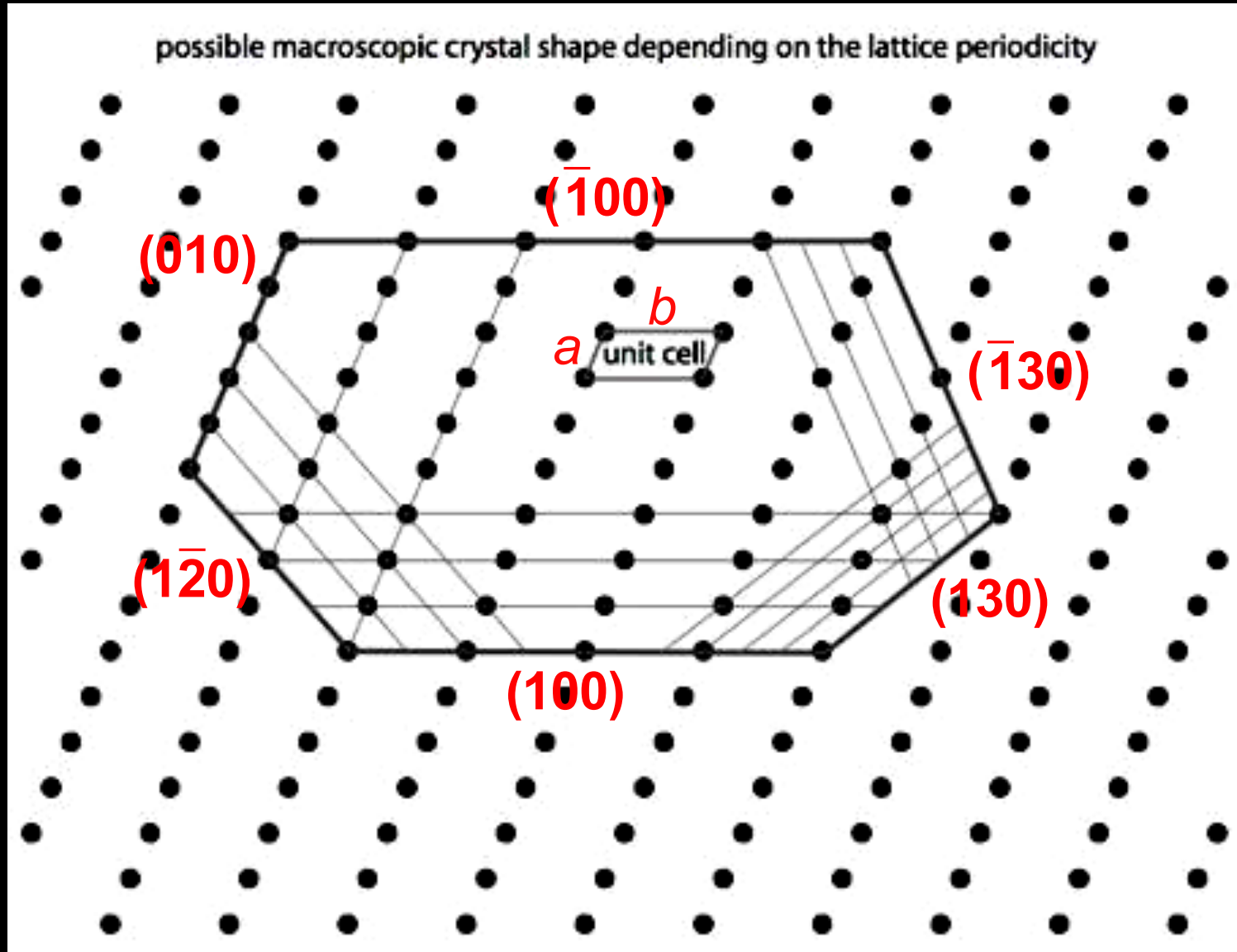
lattice planes

Haüy's Law of Rational Indices (1783)

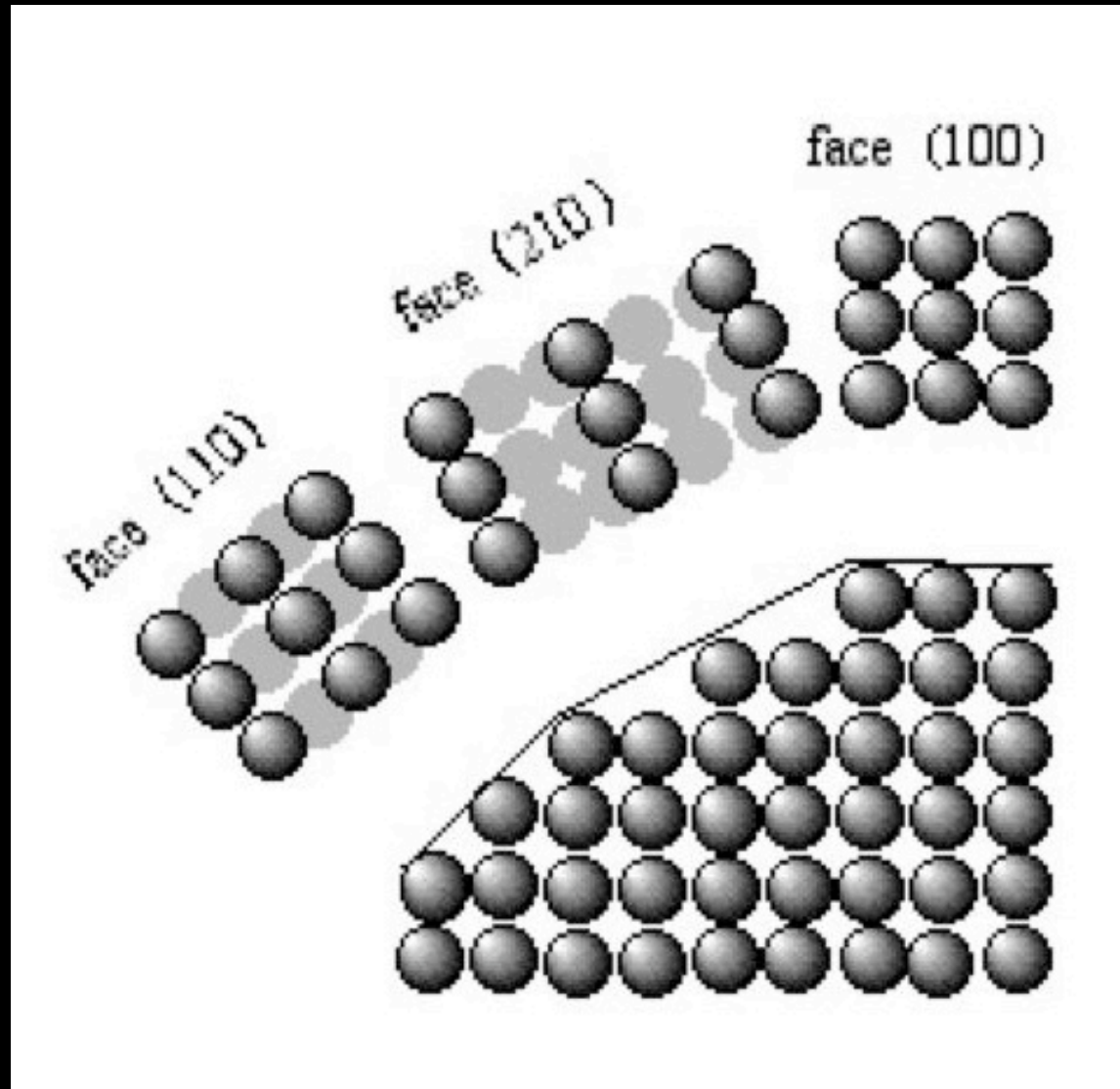
and

Miller indices (1839)

Lattice planes define the crystal faces.

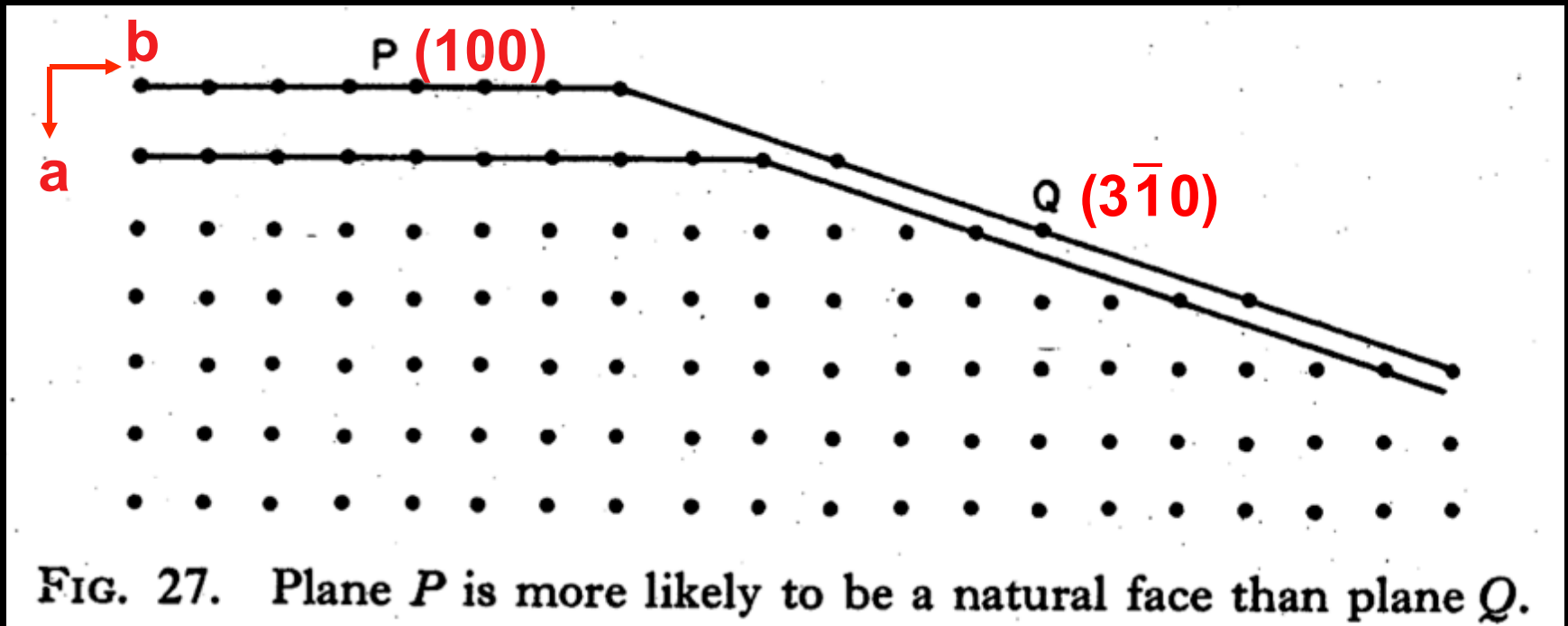


Miller Indices and Reticular Density

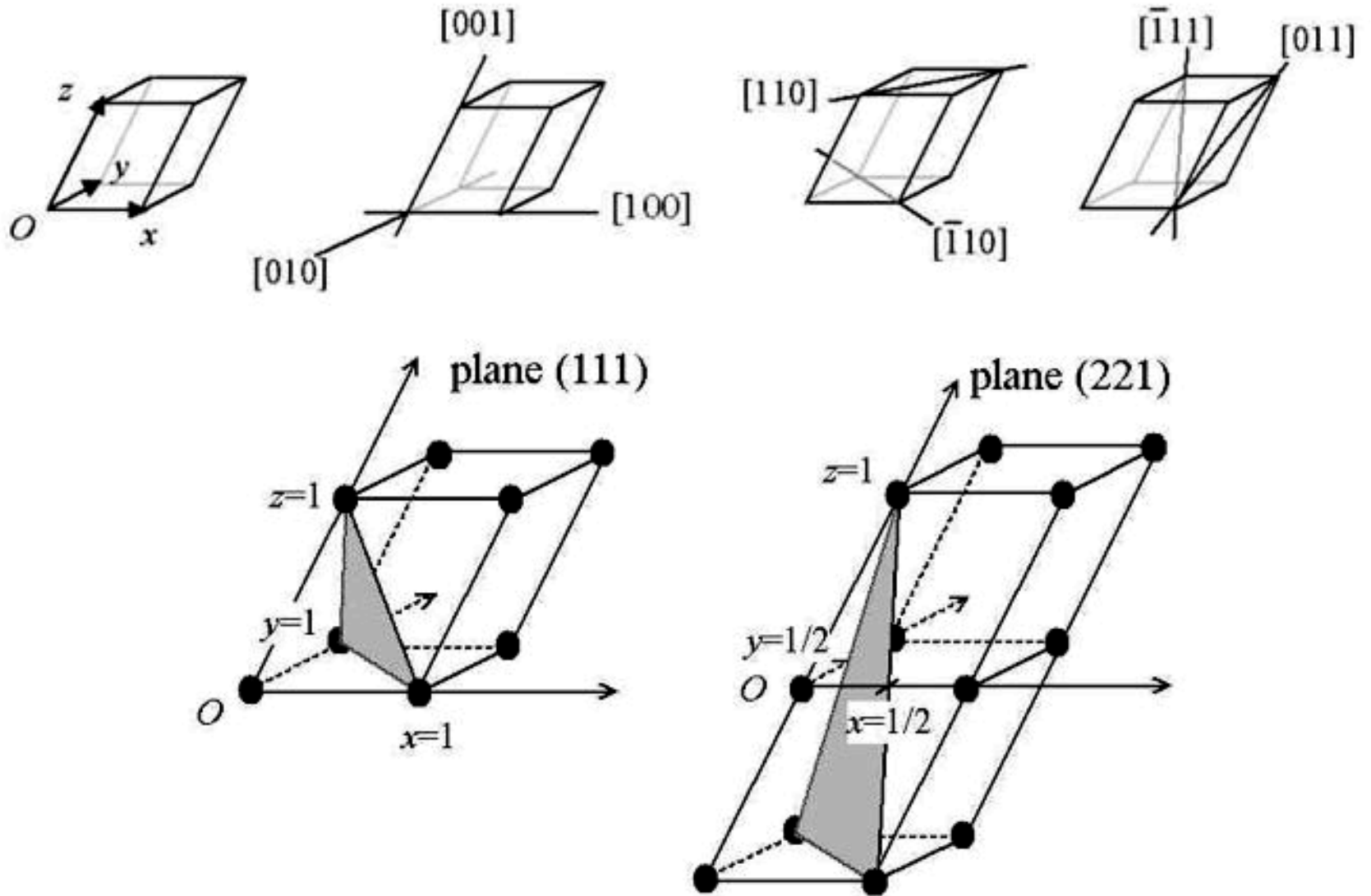


Crystal faces are lattice planes with:

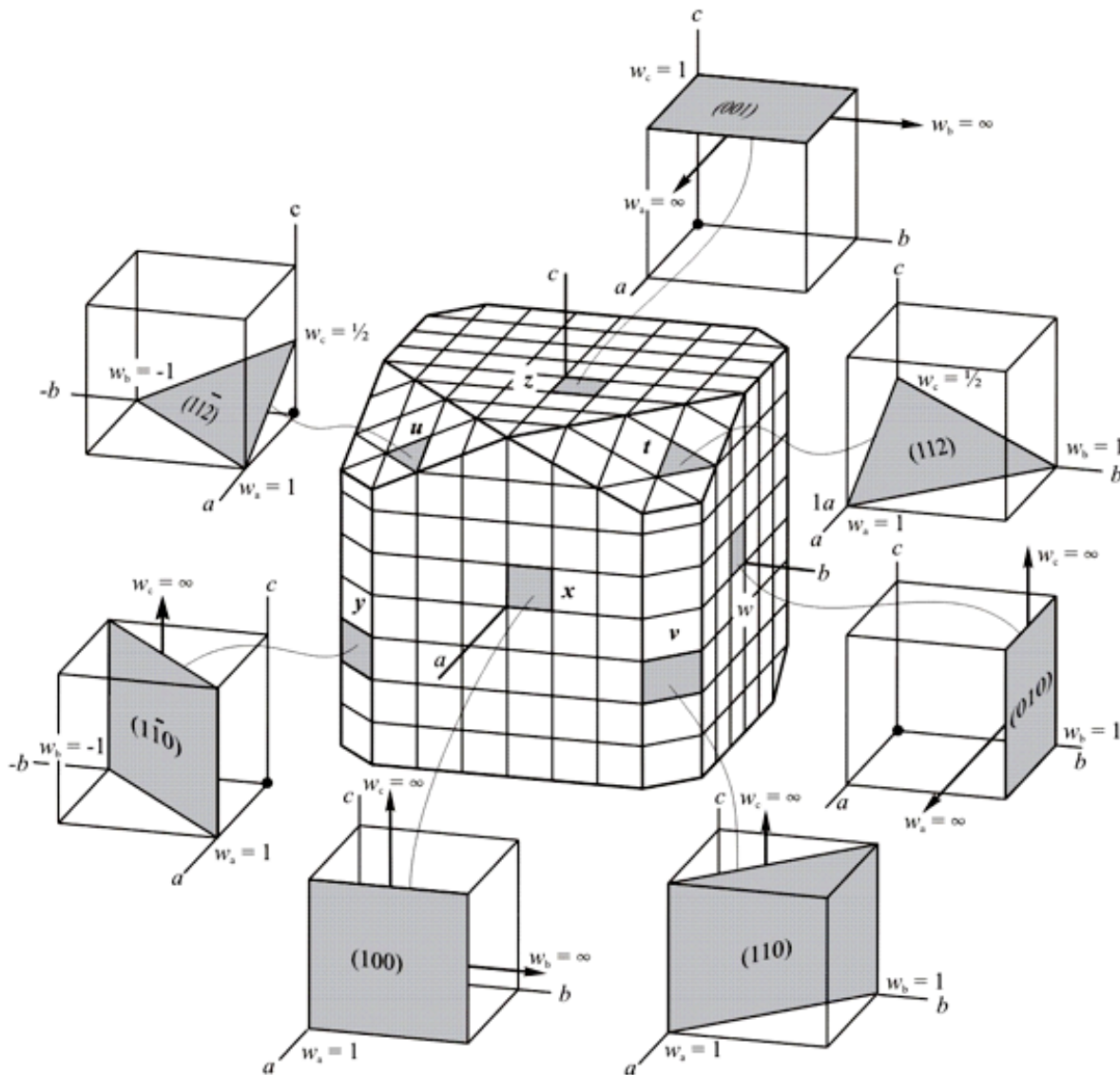
- small Miller indices,
- large interplanar spacing, and
- high reticular density.



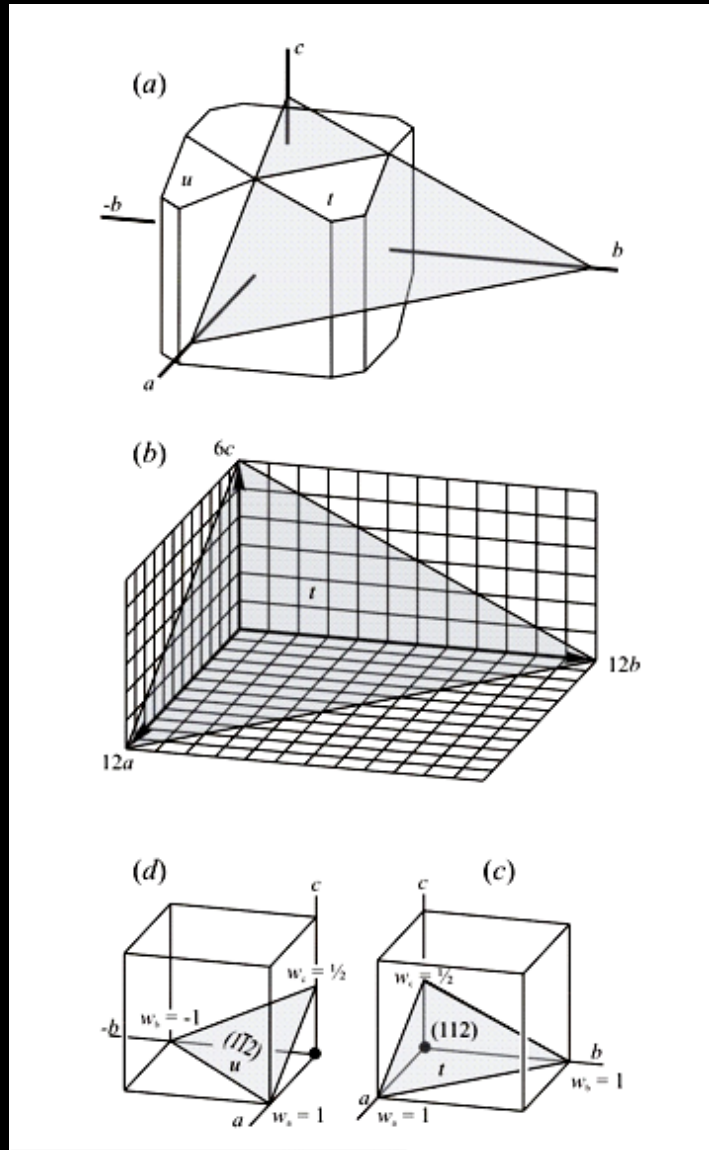
Indexing Lattice Axes $[uvw]$ and Lattice Planes (hkl)



Miller indices of some cubic crystal faces



Some faces of a truncated cube



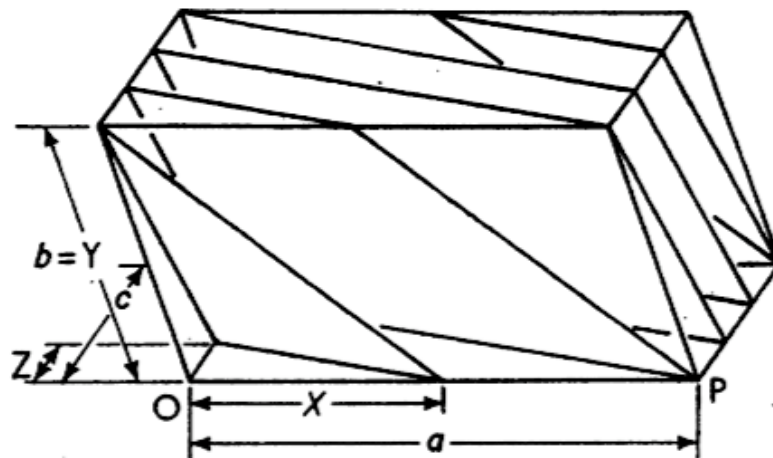


Fig. 2.15. The planes (213).

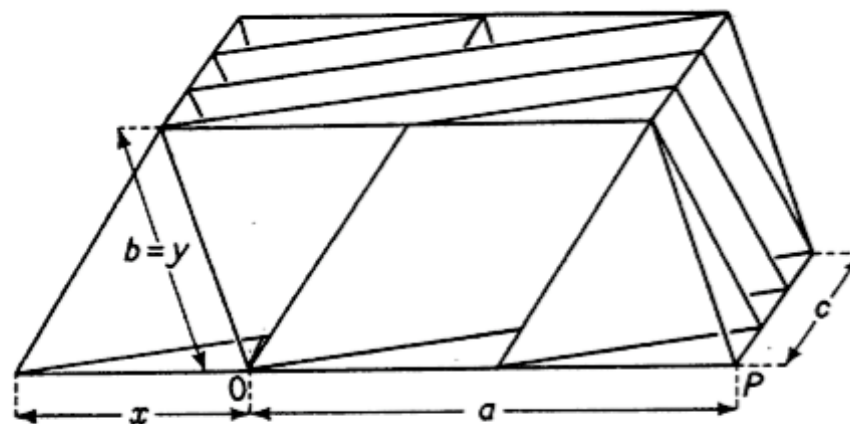
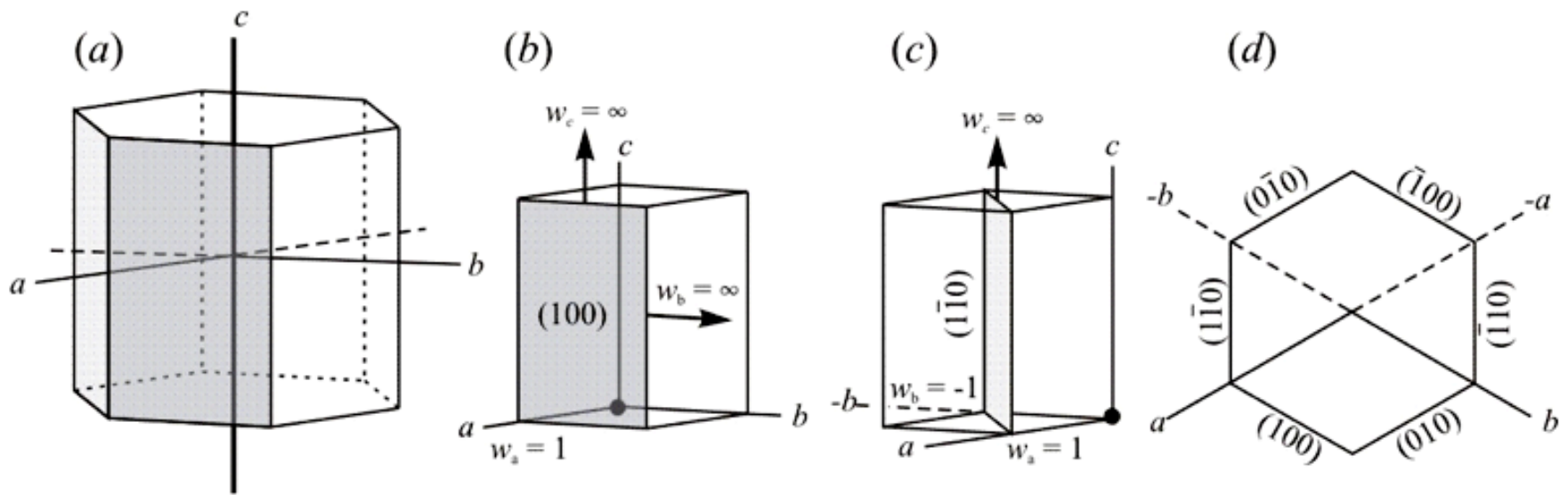
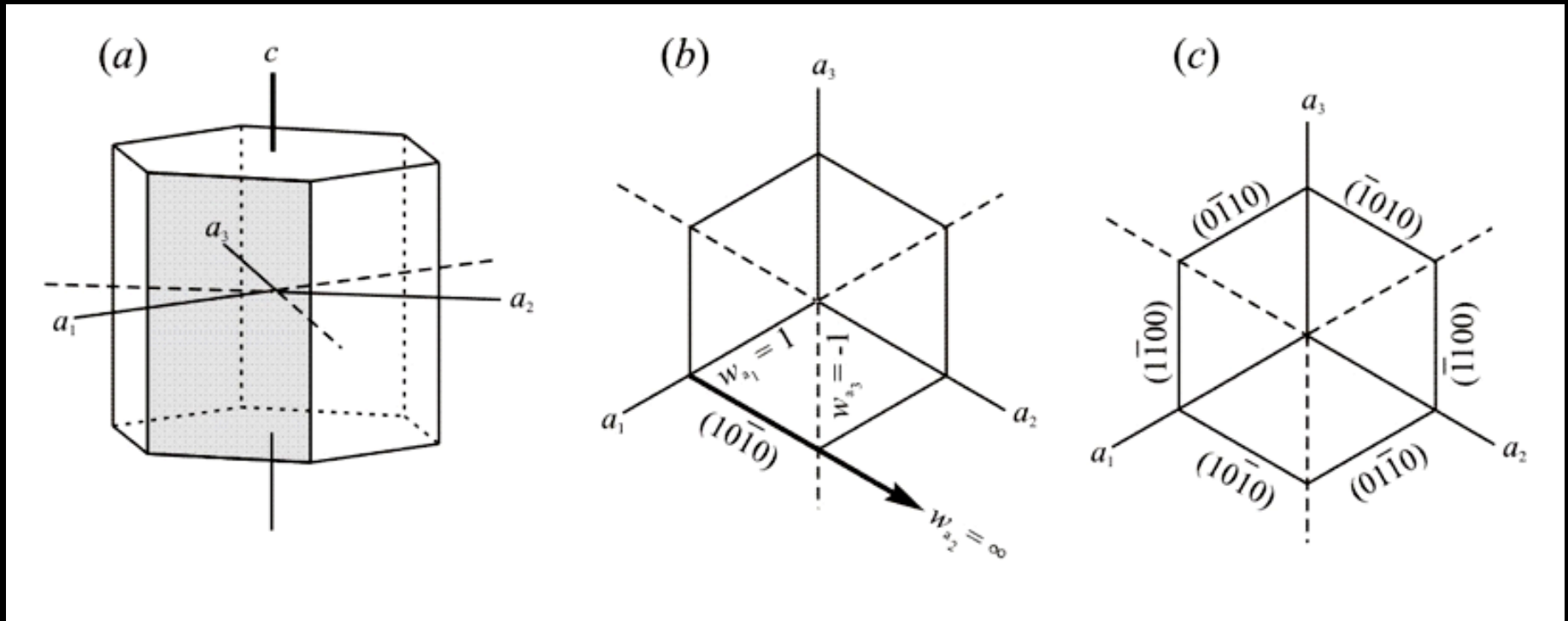


Fig. 2.16. The planes ($\bar{2}13$).

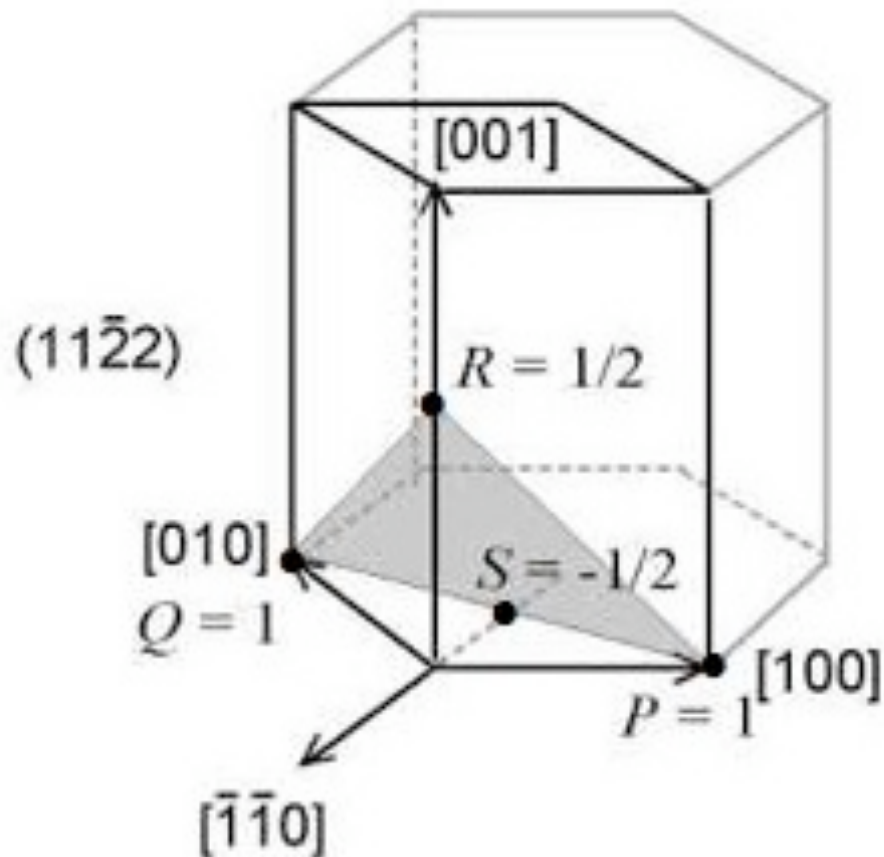
Three-index (hkl) Trigonal or Hexagonal Indexing



Four-index $(h\ k\ i\ l) = (h, k, -h-k, l)$ Hexagonal Indexing

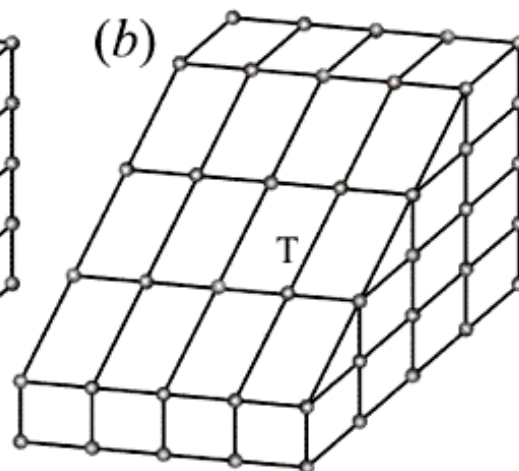
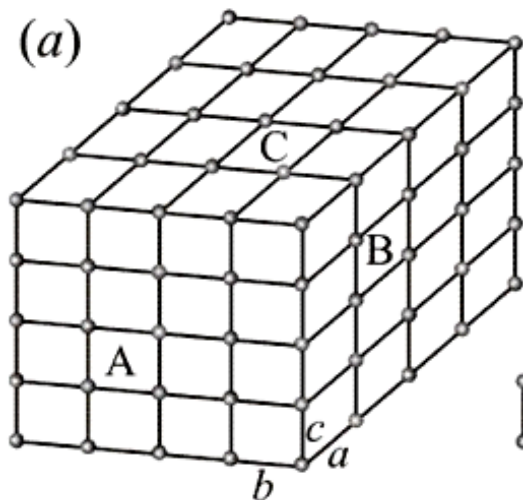


Four-index $(hkil) = (h, k, -h-k, l)$ Hexagonal Indexing



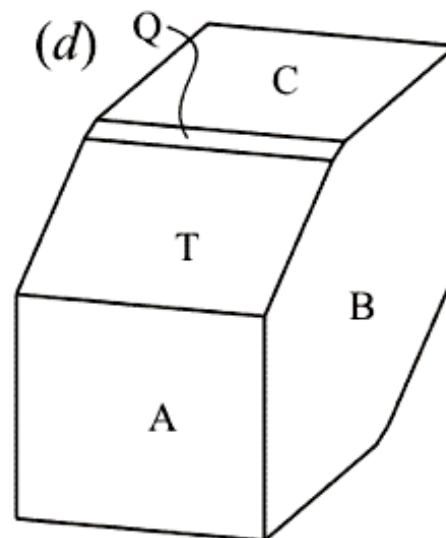
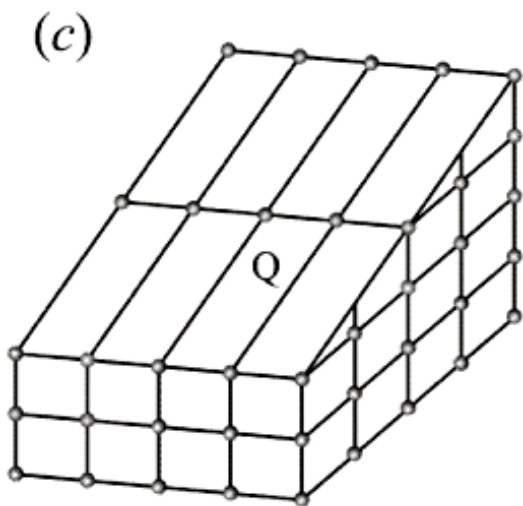
**Development of a zone of crystal faces $\{hkl\} = \{h0l\}$
 Around a zone axis $[uvw] = [010]$**

A (100)
 B (010)
 C (001)



T (101)

Q (102)



Crystal face development by omitted stacks of unit cells

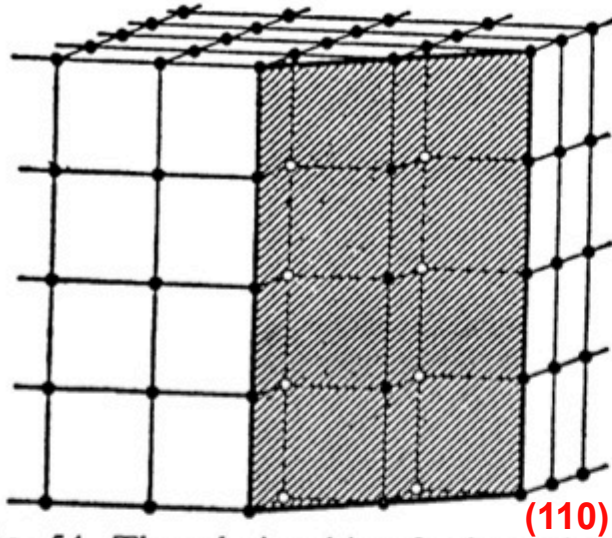


FIG. 54. The relationship of a face of the rhombic dodecahedron (shaded plane) to the structural units.

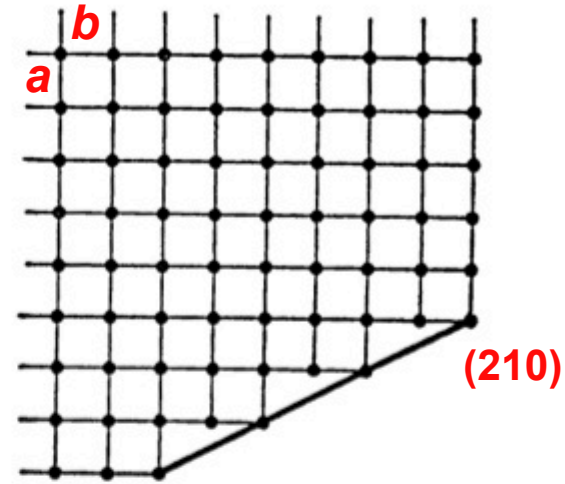


FIG. 55. Plan of the development of a further face modifying a cube edge.

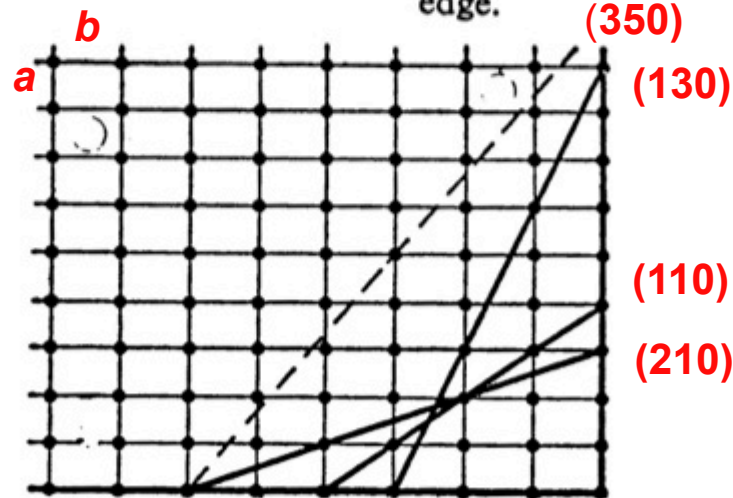
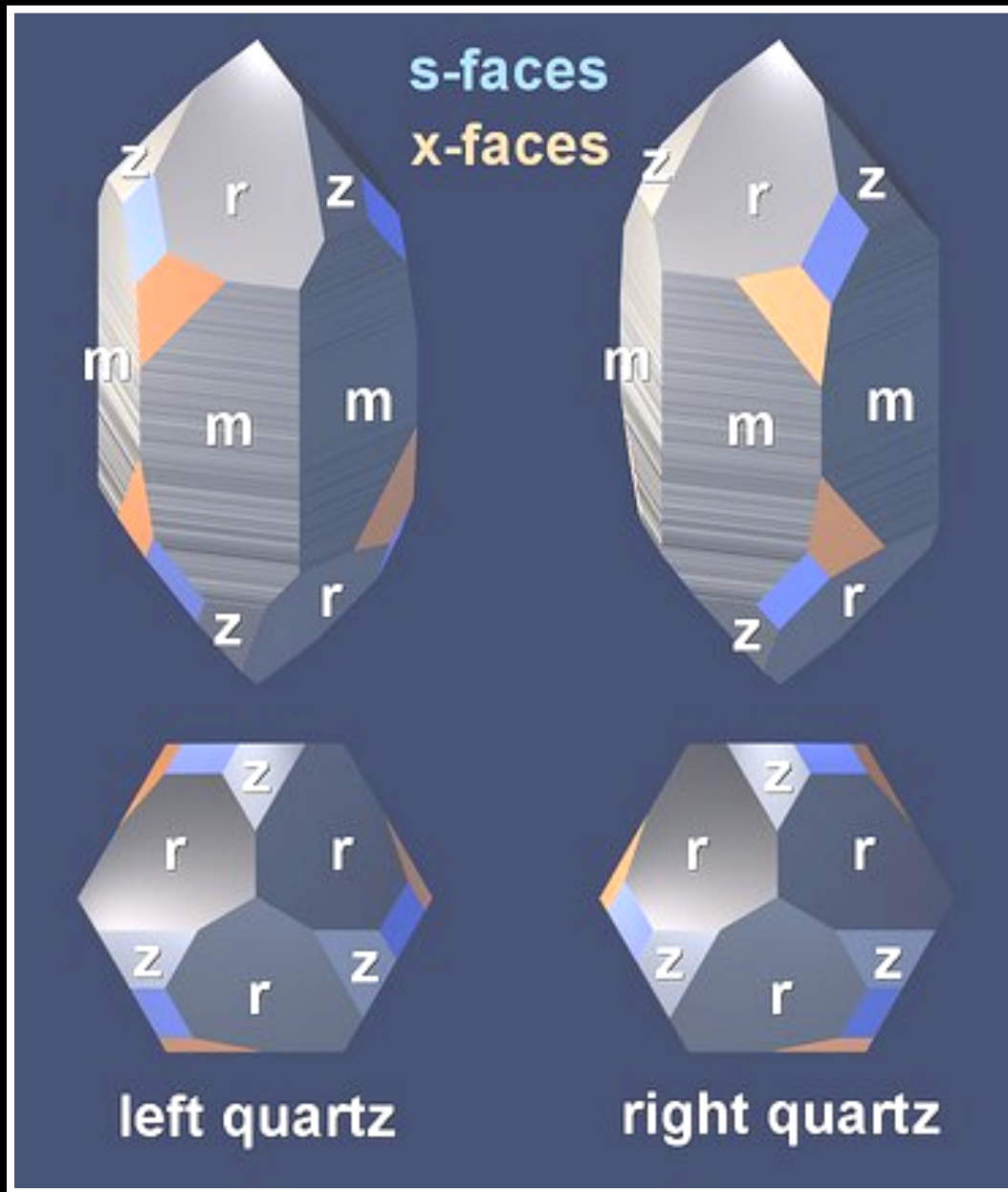
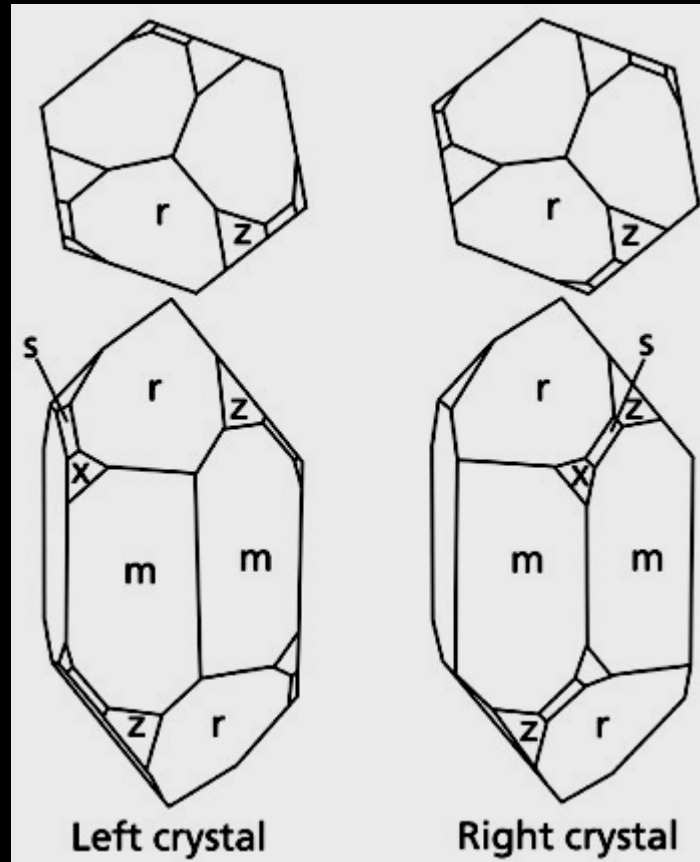


FIG. 56. The slopes of some possible planes in a crystal based on an orthorhombic structural unit.

Enantiomorphic pairs of low quartz (α -SiO₂) crystals



Enantiomorphic low quartz ($\alpha\text{-SiO}_2$) crystals



$$m = \{10\bar{1}0\} = (10\bar{1}0), (01\bar{1}0), (\bar{1}100), (\bar{1}010), (0\bar{1}10), (1\bar{1}00)$$

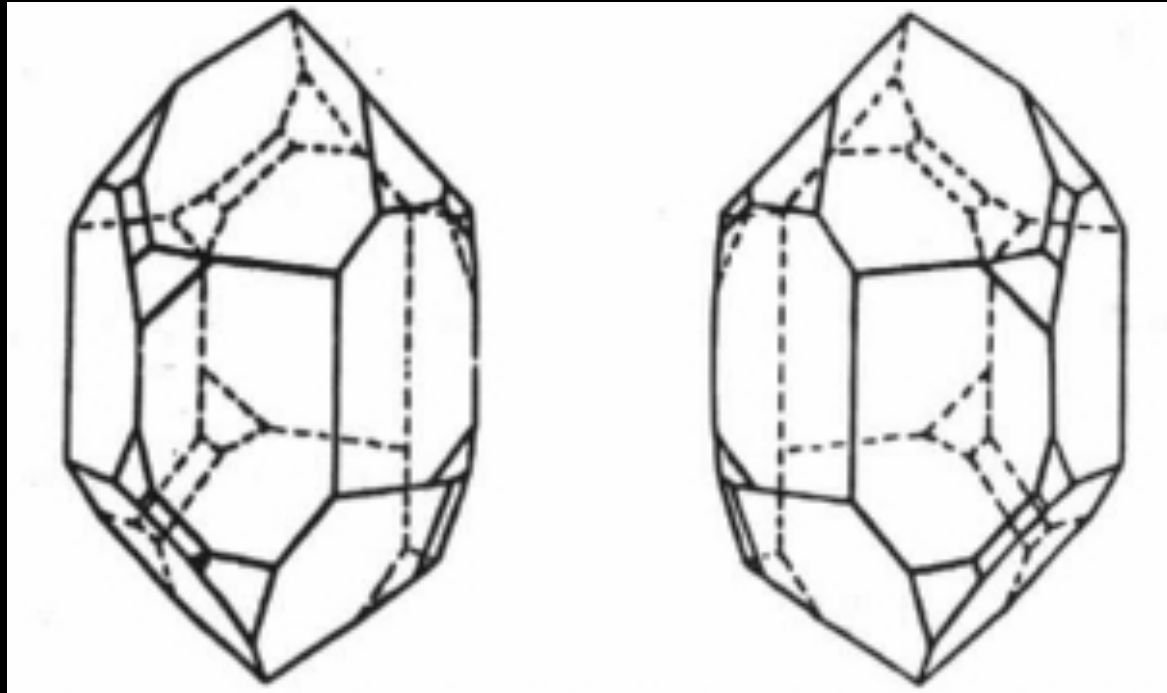
$$r = \{10\bar{1}1\} = (10\bar{1}1), (01\bar{1}1), (\bar{1}101), (\bar{1}01\bar{1}), (0\bar{1}1\bar{1}), (1\bar{1}0\bar{1})$$

$$z = \{01\bar{1}1\} = (01\bar{1}1), (0\bar{1}1\bar{1}), (\bar{1}101), (\bar{1}01\bar{1}), (0\bar{1}1\bar{1}), (1\bar{1}0\bar{1})$$

$$s = \{2\bar{1}\bar{1}1\} \text{ left, } \{11\bar{2}1\} \text{ right}$$

$$x = \{6\bar{1}\bar{5}1\} \text{ left, } \{51\bar{6}1\} \text{ right}$$

An enantiomorph pair of chiral, hemihedral,
low quartz, α -SiO₂, crystals
à la bicapped “Herkimer diamonds”



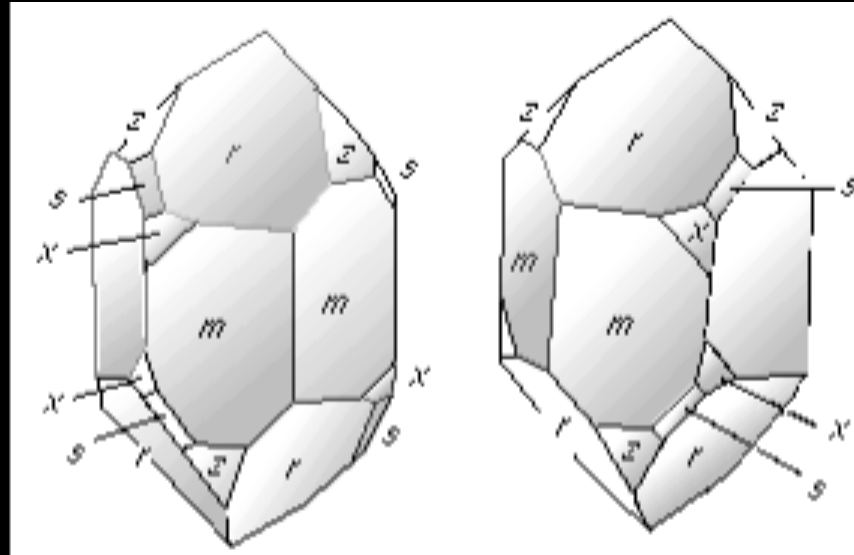
enantiomorph from $\epsilon\nu\alpha\nu\tau\iota\omicron\varsigma$ (*enantios*) “opposite” + $\mu\omicron\rho\phi\eta$ (*morphe*) “form”

chiral, chirality from $\chi\epsilon\iota\rho$ (*cheir*) “hand”

hemihedral “half the faces” from $\eta\mu\iota$ (*hemi*) “half” + $\epsilon\delta\rho\omicron\nu$ (*edron*) “seat, base, or face”

<http://cabierta.uchile.cl/revista/3/chiral1.jpg>

Enantiomorphous pairs of low quartz (α -SiO₂) crystals



left-handed
dextro-rotatory

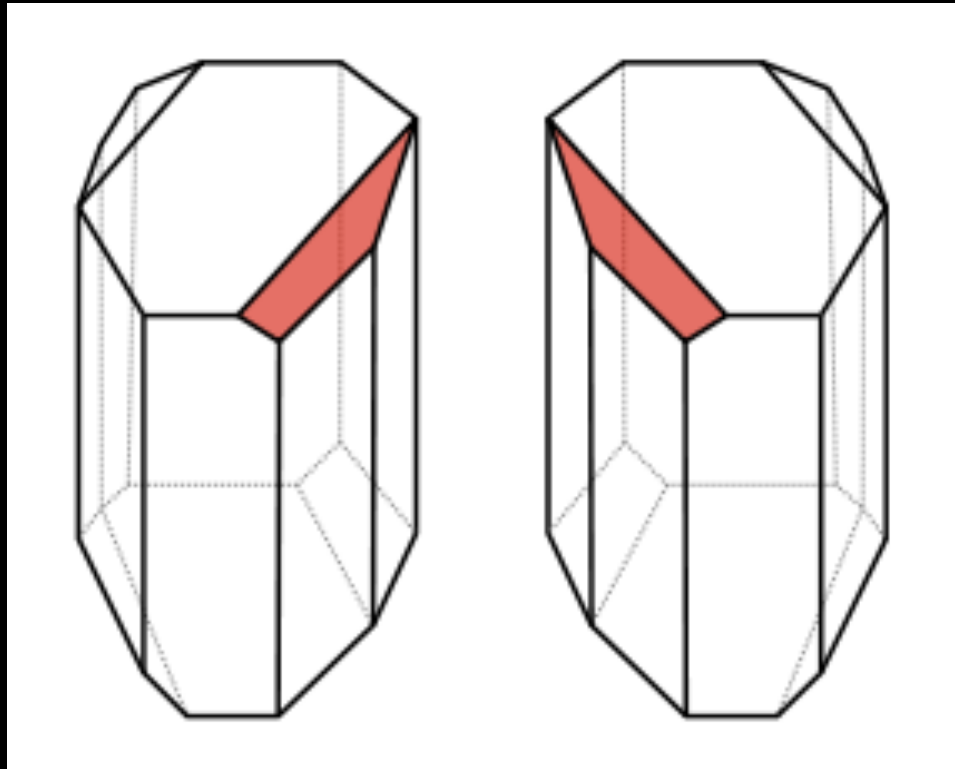
right-handed
levo-rotatory

(Photograph from Vladimir Prelog's Chemistry Nobel Lecture in 1975)

Enantiomorph pair of sodium ammonium tartrate crystals



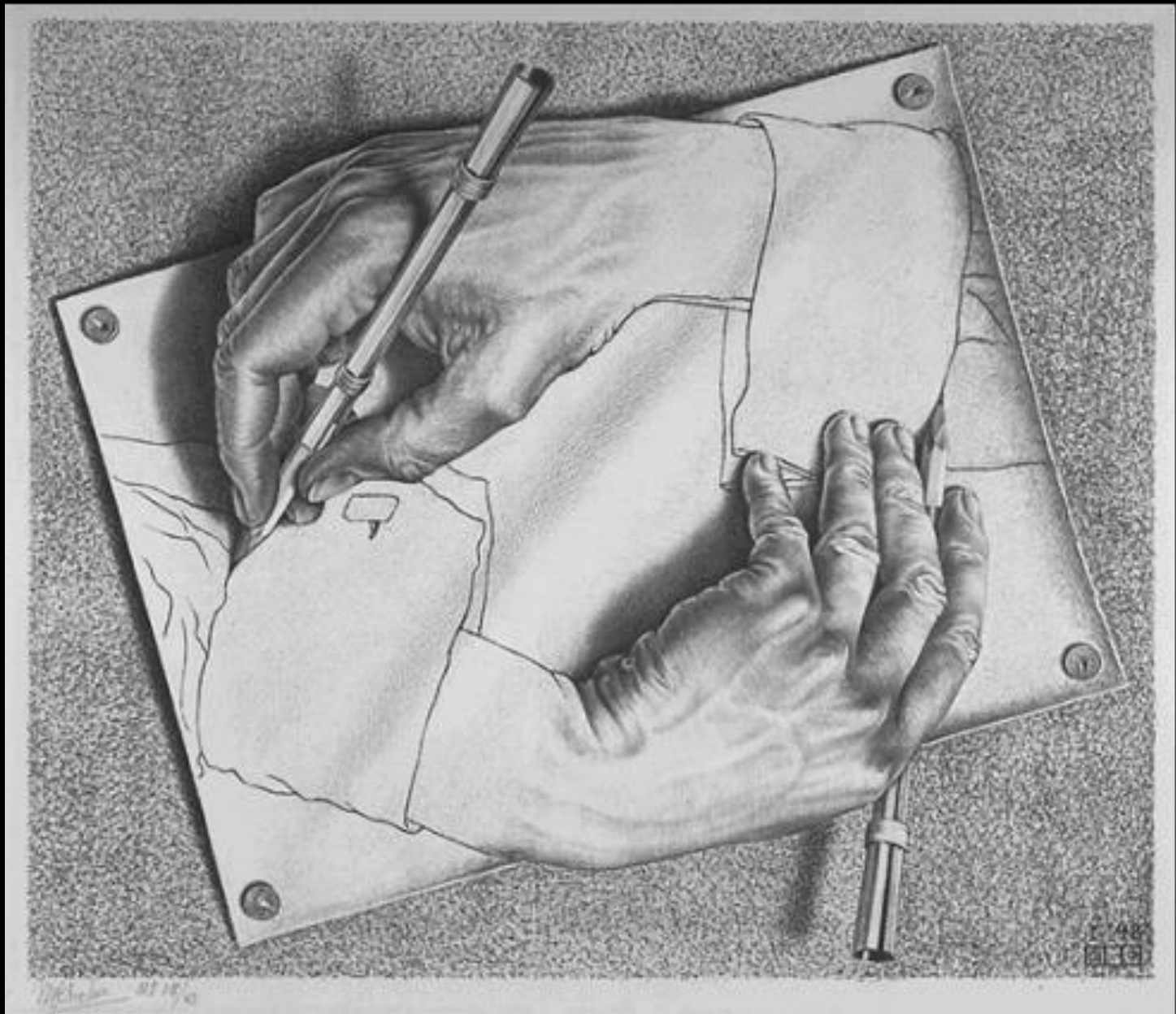
à la Louis Pasteur (1849)



The “cornerstones” of systematic stereochemistry

Charles W. Bunn (1964). *Crystals: Their Role in Nature and in Science*. New York: Academic Press

http://en.wikipedia.org/wiki/Louis_Pasteur



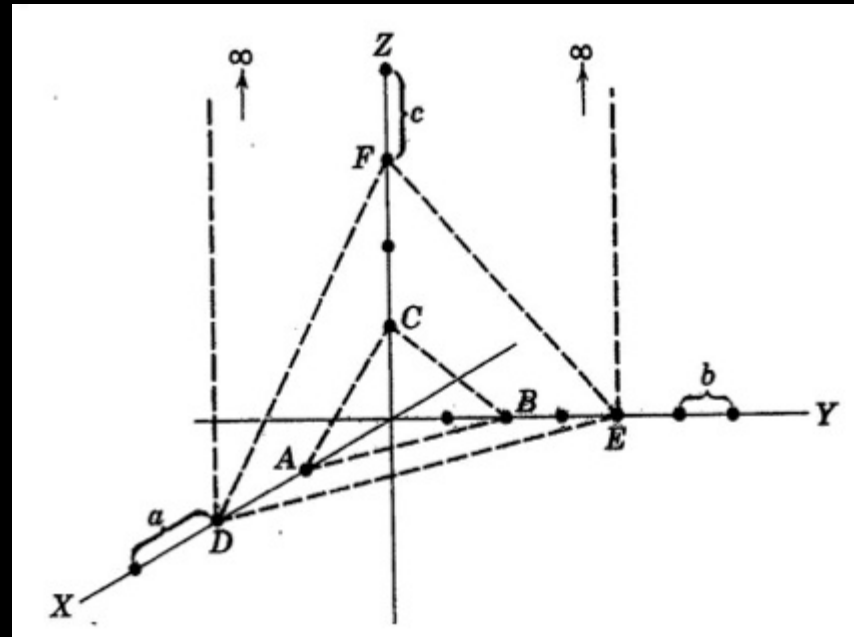
Miller indices (hkl) of crystal faces

1. Choose as *crystal axes* three non-coplanar crystal edges or directions. In particular, choose evident symmetry directions.
2. Choose as a *unit plane* or *parametral plane* a crystal face that intersects all three axes.
3. From goniometric measurements of the interfacial angles, deduce the relative lengths a, b, c of the *intercepts* of the parametral plane on the crystal axes, *i.e.*, the *axial* or *parametral ratios* $a : b : c$.
4. Determine the intercepts pa, qb, rc of the crystal faces on the crystal axes, where $p, q,$ and r are small integers or infinity. Thence determine the Miller indices (hkl) of the crystal faces as the *smallest co-prime integer values* of the *fractions-cleared reciprocals of the intercept multiples*

$$h \propto \frac{1}{p}, \quad k \propto \frac{1}{q}, \quad l \propto \frac{1}{r}.$$

Different observers might choose different crystal axes and parametral planes and hence determine different internally consistent sets of indices.

Miller indices of crystal faces



Face	Intercepts	Reciprocals of Intercept Multiples	Cleared of Fractions	Miller Indices (<i>hkl</i>)
<i>ABC</i>	$1a : 2b : 1c$	$\frac{1}{1} \frac{1}{2} \frac{1}{1}$	2 1 2	(212)
<i>DEF</i>	$2a : 4b : 3c$	$\frac{1}{2} \frac{1}{4} \frac{1}{3}$	6 3 4	(634)
<i>DE∞</i>	$2a : 4b : \infty c$	$\frac{1}{2} \frac{1}{4} \frac{1}{\infty}$	2 1 0	(210)

Harold P. Klug and Leroy E. Alexander (1974). *X-Ray Diffraction Procedures for Polycrystalline and Amorphous Materials*. New York: John Wiley.

In Fig. 59, ABC , DBC and DBE represent the slopes of three faces in a crystal the structural unit of which, with edges of lengths

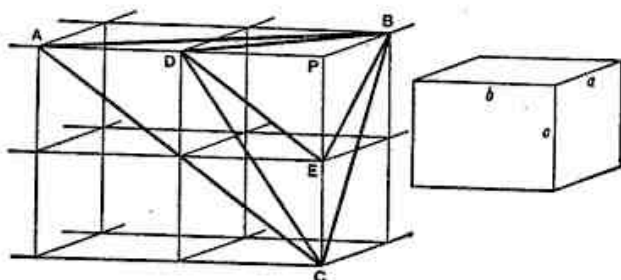


FIG. 59.

a , b , c , is represented on the right of the figure. Suppose that, for this particular substance, the ratios $a : b : c$ of the actual unit = $0.816 : 1 : 0.924$. (It is customary to express the ratio $a : b : c$ in the form $a/b : 1 : c/b$, reducing b to unity.)

The first observer selects the plane ABC as parametral plane; he therefore assigns to it the index 111. From its slope in relation to the three axial directions he would determine *axial ratios* of values $BP : AP : CP$, $0.408 : 1 : 0.924$.

The index of the plane DBC is $\frac{BP}{BP} \frac{AP}{DP} \frac{CP}{CP}$, i.e. 121.

" " " DBE is $\frac{BP}{BP} \frac{AP}{DP} \frac{CP}{EP}$, i.e. 122.

The second observer selects the plane DBC as 111, and hence calculates axial ratios $BP : DP : CP$, $0.816 : 1 : 1.848$.

The index of the plane ABC is $\frac{BP}{BP} \frac{DP}{AP} \frac{CP}{CP}$, $1\frac{1}{2}$, i.e. 212.

" " " DBE is $\frac{BP}{BP} \frac{DP}{DP} \frac{CP}{EP}$, i.e. 112.

To the third observer, DBE seems the best choice as 111. His calculated axial ratios, $BP : DP : EP = 0.816 : 1 : 0.924$, are actually those of the edges $a : b : c$ of the structural unit.

The index of the plane ABC is $\frac{BP}{BP} \frac{DP}{AP} \frac{EP}{CP}$, $1\frac{1}{2}$, i.e. 211.

" " " DBC is $\frac{BP}{BP} \frac{DP}{DP} \frac{EP}{CP}$, 1, 221.

Tabulating these results, we have three correct but different descriptions of the slopes of the three planes present on the crystal:

	Axial ratios	Indices of planes		
		ABC	DBC	DBE
Observer 1	-	111	121	122
Observer 2	-	212	111	112
Observer 3	-	211	221	111

Each description illustrates the rationality (and the simplicity) of the indices, but only when we have advanced so far that we can determine the exact arrangement of the internal structure, and hence the absolute lengths of the edges a , b , c of the unit of structure, could we say that the description given by observer 3 is preferable to those offered by observers 1 and 2.

It is clear, also, that the rationality lies only in the *ratios of intercepts* on corresponding axes, and there is no rational relationship between the intercepts on different axes unless by chance the symmetry of the system permits the choice of a symmetrically-situated plane as parametral plane. Hence the name *Law of Rational Intercepts* sometimes used is particularly misleading; it can be corrected by writing *Law of Rational Ratios of Intercepts*, but as a ratio of intercepts defines an index the correct name of the Law is that which we have used above.

Finally, it must be observed that there is nothing in this discussion which determines the relative dimensions of the whole crystal; we have been concerned only with the slopes of faces, and the habit of the crystal is in no way necessarily related to the units of measurement $a b c$ which determine these slopes. All these points will be much clearer when we have been able to practise making accurate drawings of crystals.

“The second law of crystallography”

The Law of Rational Indices

(Haüy, 1784)

The faces of a crystal have indices (*i.e.*, reciprocals of the face intercepts on the crystallographic axes) that stand in the ratio of small whole numbers.



Abbé René-Just Haüy
(1743-1822)
making goniometric
measurements on a
calcite crystal

A well-developed
 $(\text{NH}_4)_2\text{SO}_4$
crystal

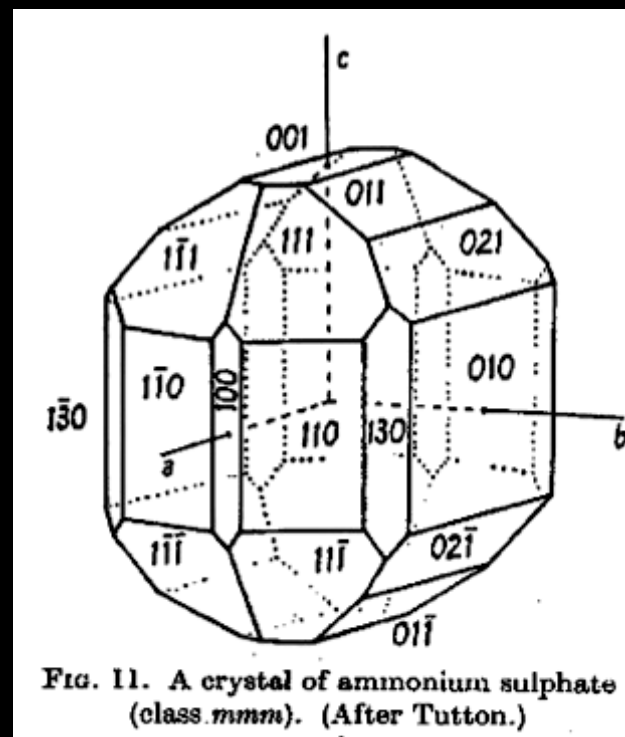


FIG. 11. A crystal of ammonium sulphate
(class *mmm*). (After Tutton.)

Axial ratios from interfacial angles

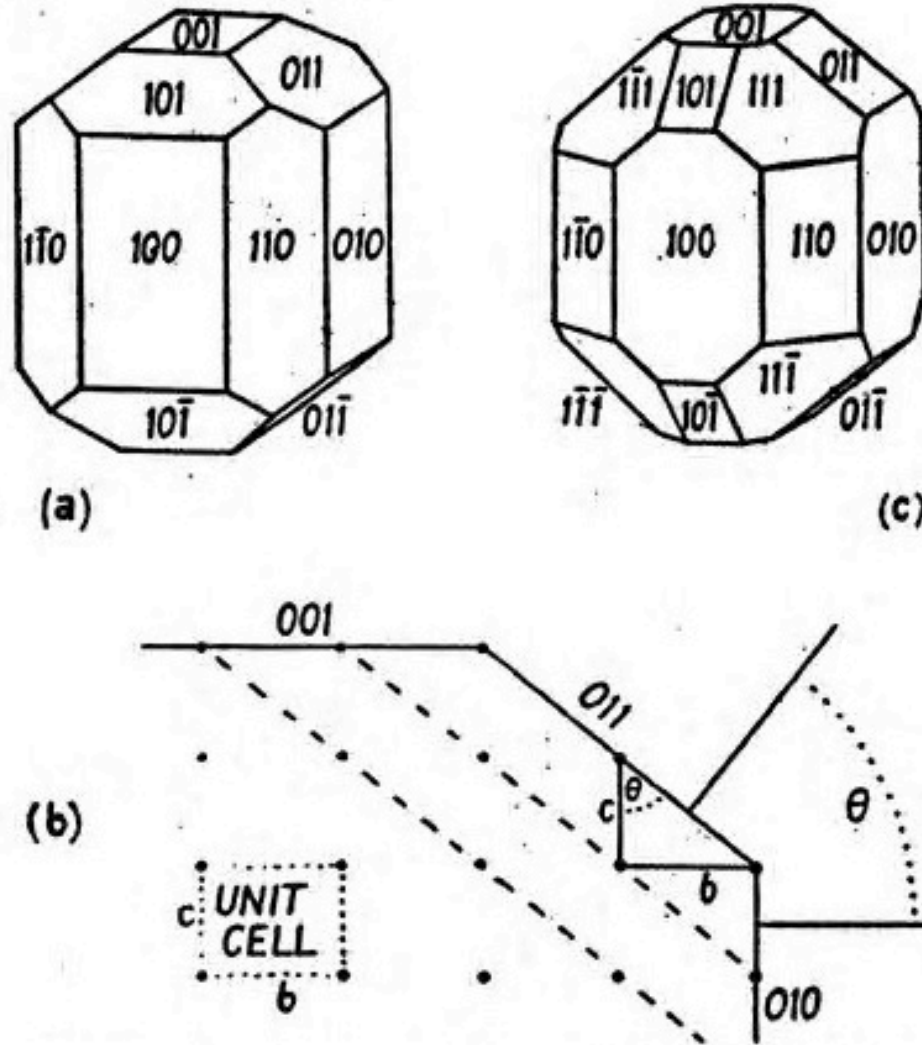


FIG. 15. Determination of the probable shape of the unit cell from interfacial angles.

Axial ratios from interfacial angles

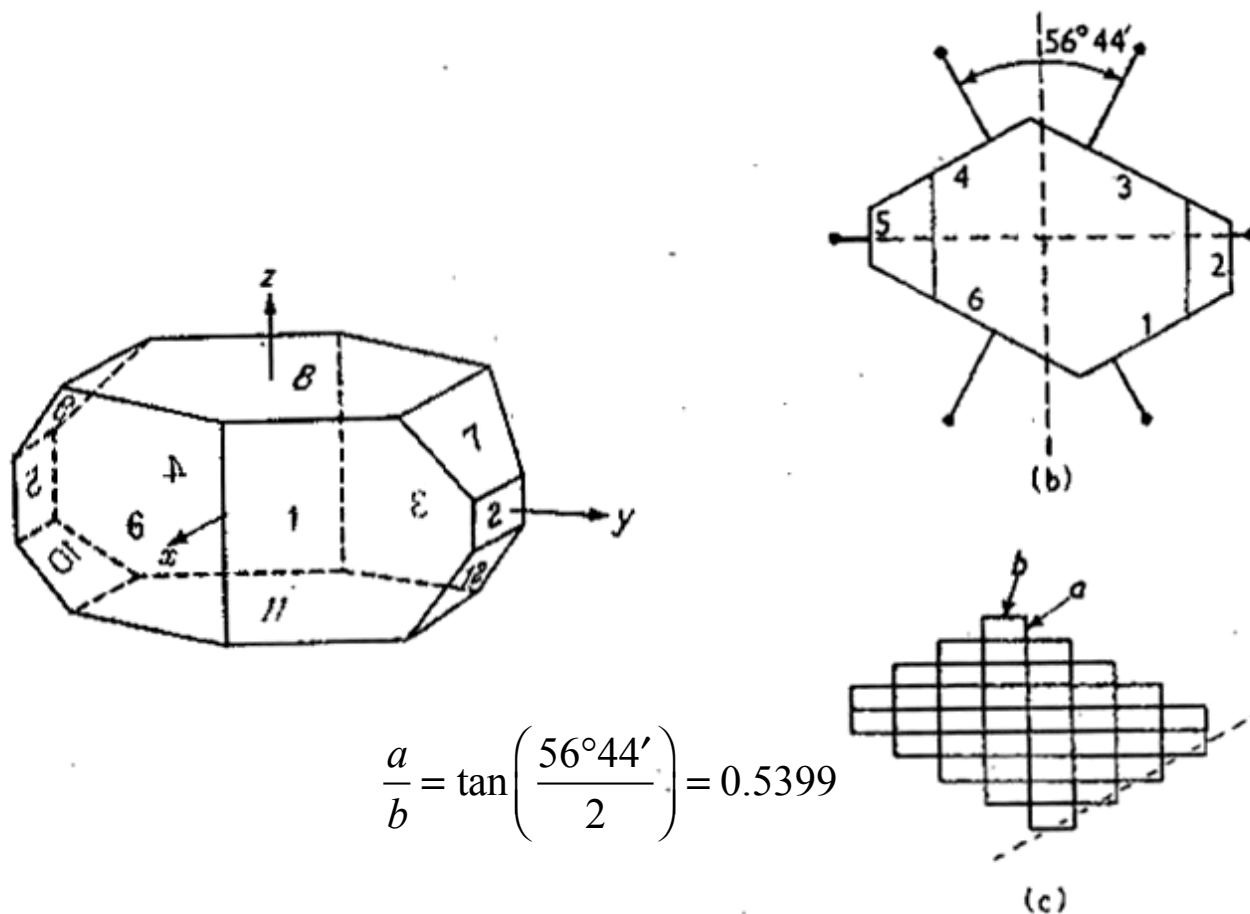
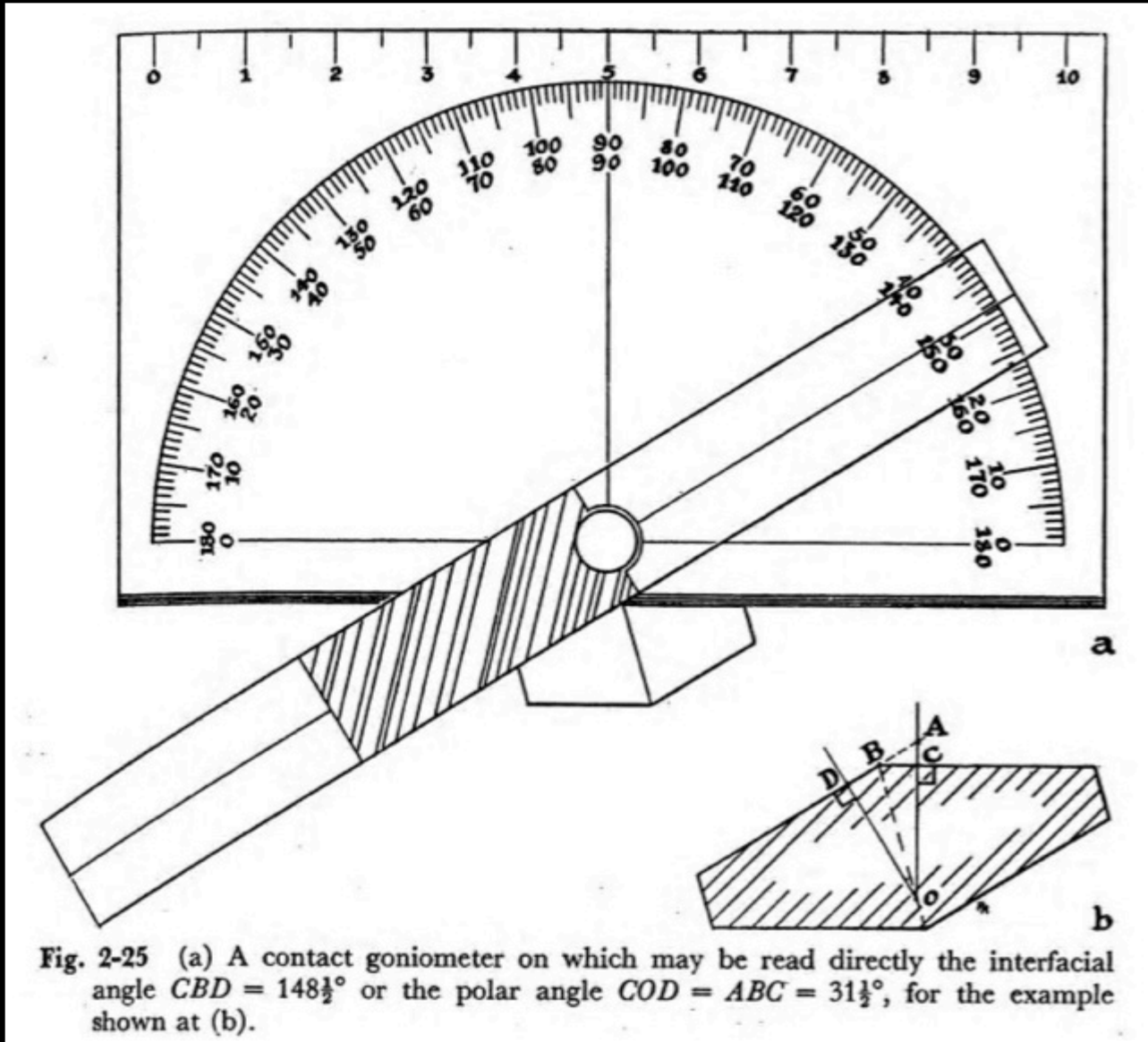


Fig. 2.12(a). Crystal of potassium succinate trihydrate.

Fig. 2.12(b). Crystal of Fig. 2.12(a) seen along z-axis.

Fig. 2.12(c). Simplest axial ratios of unit cell.

Contact goniometer



Optical goniometer

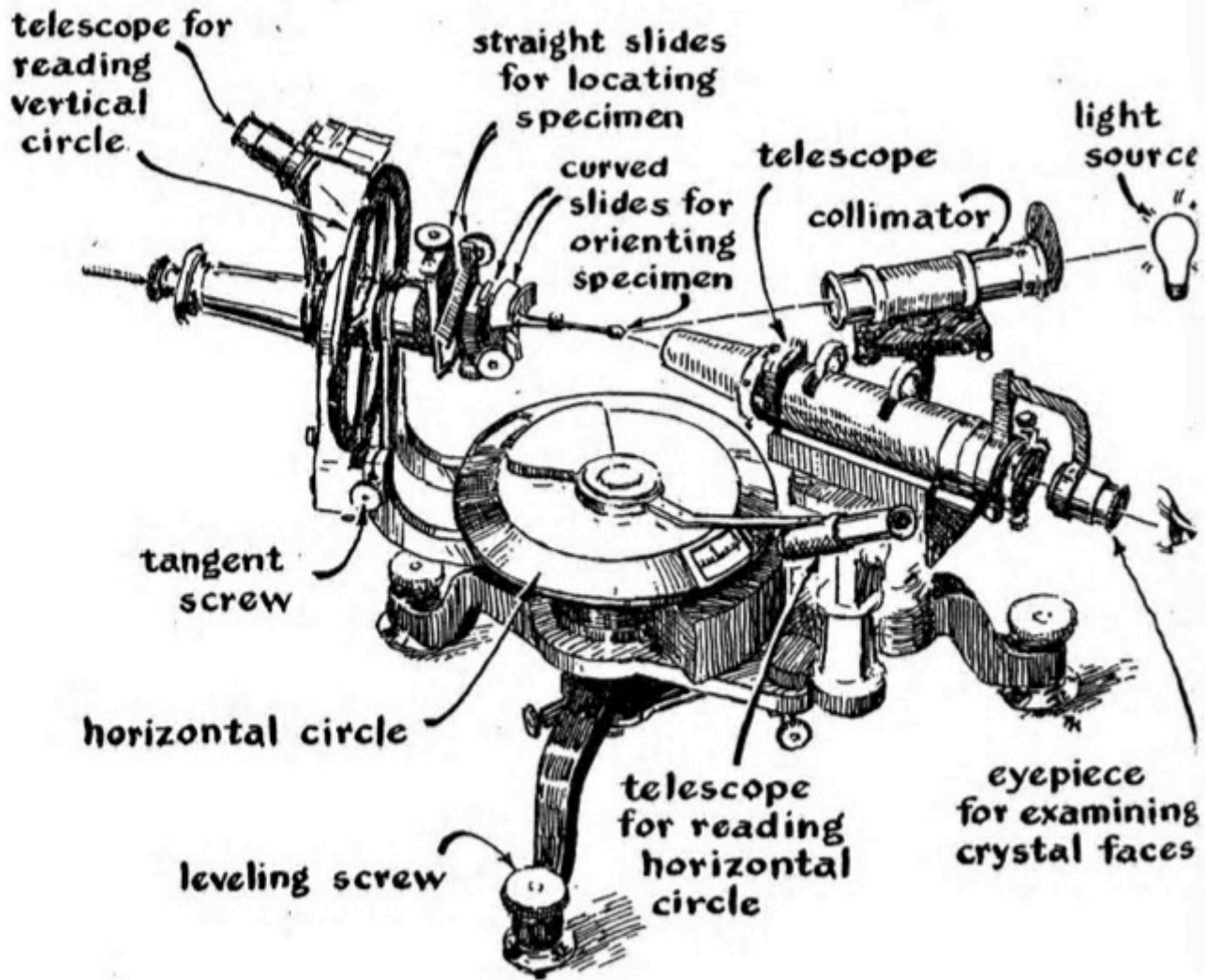


Fig. 2-26 A two-circle reflecting goniometer.

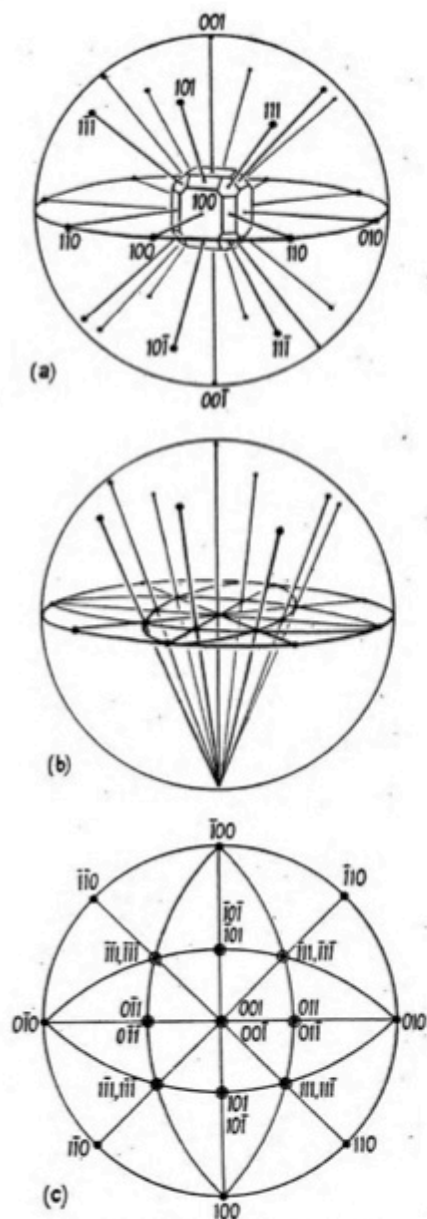


FIG. 14. The stereographic projection.

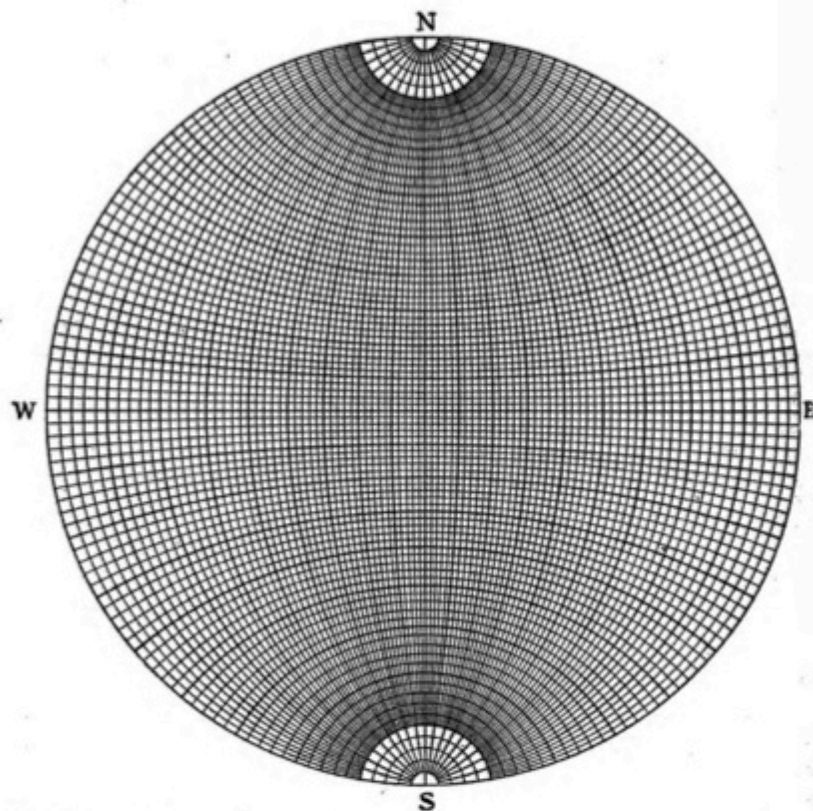


Fig. 2-19 A Wulff net. Stereographically projected great circles appear as lines of equal longitude, and small circles centered about the north and south poles appear as lines of equal latitude at two-degree intervals.

Paul Heinrich Ritter von Groth 1843-1927



In 1888, Groth was the first to suggest the possibility that spherical atoms reside at equivalent positions of space lattices.

CHEMISCHE KRYSTALLOGRAPHIE

VON

P. GROTH

ERSTER TEIL

ELEMENTE — ANORGANISCHE VERBINDUNGEN OHNE SALZ-
CHARAKTER — EINFACHE UND COMPLEXE HALOGENIDE,
CYANIDE UND AZIDE DER METALLE, NEBST DEN ZUGE-
HÖRIGEN ALKYLVERBINDUNGEN

MIT 389 TEXTFIGUREN

LEIPZIG

VERLAG VON WILHELM ENGELMANN

1906

NATURAL HISTORY

MAY 1976 • \$1.25



CHEMISCHE KRYSTALLOGRAPHIE

VON

P. GROTH

Schwefel.

α -Modification (gewöhnlicher rhombischer Schwefel).

Schmelzpunkt $113,0^{\circ} - 113,5^{\circ}$ Muthmann¹⁾.

Spec. Gew. 2,037 (aus CS_2 kryst.), 2,069 (nat.) Spring¹⁵⁾,
2,067 > Schrauf¹⁶⁾,
2,094 > Zehnder¹⁷⁾.

Rhombisch bipyramidal (natürliche Krystalle sind zuweilen auffallend bisphenoïdisch ausgebildet).

$\rightarrow a : b : c = 0,8408 : 1 : 1,9005$ Brežina¹⁸⁾.

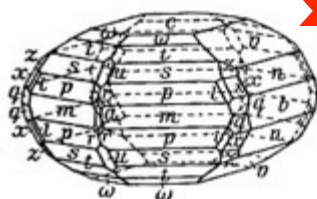
Durch Sublimation gebildete Krystalle sind gewöhnlich sehr flächenreich; hierzu gehören außer den an Vulkanen vorkommenden natürlichen Krystallen die

von Ulrich in Rösthaufen der Okerhütte am Harz beobachteten kleinen Krystalle, welche nach Brežina¹⁸⁾ folgende Formen zeigten (s. Fig. 19): $c\{001\}$, $v\{013\}$, $n\{011\}$, $b\{010\}$, $m\{110\}$, $p\{111\}$, $s\{113\}$, $t\{115\}$, $\omega\{117\}$, $x\{133\}$, $z\{135\}$, $q\{131\}$, $u\{103\}$, $l\{344\}$, $a\{100\}$, $r\{311\}$.

Aus dem Schmelzflusse kann rhombischer Schwefel krystallisieren, wenn jener unter den Umwandlungspunkt (96°) unterkühlt wird. An großen

Krystallen des sogenannten Jungfernschwefels, in Rösthaufen entstanden, beobachtete

Fig. 19.



44) Tammann, Krystallisieren und Schmelzen, Leipzig 1903, S. 58.

43) Beljankin, Journ. phys. chim. russ. 1901, 33, 670.

42) Hallopeau, Bull. soc. chim. Paris 1899, 21, 266.

41) Berthier, Traité de essais p. l. voie sèche. Paris 1848, 2, 89.

40) Spring, Bull. Acad. R. Belg. 1881 (3), 2, 83. Ber. d. d. chem. Ges. 5, 854.

39) Schrauf, Zeitschr. f. Krystall. 1887, 12, 321.

38) Zehnder, Ann. d. Phys. 1904, (4) 15, 328.

37) Brežina, Sitz.-Ber. Akad. Wien 1869, 60 (I) 539.

Ulrich¹⁹⁾ vorherrschend $p\{111\}$, ziemlich groß $n\{011\}$, untergeordnet $s\{113\}$. Auch in anderen Fällen directer Bildung der rhombischen Modification aus dem Schmelzflusse wurden nur flächenarme Krystalle beobachtet, so von Silvestri²⁰⁾ die Combination $\{111\}\{011\}$. Künstlich kann man die rhombische Krystallisation in einem unterkühlten Schmelzflusse einleiten durch Berühren mit einem rhombischen Schwefelkrystalle; am leichtesten erhält man sie, wenn man auf einem Objectglase Schwefel theilweise zum Schmelzen bringt, ohne daß er sich in die β -Modification umwandelt, und dann abkühlen läßt, wobei dann die rhombischen Krystalle weiterwachsen (Brauns⁴⁾).

Durch Umwandlung entsteht der rhombische Schwefel als die stabilste Modification aus allen übrigen Modificationen.

Aus Lösungen in Schwefelkohlenstoff, Chloroform, Bromoform u. a. bei gewöhnlicher Temperatur bildet sich $p\{111\}$ (Fig. 20) allein oder wenigstens vorherrschend; bei rascher Krystallisation stabförmige Parallelverwachsungen nach der c -Axe aneinander gereihter Bipyramiden p (Gaubert²¹⁾); bei langsamem Wachstum tritt zu $\{111\}$ häufig hinzu $b\{010\}$, ferner $s\{113\}$, $c\{001\}$, $n\{011\}$ (Fig. 21), aus CS_2 zuweilen auch $m\{110\}$, selten $a\{100\}$. Nach Mitscherlich¹⁰⁾ erhält man die besten Krystalle, wenn man eine große Quantität Schwefelkohlenstoff darstellt, ca. $\frac{9}{10}$ davon abdestilliert und den mit Schwefel gesättigten Rest langsam verdunsten läßt. Aus Acetylentetrabromid entstehen nach $c\{001\}$ tafelförmige Krystalle (Gaubert²¹⁾). Die aus CS_2 erhaltenen Krystalle wurden von Mitscherlich²²⁾ und Schrauf²³⁾ gemessen.

Fig. 20.

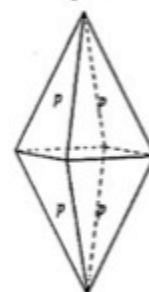
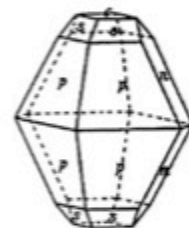


Fig. 21.



Bei der freiwilligen Zersetzung von Schwefelammoniumlösung bilden sich zuweilen sehr schöne Zwillinge nach $n\{011\}$ oder nach $\{101\}$ in Form langer Prismen, verlängert nach derjenigen Polkante von p , welche durch die Zwillingsebene gerade abgestumpft wird.

Die natürlichen Krystalle, welche theils durch Sublimation, theils durch Zersetzung von H_2S usw. entstanden sind²⁴⁾, zeigen außer den bereits angeführten Formen noch: $\{120\}$, $\{130\}$, $\{023\}$, $\{031\}$, $\{101\}$, $\{119\}$, $\{114\}$, $\{337\}$, $\{112\}$, $\{335\}$, $\{553\}$, $\{221\}$, $\{331\}$, $\{551\}$, $\{122\}$, $\{151\}$, $\{315\}$, $\{313\}$. Zwillinge wurden beobachtet nach $\{101\}$, $\{011\}$, $\{110\}$ und $\{111\}$.

19) Ulrich, Berg- u. hüttenmänn. Zeitung 1854, 97.

20) Silvestri, Gazz. chim. ital. 1873, 3, 578.

21) Gaubert, Bull. soc. fr. minér. Paris 1905, 28, 157.

22) Mitscherlich, Abhandl. Berl. Akad. 1822—1823, 43. Ann. chim. phys. 1823, 24, 264. Ms Werke 189.

23) Schrauf, Sitz.-Ber. Akad. Wien 1860, 41, 794.

24) Illosvay, »Über die Bedingungen der Bildung von gediegenem Schwefel«. Földtany Kőzlöni 1884, 14, 38, 147; Zeitschr. f. Krystall. 10, 91.

	Berechnet:		Beobachtet:			
			Brežina ^{*)} :	Mitscherlich:	Schrauf:	Silvestri:
$p:p = (111):(1\bar{1}1) = 73^{\circ}26'$		—	—	—	$73^{\circ}32'$	$73^{\circ}40'$
$p:p = (111):(\bar{1}11) = 95\ 0\frac{1}{2}$		—	—	$95^{\circ}2'$	$94\ 57\frac{1}{2}$	$95\ 0$
$p:p = (111):(11\bar{1}) = 36\ 40$		$*36^{\circ}40'$	$36\ 43$	$36\ 46$	$36\ 44$	$36\ 44$
$n:n = (011):(01\bar{1}) = 55\ 30$		—	—	$55\ 32$	$55\ 25$	$55\ 25$
$v:c = (013):(001) = 32\ 21\frac{1}{2}$		$*32\ 25$	—	—	—	—
$w:c = (023):(001) = 51\ 43$		—	—	—	—	—
$v:n = (013):(011) = 29\ 53\frac{1}{2}$		$*29\ 53\frac{1}{2}$	—	—	—	—
$n:b = (011):(010) = 27\ 45$		$*27\ 45$	—	—	—	—
$u:c = (103):(001) = 38\ 0$		—	—	—	—	—
$m:m = (110):(1\bar{1}0) = 78\ 4$		—	—	—	—	—
$r:a = (311):(100) = 16\ 59$		$16\ 35$	—	—	—	—
$l:a = (344):(100) = 50\ 41\frac{1}{2}$		—	—	—	—	—
$x:n = (133):(011) = 19\ 59\frac{1}{2}$		$19\ 56$	—	—	—	—
$\omega:c = (117):(001) = 23\ 49\frac{1}{2}$		$23\ 39$	—	—	—	—
$t:c = (115):(001) = 31\ 7$		$31\ 5$	—	—	—	—
$s:c = (113):(001) = 45\ 40$		—	—	—	—	—
$s:s = (113):(1\bar{1}3) = 53\ 3\frac{1}{2}$		—	—	—	—	—
$s:s = (113):(\bar{1}13) = 66\ 50$		—	—	—	—	—
$z:c = (135):(001) = 50\ 57\frac{1}{2}$		—	—	—	—	—
$z:x = (135):(133) = 13\ 5\frac{1}{2}$		$*13\ 5\frac{1}{2}$	—	—	—	—
$x:q = (133):(131) = 16\ 44$		$*16\ 43\frac{1}{2}$	—	—	—	—
$q:q = (131):(13\bar{1}) = 18\ 25$		$*18\ 23$	—	—	—	—

Spaltbarkeit unvollkommen nach $p\{111\}$, $c\{001\}$, $m\{110\}$.

Ebene der opt. Axen $b\{010\}$, c 1. Mittell., Doppelbr. +. Brechungsindices nach Schrauf (Zeitschr. f. Krystall. 1894, 18, 157) bei 20° (bezogen auf den leeren Raum):

Li :	$\alpha = 1,93975$	$\beta = 2,01709$	$\gamma = 2,21578$
Na :	$1,95791$	$2,03770$	$2,24516$
Tl :	$1,97638$	$2,05865$	$2,27545$

$2V = 68^{\circ}58'$ (Na), $68^{\circ}46'$ (Tl).

Vorstehende Werte, ferner die Ausdehnung durch die Wärme und die Dielektricitätsconstanten wurden an natürlichen Schwefelkrystallen bestimmt (s. Hintze, Handb. d. Min. 1, 72).

β -Modification (monokliner Schwefel).

Schmelzp. $119,4^{\circ} - 119,8^{\circ}$ (Muthmann¹⁾).

Spec. Gew. $1,958$ (Deville²⁵),

$1,915$ bei 103° (Zehnder¹⁷).

Aus Schmelzfluß; meßbare Krystalle nur bei sehr großen Mengen, Mitscherlich²²).

Protein crystals are not perfect inside

Figure 3-11 Atomic force microscope images of crystal growth. (Panel A)

The atomic force microscope images of the 001 surface of glucose isomerase show the two most common growth patterns observed in crystal growth: step growth starting from 2-dimensional nucleation islands (A, left image) and a double-spiral growth pattern (A, right image). Panel B shows formation of supercritical 2-dimensional nuclei on the 001 surface of cytomegalovirus (CMV), a member of the herpes virus family. As indicated by the arrows, in this case only two virions (B, left image) suffice to generate a critical nucleus from which new step growth commences (B, right image). Images courtesy of Alexander McPherson and Aaron Greenwood, University of California, Irvine.

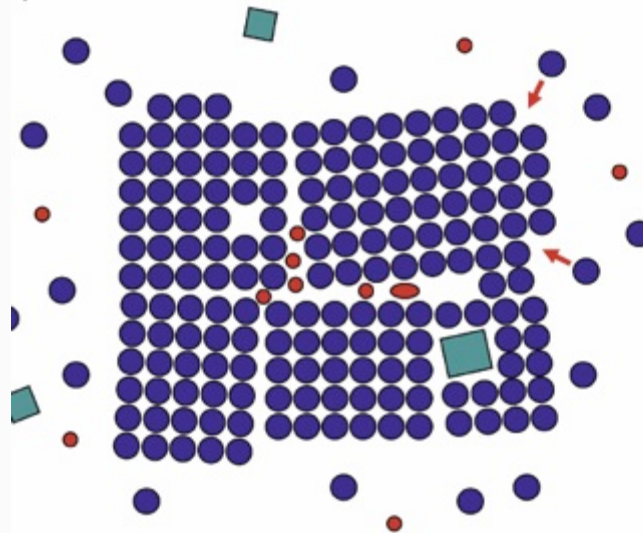
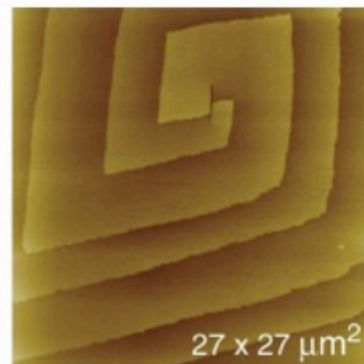
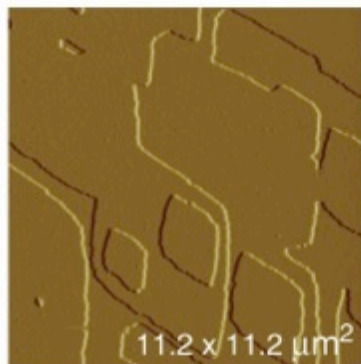


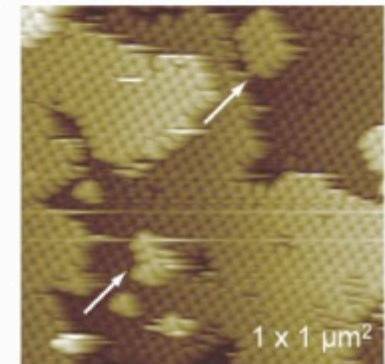
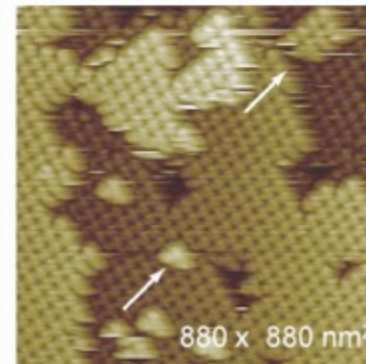
Figure 3-12 Growth of a real mosaic crystal. The schematic drawing shows a crystal growing in a solution of protein molecules (blue spheres). Small impurities (red) and some larger detritus (green squares) are also present in the solution. New molecules attach preferentially to steps and edges (red arrows) and we can recognize a growth defect in the form of a hole; impurities are enclosed at the domain boundaries; and a larger piece of detritus is incorporated at a domain boundary. Individual domains can be substantially misaligned, in this case about 6°; such a highly mosaic crystal would not be useful for diffraction experiments.

Phenomena of **mosaicity** and **twinning** complicate data collection

A



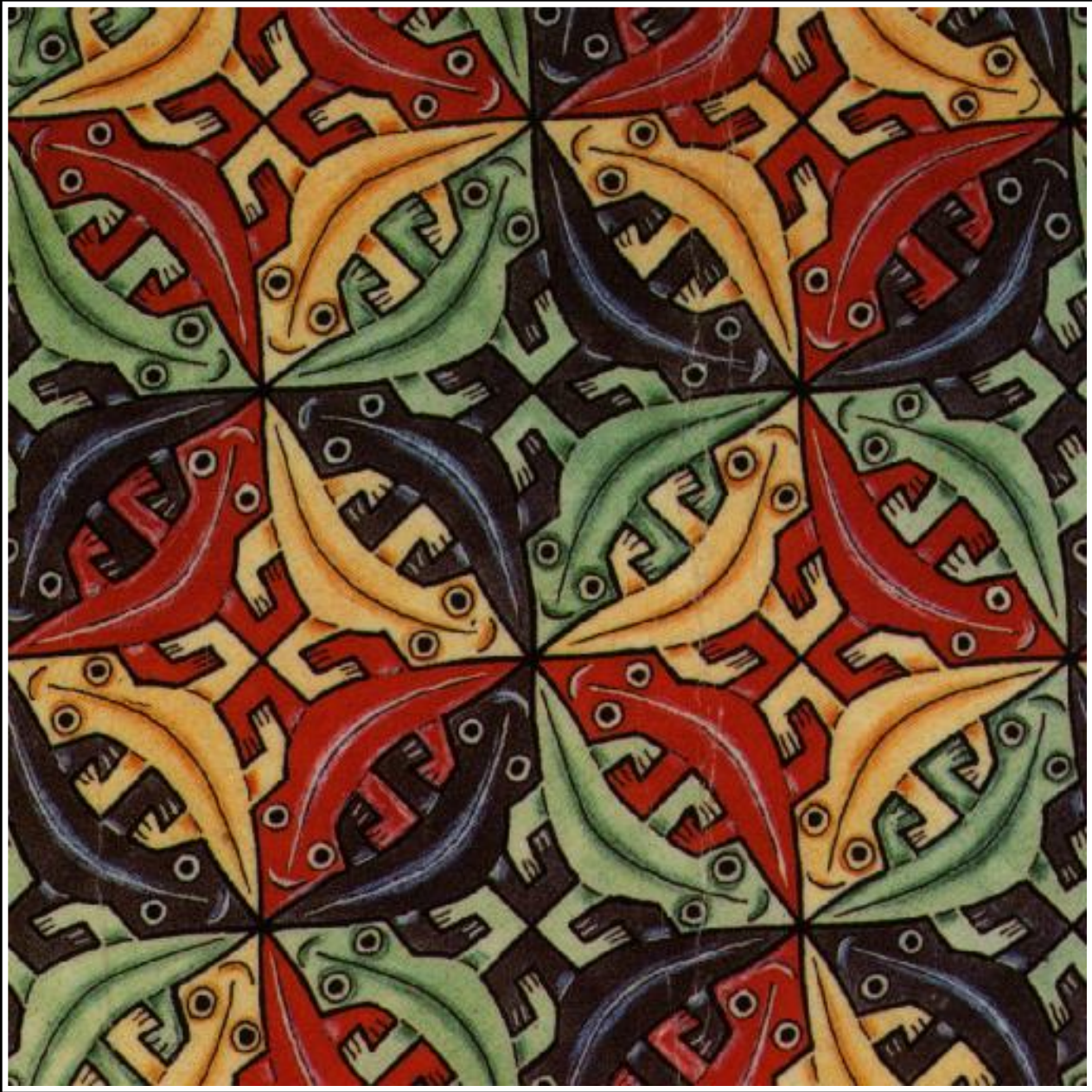
B



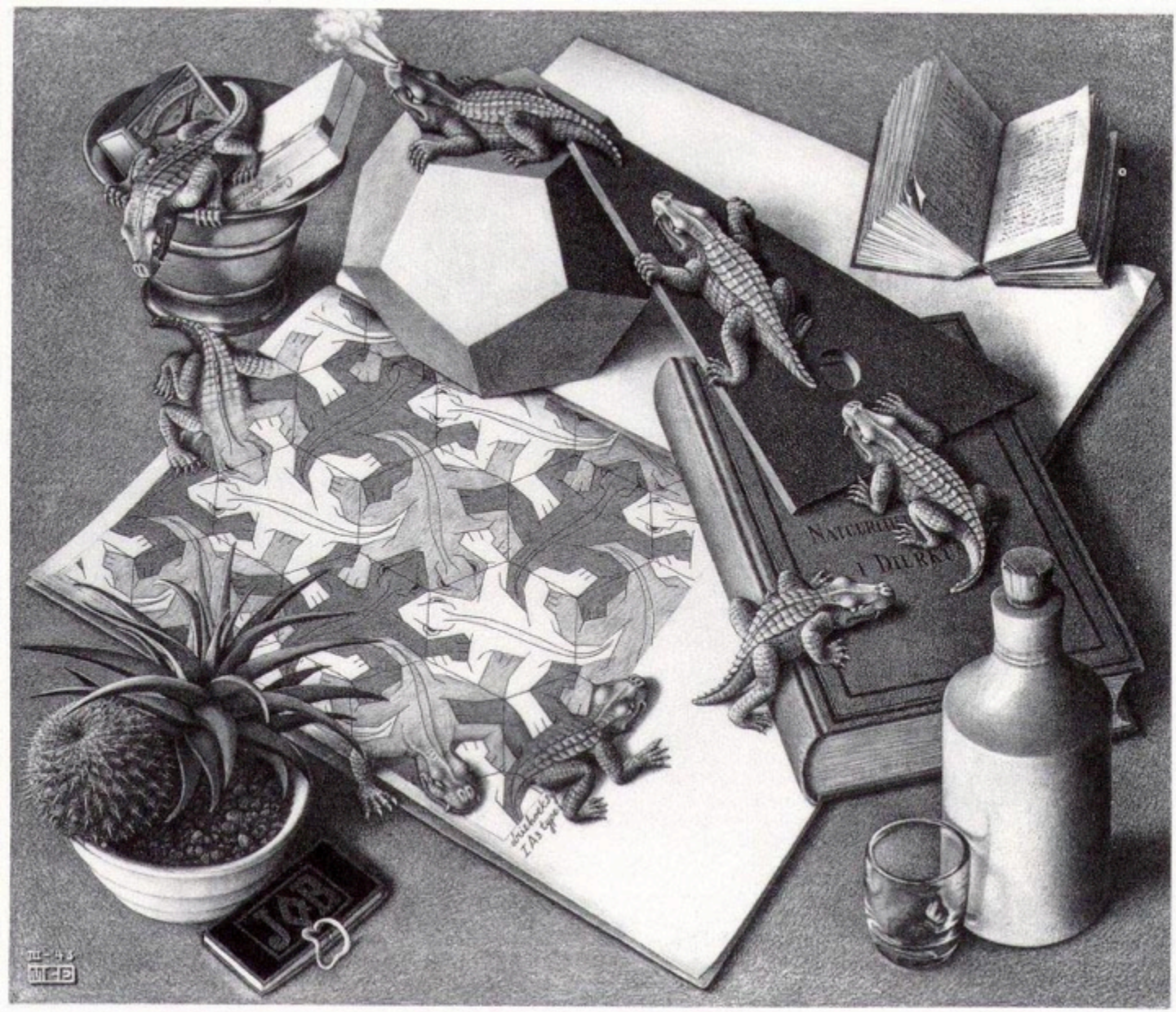
<http://escher.epfl.ch/rlattice/>



<http://www.mcescher.com/>



<http://www.mcescher.com/>



<http://www.mcescher.com/>

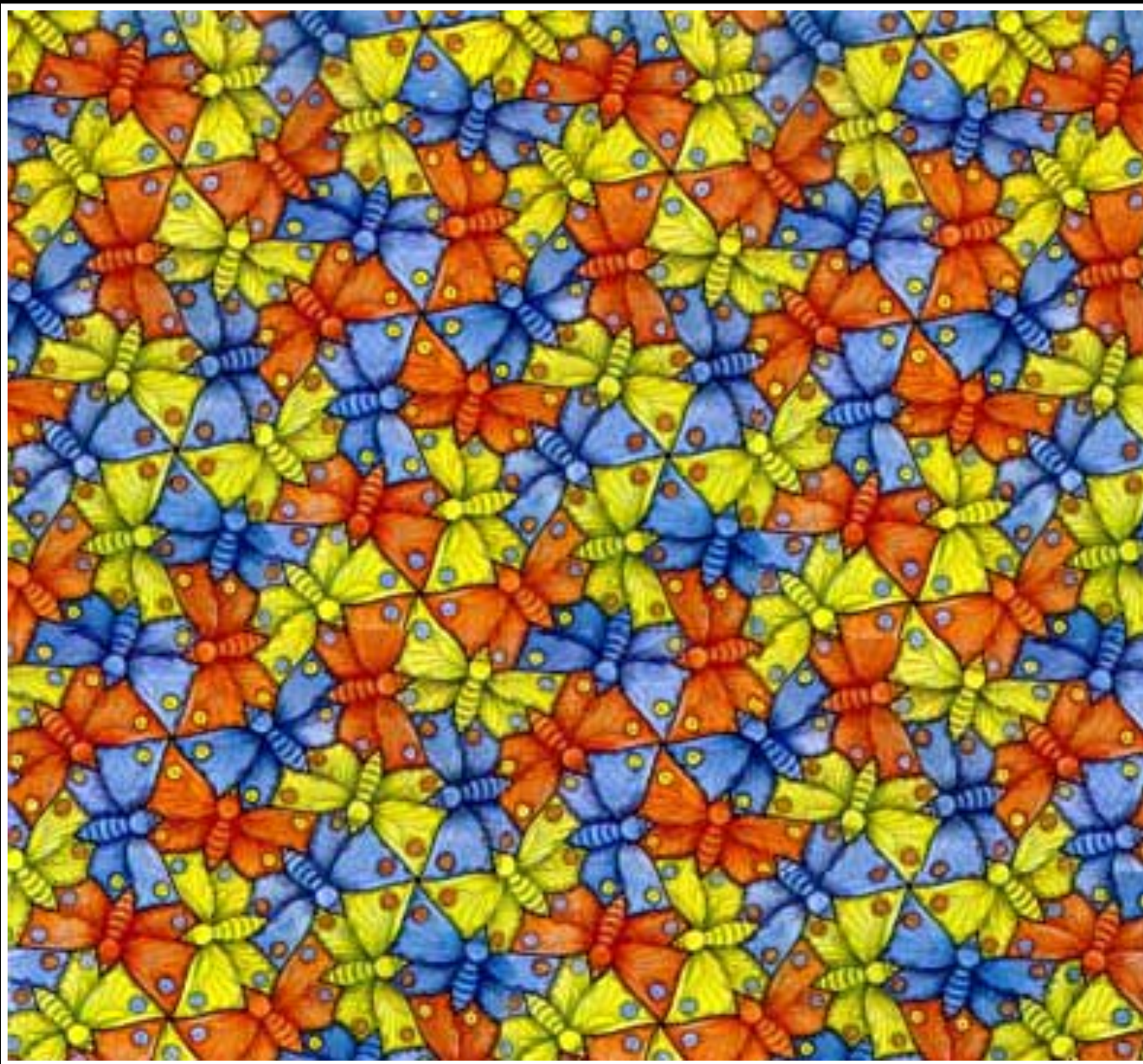
**p1
with
color**

**p3
ignoring
color**

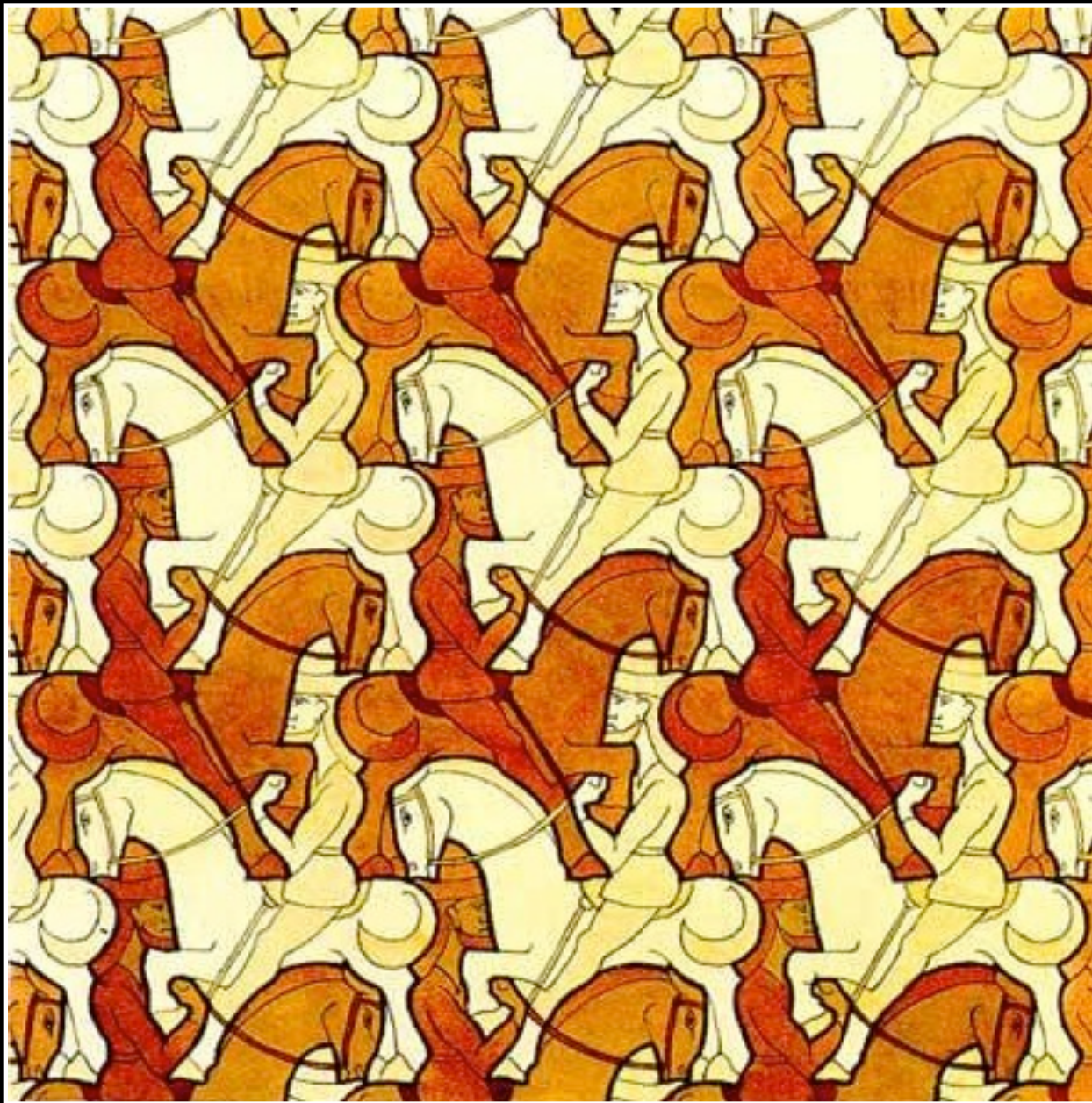


p3
with
color

p6
ignoring
color

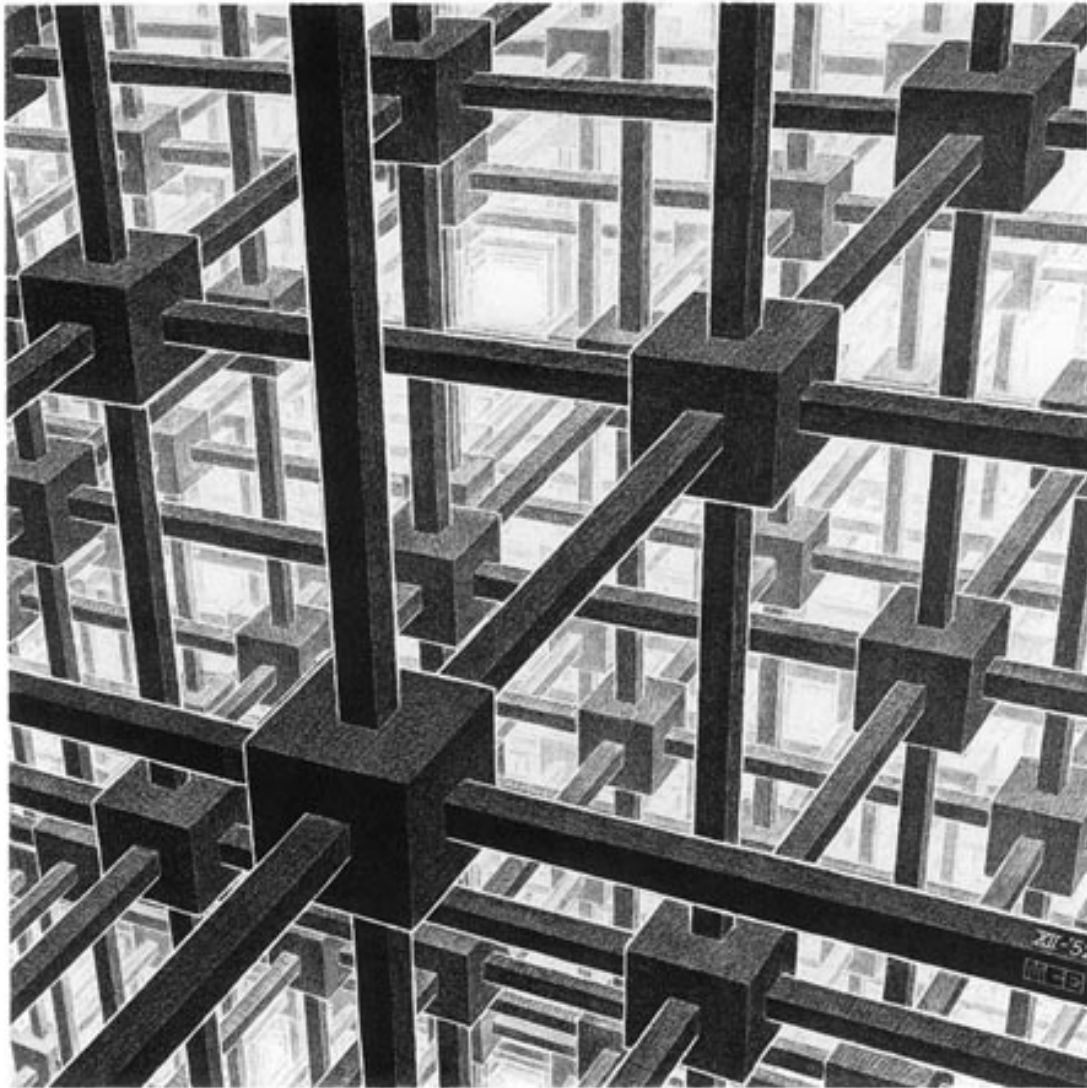


p1



p1
square



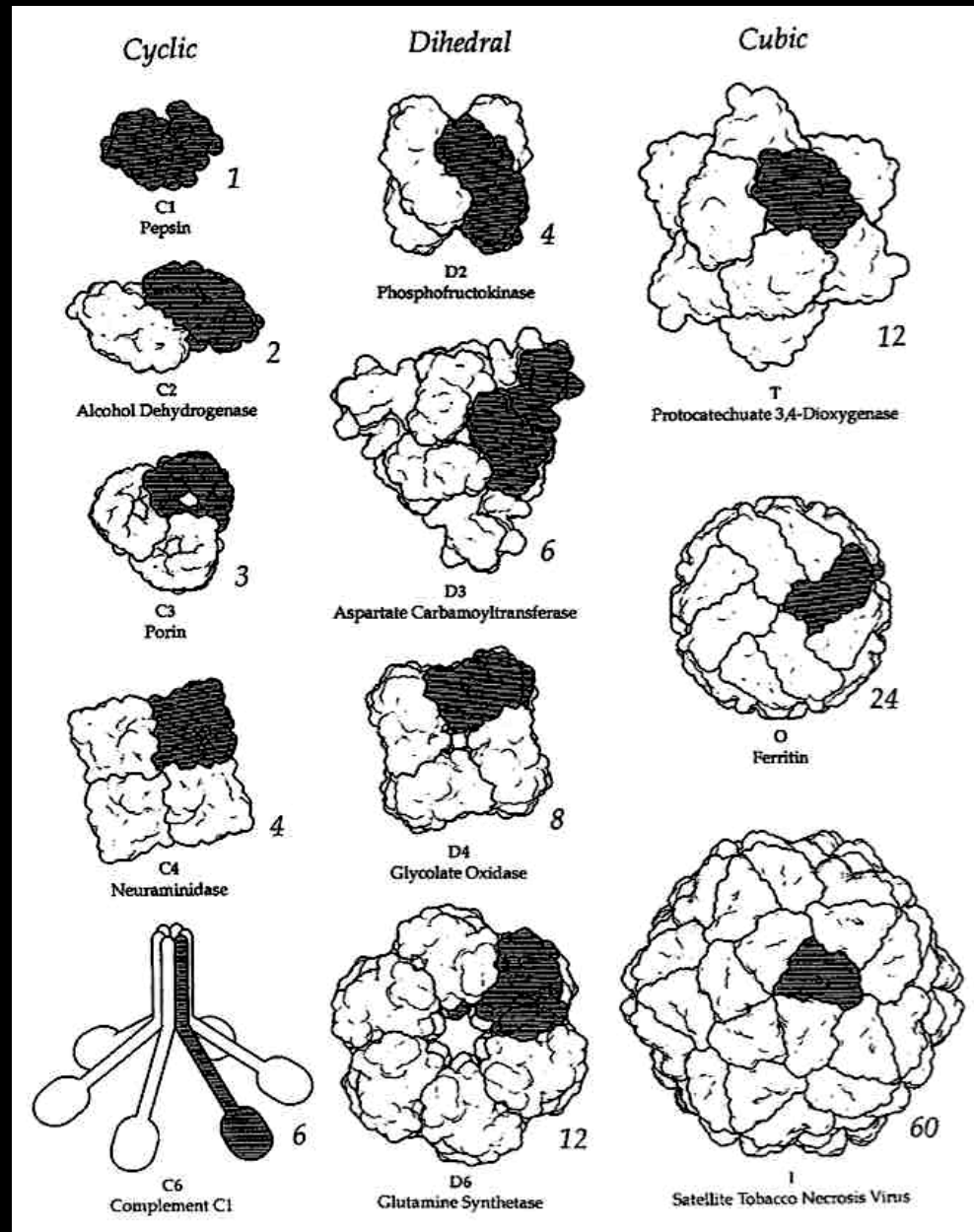


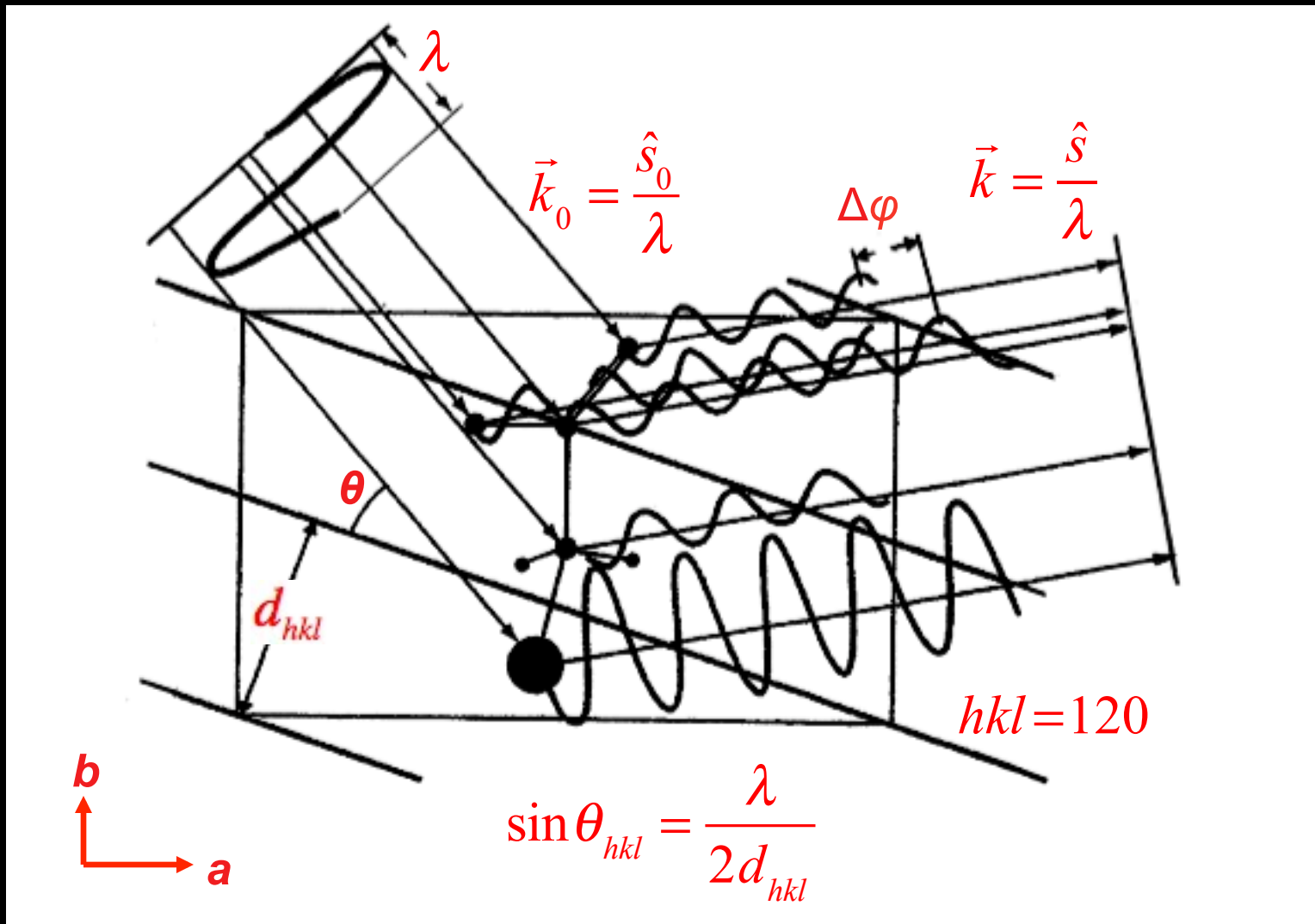
<http://www.meta-library.net/cqmedia/esch-body.html>

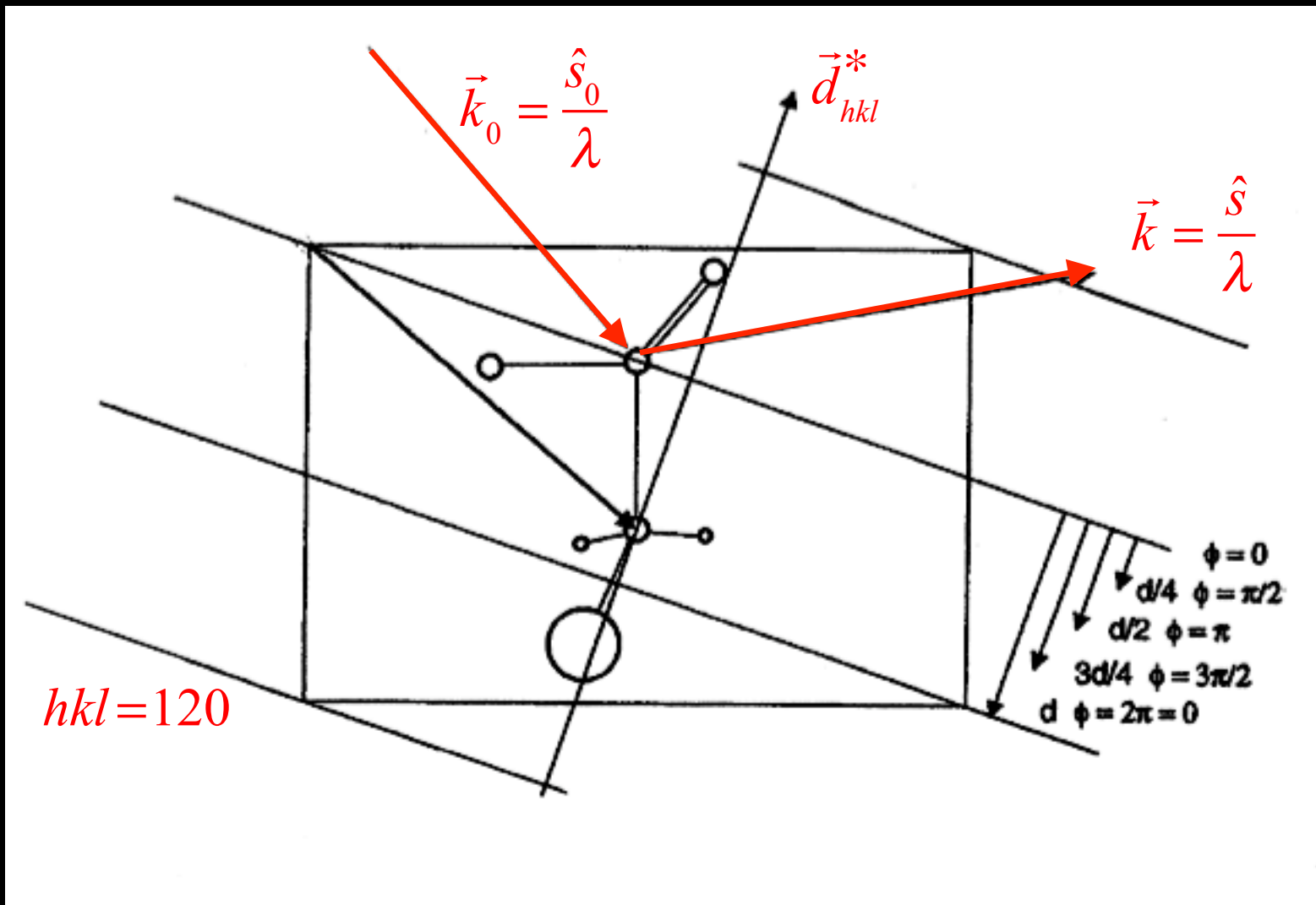
M.C. Escher (1955). Depth

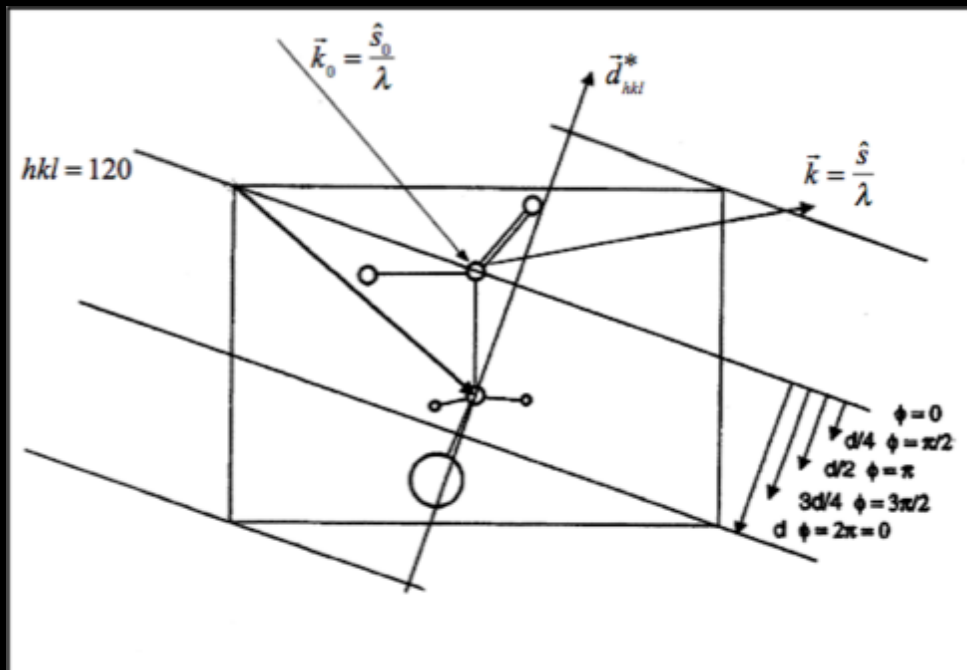
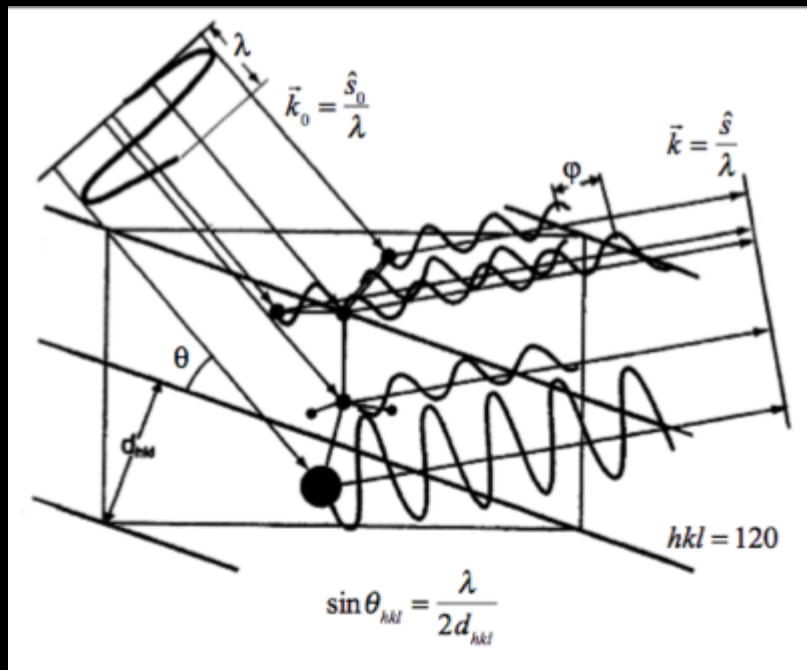


Crystallographic point groups of protein multimers





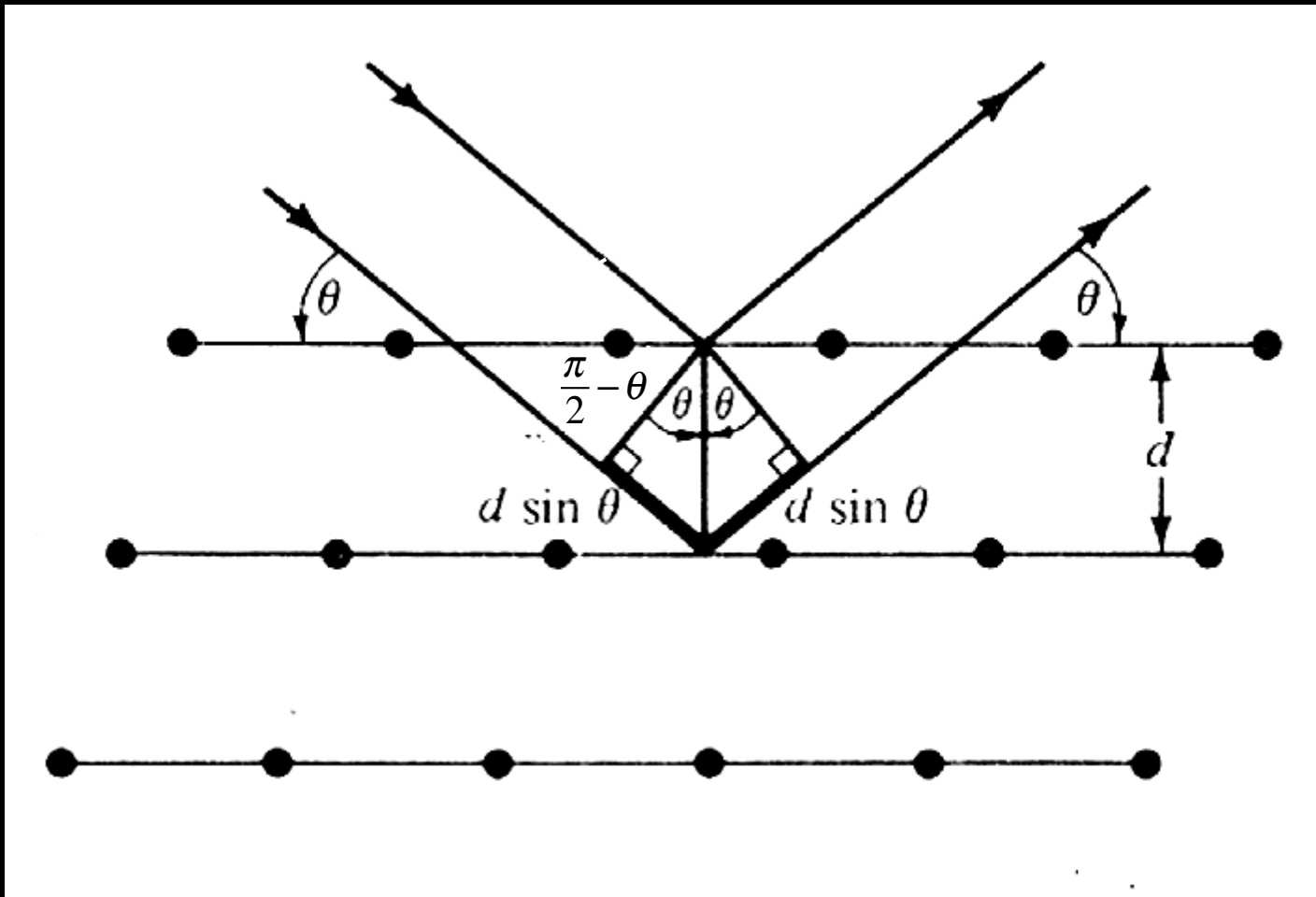




Δd_{hkl}	$\Delta \phi_{hkl}$
0	0
$d/4$	$\pi/2$
$d/2$	π
$3d/4$	$3\pi/2$
d	2π

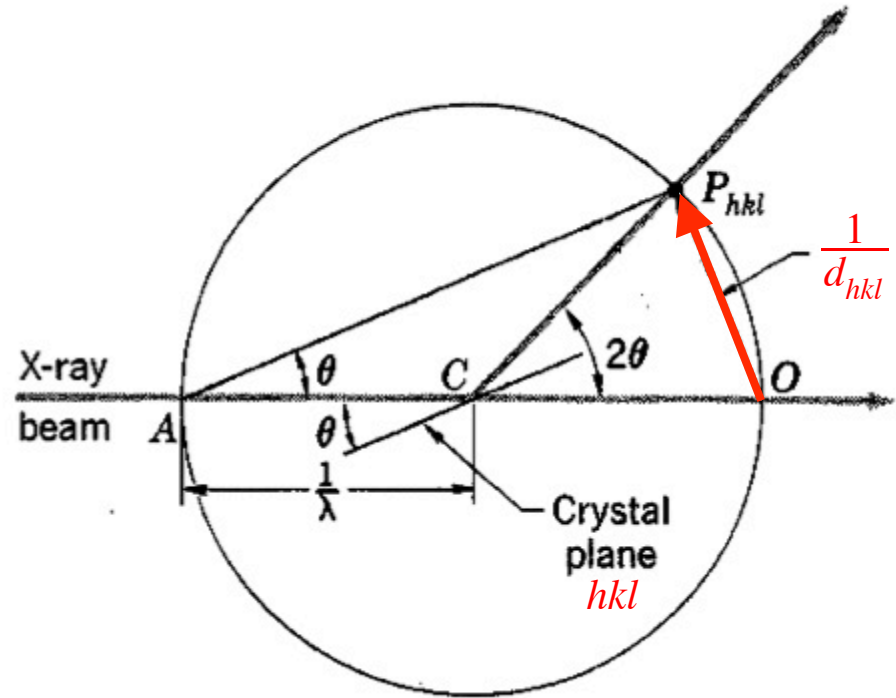
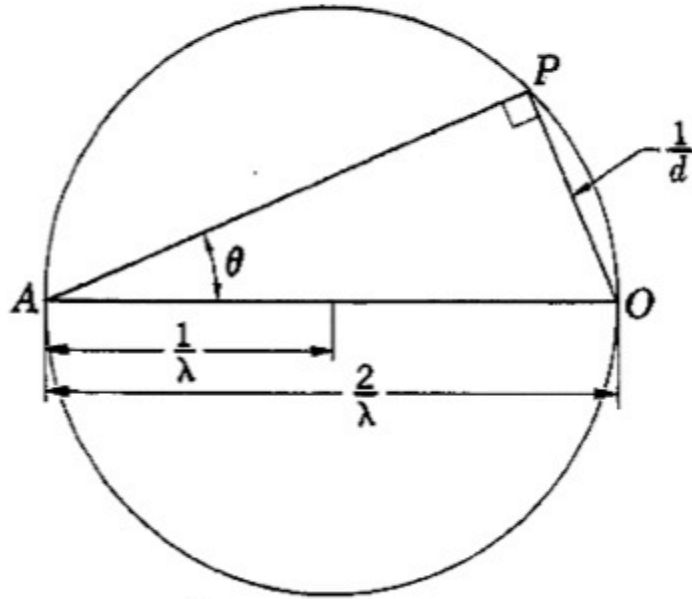
Bragg reflection from families of parallel hkl lattice planes

$$2d_{hkl} \sin \theta = n\lambda, \quad 2 \left(\frac{d_{hkl}}{n} \right) \sin \theta = \lambda, \quad 2d_{nhnknl} \sin \theta = \lambda$$



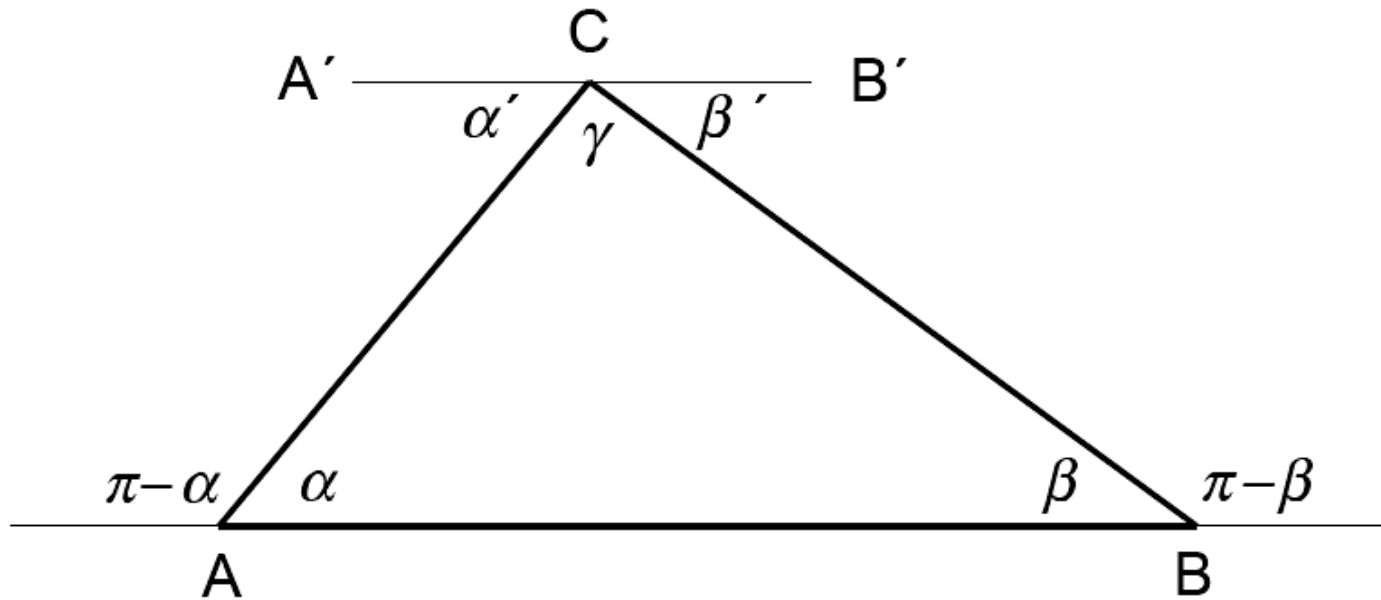
The Ewald construction

θ Bragg angle
 2θ Scattering angle



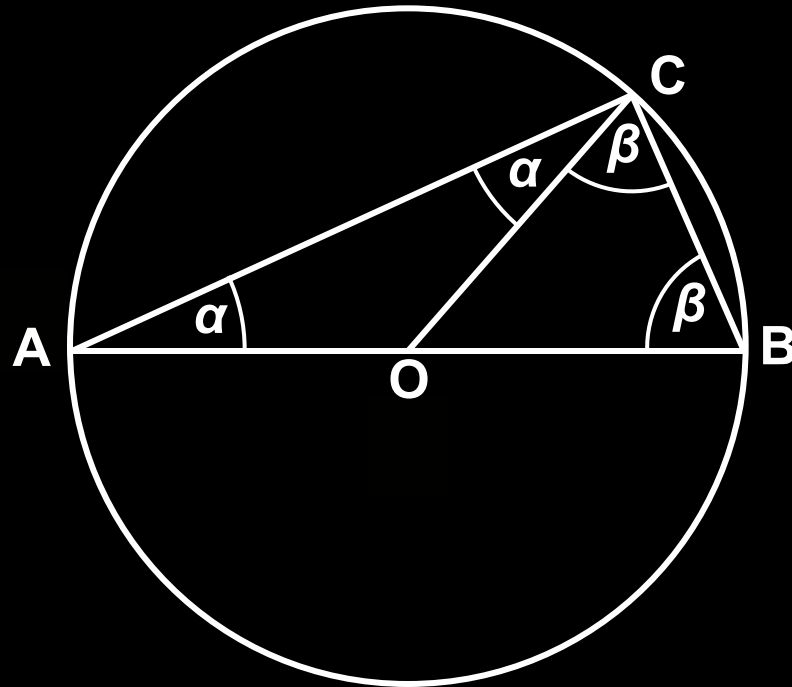
{	Wm. Henry & Wm. Lawrence Bragg (1913)	$2d \sin \theta = \lambda$
	Paul Peter Ewald (1913)	$\sin \theta = \frac{1}{d} \frac{\lambda}{2} = \left(\frac{1}{d} \right) / \left(\frac{2}{\lambda} \right)$

The sum of angles in a plane triangle equals a straight angle.



Thales Theorem

Any angle subtended by the diameter of a circle is a right angle.

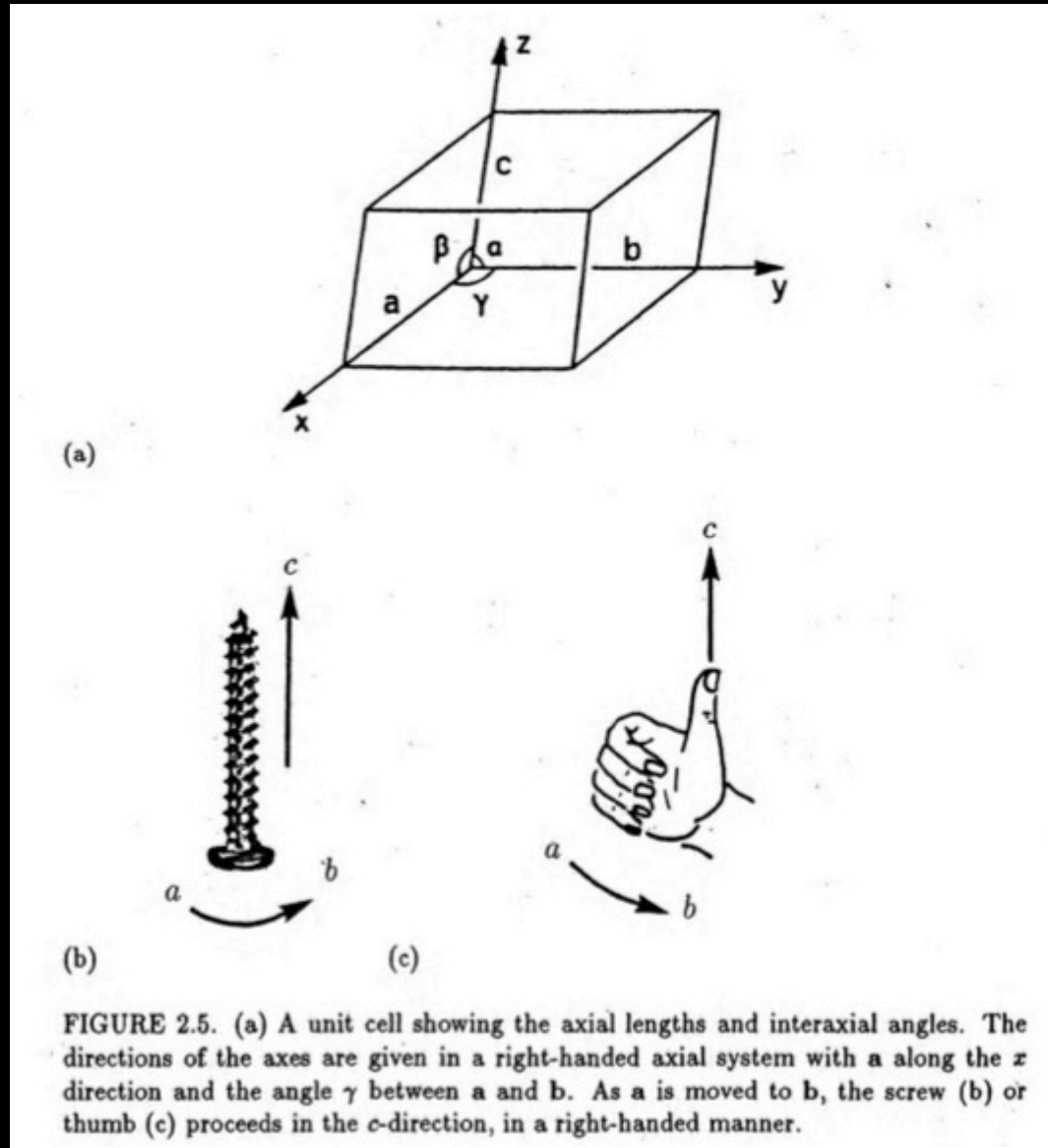


$$\alpha + \beta + (\alpha + \beta) = \pi$$

$$2\alpha + 2\beta = \pi$$

$$\alpha + \beta = \frac{\pi}{2}$$

Crystallographic axes and lattice parameters



Jenny P. Glusker, with Mitchell Lewis and Miriam Rossi (1994).
Crystal Structure Analysis for Chemists and Biologists. New York: Wiley-VCH, Inc.